NASA CR-137520

Available to the Public

STATIC NOISE TESTS ON AUGMENTOR WING JET STOL RESEARCH AIRCRAFT (C8A BUFFALO)

by C. C. Marrs, D. L. Harkonen, and J. V. O'Keefe

May 1974

Prepared under contract NAS2-7641 by

BOEING COMMERCIAL AIRPLANE COMPANY
P.O. Box 3707
Seattle, Washington 98124

for
AMES RESEARCH CENTER
NATIONAL AERONAUTICS AND SPACE ADMINISTRATION

1. Report No.	2. Government Accession No.	3. Recipient's Catalog No.
NASA CR-		

4. Title and Subtitle	5. Report Date
STATIC NOISE TESTS ON AUGMENTOR WING JET STOL RESEARCH AIRCRAFT (C8A BUFFALO)	May 1974
	6. Performing Organization Code
7. Author(s)	8. Performing Organization Report No.
C. C. Marrs, D. L. Harkonen, and J. V. O'Keefe	D6-41324-1
9. Performing Organization Name and Address	10. Work Unit No.
Boeing Commercial Airplane Company P.O. Box 3707 Seattle, Washington 98124	11. Contract or Grant No. NAS2-7641
12. Sponsoring Agency Name and Address	13. Type of Report and Period Covered
National Aeronautics and Space Administration Washington, D. C. 20546	Contractor Report
	14. Sponsoring Agency Code

15. Supplementary Notes

16. Abstract

Results are presented for full scale ground static acoustic tests of over-area conical nozzles and a lobe nozzle installed on the Augmentor Wing Jet STOL Research Aircraft, a modified C8A Buffalo. The noise levels and spectrums of the test nozzles are compared against those of the standard conical nozzle now in use on the aircraft. Acoustic evaluations at 152 m (500 ft), 304 m (1000 ft), and 1216 m (4000 ft) are made at various engine power settings with the emphasis on approach and takeoff power. Appendix A contains the test log and propulsion calculations. Appendix B gives the original test plan, which was closely adhered to during the test. Appendix C describes the acoustic data recording and reduction systems, with calibration details.

NOTE:

Further work, based on the conclusion/recommendations listed here, is reported in NASA CR-137521 and NASA CR-137522.

17. Key Words (Suggested by Author(s))	18. Distribution Statement
Perceived noise level (PNL) Tone-corrected perceived noise level (PNLT) C8A Buffalo Lobe nozzle Over-area nozzle (engine derate) Colander plate Bifurcated duct (pants section)	Unclassified–unlimited

19. Security Classif. (of this report)	20. Security Classif. (of this page)	21. No. of Pages	22. Price*
Unclassified	Unclassified	99	$3.00

*For sale by the National Technical Information Service, Springfield, Virginia 22151

CONTENTS

STATIC NOISE TESTS ON AUGMENTOR WING JET STOL RESEARCH AIRCRAFT (C8A BUFFALO)

by C. C. Marrs, D. L. Harkonen, and J. V. O'Keefe

INTRODUCTION AND SUMMARY

Previous noise measurements of the Buffalo C8A augmentor wing-jet STOL research aircraft (AWJSRA) recorded at Paine Field, Washington, indicated that the dominant noise source of the Spey engine (mk 801 SF) was the primary exhaust system. This exhaust system consists of a split flow plenum, a pressure drop "screen" (colander plate) to match the pegasus split flow plenum to the engine, and two rotatable conical nozzles.

A test program has been conducted to provide a firm technology base to reduce the noise of the AWJSRA at 152 m (500 ft) sideline, 304 m (1000 ft) overhead, and 1216 m (4000 ft) overhead at takeoff and approach power. This program was jointly sponsored by the U.S. Government (NASA with Boeing) and the Canadian Government (DITC with de Havilland and Rolls Royce). Full-scale exploratory noise data, with and without the colander plate installed, were acquired. The noise reduction potential of engine derating (primary nozzle area increase) and of lobe type suppressor nozzles was evaluated.

The test was conducted at NASA Ames Research Center, Moffett Field, California, from July 26 through August 6, 1973. The aircraft noise levels were measured with ground surface microphones located along a 30.4-meter (100-foot) sideline.

Acoustic data is presented herein for 1/3 Octave Band Overall Sound Pressure Level (OASPL), Perceived Noise Level (PNL), and Tone Corrected Perceived Noise Level (PNLT). The noise levels measured with the various configurations are compared on a constant primary (hot) thrust basis, a constant airplane lift basis at approach and a constant total thrust (primary + fan) at takeoff. Engine thrust was not directly measured during the test program but was computed from primary nozzle exit total pressure measurements. The computed hot thrust levels are approximate values but are believed sufficiently accurate for a thrust-noise evaluation.

All nozzles tested were analysed for noise suppression relative to the current configuration at three distances—152 m (500 ft) sideline, 304 m (1000 ft) overhead, and 1216 m (4000 ft) overhead—and two power settings representing the takeoff and approach operation modes. The

noise suppression results for the engine configuration with the colander plate removed are shown in figures 1 and 2 for fixed and variable area primary nozzles, respectively. In addition to the measured noise suppression increments, the noise suppression potential of each nozzle is also shown. Comparison of the two figures at approach conditions clearly shows the noise advantage for an over-area nozzle. At takeoff power (99% N_H), the superiority of the lobe nozzle is clearly demonstrated, particularly if discrete tones that were measured are removed and if the directivity effect of the rectangular array lobe nozzle for overhead applications is realized. The over-area primary nozzles would require provisions for reducing the nozzle area in order to provide sufficient thrust for emergency and takeoff modes. Similar results are obtained for the engine with the colander plate installed, but at a loss in engine thrust caused by flow losses through the colander plate.

DISCUSSION OF RESULTS

TEST HARDWARE

The standard Buffalo primary conical nozzles: 2290 cm^2 (355 $in.^2$); four other pairs of conical nozzles: 1807 cm^2 (280 $in.^2$), 2045 cm^2 (317 $in.^2$); 2639 cm^2 (409 $in.^2$), and 2942 cm^2 (456 $in.^2$); and two lobe-type suppressor nozzles 1871 cm^2 (290 $in.^2$) and 2213 cm^2 (343 $in.^2$) were tested. The conical nozzles were designed to have the same length but different conical half angles and exit diameters, as shown below:

Conical nozzle		
Exit area (cold) cm^2 ($in.^2$)	1/2 angle	Exit diameter cm (in.)
1807 (280)	16°31″	33.91 (13.35)
2045 (317)	14°03″	36.09 (14.21)
2290 (355)*	11°30″	38.1 (15.0)
2639 (409)	8°19″	41 (16.14)
2942 (456)	5°18″	43.28 (17.04)

*Standard Buffalo primary nozzle configuration

The lobe-type suppressor nozzles were tested at two exit areas: 1871 cm^2 (290 $in.^2$), and 2213 cm^2 (343 $in.^2$). The smaller-area configuration was created by blocking the two outer lobes and was tested with the colander plate removed.

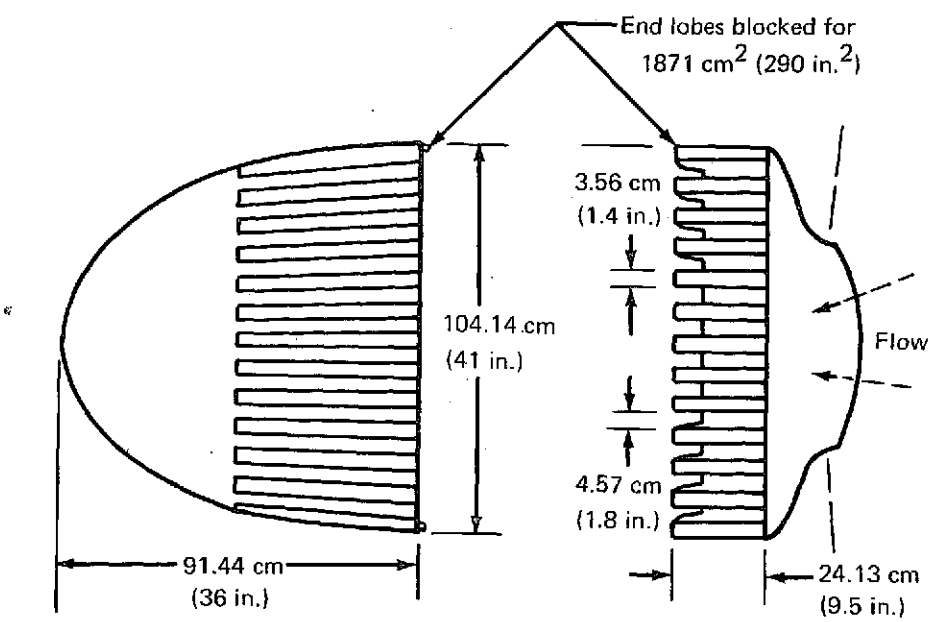

All test nozzle configurations were tested with total pressure probes installed in the nozzle exit. The dimensions and positions of the pressure rakes are shown below:

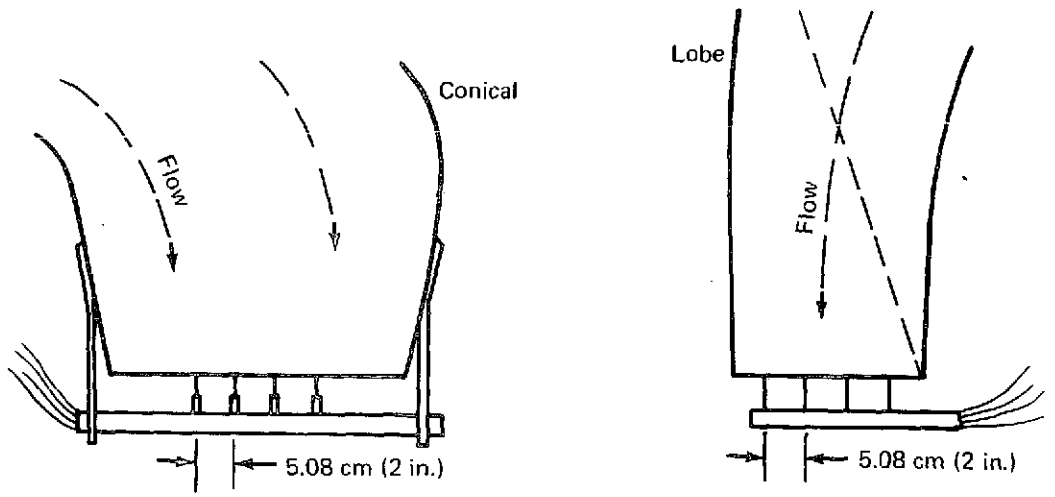

In addition to the nozzles, an engine case treatment made up of two layers of lead vinyl and one layer of fiberglass was tested. See appendix B for a complete description of this treatment.

Figures 3 through 9 are photographs of typical test configurations.

ACOUSTIC ANALYSIS

Overhead Comparisons, 304 m (1000 ft)

Figure 10 compares four nozzle configurations—conical 2290 cm^2 (355 $in.^2$), conical 2639 cm^2 (409 $in.^2$), conical 2942 cm^2 (456 $in.^2$), and lobe 2290 cm^2 (355 $in.^2$)—in terms of the overall sound pressure level (OASPL) at primary thrusts of 906 kg through 2718 kg (2000-6000 lb) for the engine with the colander plate installed. The OASPL values were taken at the angle of maximum OASPL. This comparison shows that the lobe nozzle is capable of OASPL reductions of 2 to 5 dB at 304 meters overhead because of the reduction of the low- and mid-frequency sound pressure levels. The conical nozzle "over-area" configuations—2639 cm^2 (409 $in.^2$) and 2942 cm^2 (456 $in.^2$)—should also show some suppression, especially in OASPL, because the velocity reduction due to the overarea condition should reduce the low-frequency component. Why reduction did not occur is not understood at this time.

Figure 11 shows four nozzle configurations–conical 1807 cm^2 (280 $in.^2$), conical 2045 cm^2 (317 $in.^2$), conical 2290 cm^2 (355 $in.^2$), and lobe 1871 cm^2 (290 $in.^2$)–in terms of maximum overall sound pressure levels versus thrust at 304 m (1000 ft) overhead. These configurations had the colander plate removed. The 1807 cm^2 (280 $in.^2$) conical and 1871 cm^2 (290 $in.^2$) lobe were the engine-matched configurations corresponding to the standard Spey 801-SF engine-operating line. This plot shows the lobe nozzle attaining 5 to 7 dB reduction. Again, the conical nozzle overarea configurations did not perform as expected.

Figures 12 and 13 show the nozzle configurations compared on the basis of maximum tone-corrected perceived noise level (PNLT) versus primary thrust at 304 m (1000 ft) overhead. At this distance, the high-frequency component of the spectrum is still the controlling factor in the weighted calculation of PNLT. Therefore, the resultant PNLT performance of all the nozzles is virtually the same. The lobe nozzle reduced the low-frequency noise but had a high-frequency component at 2000 and 4000 Hz which still dominated the PNLT value. The lobe nozzle does give reasonable sound reduction at the higher thrust values where the high-frequency tones were not as predominant.

Overhead Comparisons, 1216 m (4000 ft)

The 1216 m (4000 ft) overhead comparisons are based on maximum PNLT versus thrust. Figures 14 and 15 show the result of distance attenuation on the high-frequency component of the spectrum. At 304 meters the high-frequency controlled the PNLT value, and the low-frequency reduction provided by the lobe nozzle was minimized. At 1216 meters the high frequencies of the conical and lobe nozzle have been attenuated to a point where the low frequency controls the PNLT value. The resultant noise reductions shown on figures 14 and 15 reflect the low-frequency reductions attained by the lobe nozzles.

Colander Plate Evaluation

All comparisons to this point have been with either the colander plate installed or removed. For a full acoustic evaluation, it is necessary to determine the colander effect, and then cross-plot, on a constant thrust basis, the best acoustic configurations.

Figure 16 compares the conical 2290 cm^2 (355 $in.^2$) nozzle with the conical 1807 cm^2 (280 $in.^2$) nozzle for the engine with the colander plate installed and removed, respectively. The comparison is made at equal thrust. This comparison shows that it does not matter (acoustically) if the colander is installed or removed when a conical nozzle is used.

Figure 16 also shows a similar comparison of the lobe 2290 cm^2 (355 $in.^2$) nozzle with the lobe 1871 cm^2 (290 $in.^2$). As can be seen, the PNLT levels are reduced somewhat when the colander is removed. The question then occurs, what causes a change in levels when the colander is removed with the lobe nozzles, but no corresponding change with the conical nozzles? To answer this question, the respective noise spectrums must be examined.

Figures 17 and 18 are 1/3 octave band plots of the sound occurring at the angle of maximum PNLT for the configurations of colander in and out. These plots are at approximately equal thrust settings, to permit a reasonable comparison. Figure 17 shows that the spectrum shape and levels of the conical nozzle with and without the colander are virtually equal. In contrast, figure 18 shows that when the colander is removed with a lobe nozzle, the mid-frequencies (200 to 1600 Hz) are slightly reduced, thereby reducing the PNLT slightly. Figure 18 also shows that the "tone" which occurs at 160 Hz when the colander is installed shifts down to 100 Hz and also increases in amplitude when the colander is removed.

This change in frequency most likely occurs because of the acoustic volume increase in the "pants" section* when the colander is removed. The increase in amplitude still requires analysis. It is possible that a change in spectrum shape and level does occur with the conical nozzle when the colander is removed, but that the effect is masked in the absence of the noise reduction brought about by the lobe nozzle.

Comparison of Best Conical Over-Area and Lobe Nozzles

The next step in the analysis is to compare the best conical over-area configuration and the best lobe nozzle configuration against the baseline—conical 2290 cm^2 (355 $in.^2$) colander in—and determine which configuration shows the best suppression potential.

Figures 19 and 20 show three nozzles—lobe 1871 cm^2 (290 $in.^2$), colander out; conical 2045 cm^2 (317 $in.^2$), colander out; and conical 2290 cm^2 (355 $in.^2$), colander in (baseline)—plotted at four distances from the source. These plots are extrapolations of data measured at 30.4 m (100 ft) sideline, and do not show any effect of a directivity advantage when sound from the narrow side of the lobe nozzle is measured. This effect is discussed later in the text.

Additional Potential of Lobe Nozzle

It is felt that an evaluation of the effect of removing the spikes at 2000 and 4000 Hz and removing the low-frequency spike is necessary in evaluating the future potential of the lobe nozzle.

*Split flow plenum

Figures 21 and 22 show the 1/3 octave spectrum of the lobe nozzle, measured at four power settings. These spectrums are at the angle of maximum PNLT. The dashed lines show how the spectrums would appear if the high- and low-frequency "problem" areas were removed.

Figures 23, 24, and 25 show the additional suppression potential of the lobe nozzle at various distances when the high-frequency spikes are removed, when both high and low frequencies are removed, and when the additional directivity effect is included. The directivity effect does not depend on future nozzle development as do the high and low frequency removal. It should be noted that when the conical or lobe nozzles are vectored down, the peak level (PNLT) can increase, due to a reduction in transmission path length at critical angles, but the directivity effect of the lobe nozzle will not change; therefore the PNL increments of the conical and lobe nozzles at a given rotation angle remain constant.

Effect of Flap Angle on Sound Directivity

Figure 26 plots PNLT versus angle for flap angles of "up," 30° down and 50° down. The results shown are very predictable: as the flap is lowered, the sound level decreases in the aft quadrant and increases in the forward quadrant. This is caused by sound reflecting off the airstream from the blown flap. As the data was measured on a sideline, the results are only valid for a sideline display. Overhead directivity changes are not predictable at this time.

Engine Case Blanket* Evaluation

Figures 27 and 28 plot the 1/3 octave spectrums as measured by the two close-in microphones for blanket-on and -off configurations. Because the blanket had a tendency to blow off during the test, data were obtained at only two power settings. The test configuration was the lobe nozzle with colander plate removed and flaps in the up position.

Three conclusions can be drawn from figures 27 and 28:

a) The engine case radiated noise does not appear to be a large contributor to the noise levels measured in the far field. Because the blanket should have made a large reduction in the measured levels from 0.5 through 10 kHz if the engine case radiation were the dominant noise source, it can be deduced that the major portion of the noise is either generated outside of the engine or is internally generated and escapes through the exhaust.

*Two layers of lead vinyl plus one layer of fiberglass

b) The large "spike" also changed to a lower 1/3 octave when the engine thrust was lowered. All indications are that the lobe nozzle is generating this tone. How this tone is being generated is unexplained at this time.

c) The 100 to 125 Hz noise levels were reduced by the blanket. This indicates that the source of this sound is inside the engine. Figure 18 also shows a change in the low frequency when the colander is removed, indicating that the pants section of the engine could be the source of this sound. The reduction of low-frequency noise, measured by the forward close-in microphone, shows that this sound may be transmitting internally forward through the engine. A modification to the pants section might help in eliminating these low frequencies.

Comparison of Paine Field and Ames Data

Figure 29 shows the Paine Field static data as measured on a 45.6-m (150-ft) polar array. The Ames data measured on a 30.4-m (100-ft) sideline and extrapolated to the above polar array are also shown.

The flaps were at 30° in each case. This is the only common data point between Ames and Paine Field, and unfortunately, the 30° flap position gives a directivity change (see figure 28) which could cause the polar and sideline arrays to give different values when data are extrapolated from an assumed point source.

It would appear that if the directivity pattern of the Paine Field data were "pivoted" about the 120° angle, the two plots (Ames 94.7% N_H and Paine Field 96% N_H) would agree within acceptable tolerances. As can be seen, the peak levels of the PNL for Ames and Paine Field are close in value, but the angle at which the peak occurs varies.

There are two possibilities identified at this time as to the cause of this directivity shift:

a) The shift that results when the flaps are lowered to 30° is probably caused by the slot nozzle airstream reflecting the sound forward. Any external force (for example, the wind) that changes this airstream could change the sound directivity pattern. As the wind at Paine Field was approximately 9 knots during the test, whereas the wind at Ames was 0-3 knots, a difference in the directivity pattern would be expected.

b) The microphone array at Paine Field was a 45.6-meter (150-ft) polar layout centered about the exhaust nozzle exit while the array at Ames was a 30.4-meter (100-ft) sideline, with angles measured from the exhaust exit. Under normal conditions these two arrays should measure comparable values if the nozzle is indeed the point noise source. However, if the nozzle exit is not the point noise source, the angles designated for the microphones will be wrong.

A cross correlation of the data from Ames and Paine Field might possibly establish the actual sound source. If the source location is known, the microphone angle identification could be changed, for Ames and Paine Field, to represent the true angles from the source. With this new angle designation, the data could be replotted and it is felt that correlation between Paine Field and Ames could exist.

Over-Area Potential of Lobe Nozzle

All the acoustic evaluations up to this point have been based on equal primary thrust. It is felt that additional potential noise reductions exist at approach power by going over-area with the lobe and conical nozzles, and then taking advantage of the excess lift by pulling the throttle back.

Tables 1 and 2 list the maximum PNLT values at approach and takeoff power as a function of primary exhaust geometry area for the lobe and conical nozzles. The values for the lobe nozzle were derived by picking a nozzle area, establishing a hot thrust value, and then going back to the 1871 cm^2 (290 $in.^2$) lobe nozzle thrust versus PNLT plots and establishing a PNLT value for that thrust. When it was found that an excess of thrust existed relative to the baseline, a theoretical throttle reduction was made until either the total airplane lift was matched (approach) or the total primary and fan thrust was attained (takeoff); a new PNLT value was then established.

The PNLT values for the various exhaust nozzle areas at approach conditions are plotted on figures 30 through 35. These plots show that going over-area with the conical or lobe nozzle gives a potential of approximately 1/2 PNdB decrease per 64.5 cm^2 (10 $in.^2$) increase in area. This potential decrement approximately doubles when over-area plus throttle pull is employed.

The takeoff values shown in tables 1 and 2 do not show enough reduction potential to warrant further analysis. Also, the larger areas do not provide adequate thrust to provide a margin for emergencies.

Acoustic Directivity of Rectangular Array Lobe Nozzle

The data measured during this test program was recorded on a 30.4-m (100-ft) sideline, relative to the long axis of the nozzle.

Existing data (ref. 1) shows that if the acoustic recordings had been made relative to the short axis of the lobed nozzle, a reduction of 2 dB below measurements relative to the long axis would have been found. As it was impossible to measure the data relative to the short axis during this test, it is reasonable to assume that the 2 dB reduction does exist and should be considered in this report.

The 2 dB directivity effect will not be changed when the nozzles are vectored down. However, a change in the peak PNLT value for both the conical baseline and the lobe nozzle can occur. This change is brought about by the different sound transmission path lengths from the source. The differences between the lobe nozzle and baseline nozzle will still remain constant when measured at constant nozzle vector angles relative to the nozzle.

Acoustic Data Summary

Table 3 summarizes the measured noise reductions produced by conical and lobe type nozzles that were tested on the C-8A Buffalo aircraft. Noise suppression increments including potential reductions relative to the current configurations at takeoff and approach power levels are tabulated for 152-m (500-ft) sideline, 304-m (1000-ft) overhead, and 1216-m (4000-ft) overhead distances. This table shows the best conical and lobe nozzle configuration, as well as an over-area (thrust derating) analysis of both types of nozzles. Noise suppression for two power conditions, approach and takeoff, are shown with throttle reductions where excess thrust or airplane lift relative to the baseline exists.

The table shows the peak tone-corrected PNL reduction values of each nozzle relative to the airplane baseline configuration. All the values are progressive and show the total PNLT reduction for each step of the analysis. For example, consider the evaluation of the 1936-cm^2 (300-$in.^2$) lobe nozzle at 1216-m (4000-ft) overhead distance at approach power. At 93% N_H, the nozzle attained 2.5 PNdB reduction at 304 m (1000 ft). If the cold thrust is higher than that produced by the baseline configuration, the engine speed can be reduced (throttle back) until the aircraft lift is equivalent. In this particular case the engine is close to match conditions, and therefore no excess lift exists to allow cut-back. Removing the 150 and 2000 Hz tones results in an additional potential of 3.4 PNdB reduction with a resultant total decrement of 5.9 PNdB, as shown.

The last step is to include the directivity effect of the lobe nozzle having an aspect ratio of 4. Test data (ref. 1) shows that nozzles with similar aspect ratios and shapes are quieter when

measurements are made relative to the nozzle short axis. Therefore, it is reasonable to assume that we can add 2 dB suppression to the overhead reductions, and thus show a total reduction of 7.9 PNdB.

It should be noted that in tables 1 and 2 the PNLT values for a reduced throttle condition are firm. In table 3, however, the potential reductions shown for tone removal and directional effects require further testing and therefore should be considered risk items.

PERFORMANCE ANALYSIS

Hot Thrust Computations

All measured noise data presented here is compared on an equivalent hot thrust basis or a combination of hot and cold thrust. The hot thrust data is computed as a product of the fully expanded isentropic velocity, the measured primary mass flow, and a velocity coefficient:

$$F_G = C_V \cdot M_m \cdot V_J$$

The ideal jet velocity (V_J) is found as a function of the nozzle total pressure ratio, P_{T_8}/P_{AMB}, using conventional compressible flow relationships:

$$V_J = \sqrt{\frac{2\gamma g R T_T}{\gamma - 1}\left[1 - \left(\frac{P_S}{P_T}\right)^{\frac{\gamma - 1}{\gamma}}\right]}$$

where $P_S = P_{AMB}$.

Hot thrust could also be computed by knowing the discharge coefficient, C_D, of all the nozzles tested. The nozzle pressure ratio is solved by an iteration process—matching the measured mass flow rate, C_D and nozzle pressure ratio.

Figures 36-40 from Boeing reference documents show the desirability of computing thrust from the C_V method. They are model test data measured on test facilities with uniform and well-controlled entrance flow conditions.

Figure 36 shows the large sensitivity of C_D with nozzle 1/2 angle and nozzle pressure ratio. Figures 37 and 38 show the same trends but in addition show insensitivity to diameter ratio (D/d). Figure 39 shows the relative insensitivity of peak velocity coefficient (C_V) with nozzle 1/2 angle

and diameter ratio. Figure 40 shows the relative insensitivity of C_V with nozzle pressure ratio in the range of NPR = 1.2 to 2.4.

Accordingly, even with well-controlled nozzle entrance flow conditions the discharge coefficients can vary over a large range while the nozzle velocity coefficient is normally quite constant for conical nozzles. Consequently, the primary thrust from the present test program was computed using the C_V method.

The nozzle pressure ratios were measured by installing a four-probe total-pressure rake on each of the nozzles tested. The rakes were not installed to survey the nozzle exit pressure profiles. Instead they were positioned mainly in the center portion of the nozzles, away from the nozzle walls, to measure the nozzle supply total pressure. Normally, the total pressure in the central zone of a nozzle is essentially uniform. The nozzle exit total pressures measured on the conical and lobe nozzles are plotted on figure 41. Generally, the highest values of pressure distortion were measured with the larger conical nozzles with colander plate installed. The pressure data measured with the 1871-cm^2 (290-$in.^2$) lobe nozzle (run 18) indicates the existence of uniform velocity distribution except for the probe nearest the bottom of the lobe, which is most likely sensing a loss from nozzle wall boundary. Unfortunately, three of the four probe leads broke during run 22 due to severe vibration caused by the induced flow in the lobe secondary passages. Probe 4, which consistently indicated a lower value than the other three, was not used in the hot thrust or primary velocity computations. The maximum exit pressures measured with the conical nozzles were sensed by probes 1 and 2, as indicated in figure 41. The exit pressure data from runs 26, 27, and 28 indicate that total pressures measured by probes 1 and 2 are clearly higher than the pressure level sensed by probes 3 and 4. Consequently, the conical nozzle thrust values were computed using the pressures measured by probes 1 and 2, which were selected to represent the nozzle supply pressure.

The adjusted velocity coefficient (C_{VA}) used in the hot thrust computations for the conical nozzles (see fig. 45) was computed from the nozzle exit velocities, primary mass flows (run 28), and test bed primary thrust:

$$C_{VA} = \frac{\text{test bed primary thrust}}{M_{PRI} \cdot V_J}$$

For the three highest power settings the C_{VA} is within 1 percent of the value that normally would be selected (0.990-0.995) for a conical nozzle. Figure 42 shows the C_{VA} as a function of primary flow rate. It is not clear if this is the proper correlating parameter. The C_{VA} used for the lobe nozzle is shown adjusted down from conical nozzle level by 2 percent.

Figure 43 shows the estimated peak velocity coefficients for lobe-type suppressor nozzles as a function of the number of lobes and the lobe aspect ratio. The estimated C_V for the lobe nozzle, based on its aspect ratio and number of lobes, is 0.97, about 2 percent below the predicted conical nozzle level.

Nozzle Discharge Coefficient

The nozzle discharge coefficients (C_D = measured mass flow/ideal mass flow) were computed and are shown in figure 44. The C_D values are not involved in the hot thrust computations but are included to aid with the analysis. Normally, the larger conical nozzles would produce the highest values of C_D due to their small internal 1/2 angles (smaller vena contracta). The trend here is just the opposite, with the larger nozzles indicating very low C_D values. The 1807 cm^2 (280 $in.^2$) conical nozzles, with the most favorable contraction ratio (lowest entrance mach number) and most uniform pressure profiles, produce C_D values very close to those predicted for a nozzle of its 1/2 angle, as indicated in figure 44. The 1871-cm^2 (290-$in.^2$) lobe also produces C_D values close to those expected but indicates some exit area growth under increased temperature and pressure. The low C_D values for the larger conical nozzles indicate the presence of zones of flow separation or very low total pressure, which probably are not filling well. If separation exists with attendant base drag forces, then the actual hot thrust will be somewhat lower than that computed here. It is also noted that the C_D values are subject to more uncertainty when using limited nozzle pressure data and when pressure profiles are not uniform.

The 2290-cm^2 (355-$in.^2$) lobe nozzle also indicates low C_D values in figure 44. This is most likely due to the outer lobes, which were blocked for the 1871-cm^2 (290-$in.^2$) configuration not flowing full. Structural requirements for the outer lobes resulted in considerable blockage in these passages. This problem will be avoided in any flight nozzle by redesign of the internal struts in the outer lobes.

The discussion on discharge coefficients, above, has been restricted to the definition of discharge coefficient as it applies to a normal nozzle installation. With the nozzles attached to the split-flow plenum, a system discharge coefficient might better apply here. The low C_D values would then be attributable to the sharp turning angles in the elbow.

In summary, the hot thrust computations based on limited nozzle pressure instrumentation are approximate but are believed sufficiently accurate to be applied in a noise-thrust analysis. More uncertainty exists in computed hot thrust for the larger conical nozzles due to the more distorted flow conditions. As noted above, separated flow in the larger nozzles would result in thrust levels lower than the computed values presented here.

Performance Data Analysis

Table 4 lists the computed nozzle performance for all test nozzles except the 2290-cm^2 (355-$in.^2$) conical nozzle with colander plate removed. This configuration was not tested with the pressure rakes on due to time limitations. The hot thrust levels for this configuration are derived from an extrapolation of the 1807-cm^2 (280-$in.^2$) and 2045-cm^2 (317-$in.^2$) colander-out data, as shown in figure 45.

The hot thrust values (F_g) listed in table 4 are not corrected for ambient pressure as runs 24-28 were conducted with the barometer constant and the ambient pressures during runs 18 and 22 were only slightly different.

Figure 46 shows the computed hot primary thrust values plotted versus $N_L/\sqrt{T_1}$. The highest computed hot thrust level was produced by the 1807-cm^2 (280-$in.^2$) conical nozzle and the lowest was developed by the 2290-cm^2 (355-$in.^2$) conical nozzle, colander out. The 1871-cm^2 (290-$in.^2$) lobe nozzle, operating with an exit area of approximately 1936 cm^2 (300 $in.^2$), produces considerably lower thrust levels than the 1807-cm^2 (280-$in.^2$) conical. This is due mainly to the partially derated condition produced by the over-area lobe nozzle. The computed thrust levels for the 2290-cm^2 (355-$in.^2$) lobe nozzle are seen to be slightly higher than the baseline configuration 2290- cm^2 (355 $in.^2$) conical, colander in. This may be due to base drag forces in the test bed thrust levels and/or inability to measure accurately a representative nozzle supply total pressure from distorted pressure profiles.

The 2639-cm^2 (409-$in.^2$) and 2942-cm^2 (456-$in.^2$) conical nozzles, tested with colander plate installed, produced hot thrust levels significantly lower than the baseline configuration, as expected. Examination of the speed match data ($N_L/\sqrt{T_1}$ and $N_H/\sqrt{T_1}$) (see fig. 49) indicates that "true" derating occurs ($N_L/\sqrt{T_1}$ increases relative to $N_H/\sqrt{T_1}$) with the 2639-cm^2 (409-$in.^2$) nozzle. At this point the colander plate is fully choked, for the 2942-cm^2 (456-$in.^2$) nozzle produced no further change in the speed match characteristics. The lower hot-thrust level produced by the 2942-cm^2 (456-$in.^2$) nozzle reflects the increase in shock losses across the colander plate as the flow becomes supersonic. Extrapolation of the hot thrust levels beyond the highest power setting tested is done with some uncertainty.

Table 4 also shows the computed fully expanded jet velocities for all test configurations. The jet velocities are plotted versus $N_L/\sqrt{T_1}$ in figure 47. Except for the 2290-cm^2 (355-$in.^2$) conical nozzle, colander plate out, all jet velocities were computed from the nozzle exit total pressure measurements discussed above. The jet velocities for this configuration are derived from an extrapolation of the 1807-cm^2 (280-$in.^2$) and 2045-cm^2 (317-$in.^2$), colander-out data as shown in figure 48.

Over-Area Effects on Total Thrust Performance

To take advantage of any hot jet noise reduction from over-area nozzles (derating), particularly during approach, the noise levels were estimated for several primary nozzle areas ranging from 1807 cm^2 (280 $in.^2$) to 2942 cm^2 (456 $in.^2$). The example discussed below pertains to an over-area lobe nozzle—up to 2290 cm^2 (355 $in.^2$)—but the procedure applies to conical nozzles as well. An explanation of the procedure used in estimating the hot and cold (isentropic) thrusts follows.

A 1936-cm^2 (300-$in.^2$) cold-geometric lobe nozzle was selected to produce the same hot thrust versus $N_L/\sqrt{T_1}$ characteristic as the baseline nozzle, 2290 cm^2 (355 $in.^2$), colander in. Estimating an area growth to about 2000 cm^2 (310 $in.^2$) under operating conditions and accounting for lobe C_D levels somewhat greater than those of the 2045-cm^2 (317-$in.^2$) conical nozzles would produce an effective flow area close to that of the 2045-cm^2 (317-$in.^2$) nozzles. The speed match N_H versus N_L would then be identical to that produced by the 2045-cm^2 (317-$in.^2$) nozzles. With a 2 percent friction loss factor applied to the lobe 1936-cm^2 (300-$in.^2$) nozzle, the hot thrust versus $N_L/\sqrt{T_1}$ would be very close to that produced by the baseline configuration.

Hot and cold thrust are also shown for lobe-type suppressor nozzles of 1807 cm^2 (280 $in.^2$), 2194 cm^2 (340 $in.^2$), and 2290 cm^2 (355 $in.^2$). Figure 49 shows the speed match characteristics of the configurations examined. Figure 50 plots the computed hot thrust values versus $N_H/\sqrt{T_1}$. Figure 51 shows the computed cold isentropic thrust values versus $N_H/\sqrt{T_1}$.

In general, noise and thrust estimates were made at approach power (93% N_H) and a takeoff condition of 99% N_H. For approach, the N_L was selected from the speed match curve (fig. 49) for each primary nozzle area at a constant N_H, and the hot and cold thrusts were selected from figures 50 and 51. If excess cold thrust (lift) existed, compared to the baseline, the engine speed was "reduced" until the excess lift (compared to baseline) was approximately 1/4 the decrement in hot thrust. The noise values were then selected from the curves of noise versus hot thrust. In an attempt to identify the appropriate noise values with the thrust values and speed match points, circled letter-number codes are used on figures 49, 50, and 51 and the tabulated noise summary sheet, table 1.

For the takeoff case, a 99% N_H was selected and the appropriate N_L identified for each nozzle area from the speed match curves, figure 49, The N_L limit used in this analysis was arbitrarily selected as maximum continuous. The hot and cold thrusts were selected from figures 50 and 51 for the appropriate primary areas and N_H (99%) setting. The total thrusts (hot and cold) were then compared with the baseline total thrust value. If the total thrust was in excess of the baseline total thrust, the engine speed was reduced until the total thrusts were approximately equal. The noise level was then estimated from the curves of noise versus hot thrust.

The speed match characteristics in the above analysis are based on the conical nozzle tests and the appropriate primary areas. These primary areas represent the effective areas of the lobe-suppressor nozzles evaluated in this analysis.

CONCLUSIONS

The primary conclusions drawn from the noise tests are as follows:

a) The over-area conical nozzle concept demonstrates insignificant noise suppression at takeoff power, based on a comparable total thrust basis.

b) At approach power, 304-m (1000-ft) overhead, the over-area concept produces approximately 4 PNdB suppression based on a constant airplane lift.

c) At takeoff power (99% N_H) the lobe nozzle shows 5.2 PNdB reduction at 1216-m (4000-ft) overhead. At approach power at this distance, a reduction of 2.5 PNdB is shown; however, to show suppression at closer distances, an over-area configuration is required.

d) To use an over-area concept, which is acoustically effective, a variable area nozzle is required.

e) The lobe nozzle appears to create 2000- and 4000-Hz tones which limit suppression. If these tones can be removed, additional suppression of approximately 2 PNdB could be realized. (Magnitude of this suppression would depend on sideline distance and power setting.)

f) The directivity effect of the sound from a nozzle with a geometric configuration similar to the 13 lobe nozzle tested has shown an additional 2-dB reduction in the overhead (nozzle short axis) direction. If this is true, the lobe nozzle would demonstrate an addition 2-PNdB suppression if measured in an overhead location.

g) The engine bifurcated ("pants") section appears to create a low-frequency tone (150 Hz) which limits the suppression potential of the nozzles, especially over long distances.

h) Flap angle has a direct effect on the sound directivity from the nozzles.

i) Test results show that an engine case treatment would not appreciably change noise levels.

RECOMMENDATIONS

Our suggestions for further work in this program fall into five main categories, as follows:

a) Perform diagnostic static test on existing lobe nozzle (BNS-1)

1) Run test on a model facility, blocking approximately four lobes so that an airflow of 18.2 kg/sec (40 lb/sec) at 371 C (700 F) at 1.6 nozzle pressure ratio can be attained.

2) Determine source of 2000- and 4000-Hz tones by modifying the nozzle in logical steps to isolate the source.

3) Determine nozzle directivity effect using 11 lobes flowing at approximately 1.3 nozzle pressure ratio.

4) Define nozzle propulsion performance.

At this point, a decision must be made whether to go ahead with modifications to the existing BNS-1 nozzle or to design a new nozzle, BNS-2, with a target of 3 PNdB suppression more than BNS-1. This nozzle design would be based on the extra thrust available when the colander is removed or modified.

b) Modify existing lobe nozzle (BNS-1)

1) Make one flightworthy nozzle.

2) Retest on static rig for confirmation of tone absence and propulsion performance.

3) Fabricate three additional flightworthy nozzles.

4) Install on the airplane and ground static and flight test.

c) Develop new nozzle concept (BNS-2)

1) Design and fabricate one nozzle with a target of 3 PNdB suppression more than BNS-1.

2) Static test on Boeing facility to confirm tone absence and determine propulsion performance.

3) Test on full scale engine at engine overhaul.

4) Fabricate three nozzles to complete the airplane set.

5) Install on the airplane for static and flight test.

d) Develop "pants" section for low-frequency elimination

1) Design and fabricate various splitter concepts for the pants section.

2) Test full scale at engine overhaul.

e) Develop design for variable area lobe nozzle.

Boeing Commercial Airplane Company
P.O. Box 3707
Seattle, Washington 98124, May 15, 1974

APPENDIX A

TEST RUN LOGS

Run	Configuration	Condition	Nozzle and area, in.^{2}	Colander	Flap	Cage lining	Microphone array	Engine no.	Outside air temp, F°	Relative humidity, %	Wind azimuth, °	Wind velocity, mph	Wind gusts, mph	N_L rpm %	N_H rpm %	T_6	V_j ft/sec	P_s8	Orifice diameter, in.	$N_L\sqrt{T}$	Primary thrust, lb	Configuration description and comments
	Configuration Data							Atmospheric						Engine Data								
4	9	1	con	280	out	up	no	A	1	59.9	90.6	10	4	1	55	85	390		17.3	2.99			Close-up microphones will be referred to as 10 for the forward unit and 20 for the aft. Runs 1, 2 and 3 are propulsion, airplane pointed north. Run 104 is ambient with auxiliary power cart running.
4	9	2	con	280	out	up	no	A	1	60.1	90.5	10	4	0	60	86.3	370		18.0	2.99			
4	9	3	con	280	out	up	no	A	1	60.2	90.4	0	4.2	0	70.2	89	375	1323	19.6	2.99	392.4	3360	
4	9	4	con	280	out	up	no	A	1	60.5	90.3	0	4.5	1	78	92.2	410	1480	22.7	2.99	415.7	4260	
4	9	5	con	280	out	up	no	A	1	61.0	90.3	20	4.0	1	89	95.5	470	1724	27.5	2.99	449.2	5730	
4	9	6	con	280	out	up	no	A	1	61.1	90.1	10	4.5	1	99	100.3	570	1971	32.5	2.99	481.2	7230	
104	9	1	con	280	out	up	no	A	1	60.1	90.7	0	5.5	2	–	–	–	–	–	–			Ambient taken prior to run 4
105	10	1	con	317	out	up	no	A	1	61.7	87.3	340	3.0	0	–	–	–	–	–	–			Ambient prior to run 5
5	10	1	con	317	out	up	no	A	1	62.8	83.4	340	3	0	79.5	90.5		1152		4.2	401.2	2880	No engine match prior to this run
5	10	2	con	317	out	up	no	A	1	63.6	83.5	20	4	2	88.8	93.8		1442		4.2	446.7	4630	
5	10	3	con	317	out	up	no	A	1	62.2	83.1	340	5	1	96.2	96.6		1691		4.2	4826	6030	
106	11	1	lobe	288	out	up	no	B	1	72	67	20	6	+2	–	–	–	–	–	–			Pre-run ambient.mic 135 now at 20 loc Mic 145 now at 10 loc close up Engine match no good
6	11	1	lobe	288	out	up	no	B	1	72	67	20	6	2	78.9	91.0	395		21.6	4.2			
6	11	2	lobe	288	out	up	no	B	1	69	66	20	6	0	90.7	94.7	438		25.5	4.2			
6	11	3	lobe	288	out	up	no	B	1	66	70	20	4	+3	96.4	96.5	465		26.5	4.2			
107	1	1	con	355	in	up	no	B	2	59.3	88.4	350	1	0	–	–	–	–	–				Ambient run 7 aborted, truck ran over 3 mics 10 and 20 nearfield mics were put on 100' S/L as no spares were available * no data at 135 and 145 Amb 108 taken prior to run 8 weather cond's for amb are same as cond 1
7	1	1	con	355	in	up	no	B	2	59.3	88.4	0	0	0	–	–	–	–	–				
8	1	1	con	355	in	up	no	B*	2	59.7	87.6	250	2	0	45.2	80.2	400			–			
8	1	2	con	355	in	up	no	B	2	59.4	87.5	330	3	0	69.0	86.7	355			–	345.9	–	
8	1	3	con	355	in	up	no	B	2	59.3	87.5	0	0	0	82.5	91.0	408	1180		–	409.7	3080	
8	1	4	con	355	in	up	no	B	2	59.4	87.6	0	0	0	86.3	92.7	418	1308		–	429.4	3790	
8	1	5	con	355	in	up	no	B	2	60.1	87.6	0	0	0	91.8	94.8	485	1486		–	455.6	4810	
8	1	6	con	355	in	up	no	B	2	60.0	87.5	0	0	0	98.9	99.0	565	1734		–	489.8	6280	
9	2	1	con	355	in	30	no	B*	2	59.6	87.1	0	0	0	78.6	90.9	390	1062		–	390.5	2470	Engine was not shut down between runs 8 and 9 100% NL=8393 RPM 100% NH=12135 RPM
9	2	2	con	355	in	30	no	B	2	59.9	87.0	0	0	0	91.5	94.7	480	1472		–	453.4	4730	
9	2	3	con	355	in	30	no	B	2	60.5	87.1	0	0	0	98.8	98.9	555	1725		–	488.5	6230	
11	3	1	con	355	in	50	no	B*	2	60.7	83.0	320	1	0	81.5	91.0	412	1135		–	402.5	2860	Jitney ran over mic at 150 -engine shut down Run 10 aborted amb 111 taken prior to run 11 Traffic on road behind acoustic van during data recording
11	3	2	con	355	in	50	no	B	2	61.0	82.7	300	1	0	92.1	95.0	494	1471		–	453.3	4730	
11	3	3	con	355	in	50	no	B	2	61.2	82.3	350	1	0	98.8	99.0	558	1691		–	484.8	6060	
112	5	1	con	405	in	up	no	B*	2	60.7	89.1	100	1	0	–	–	–	–	–	–			Amb112 taken prior to run12. The 60 and 20 mics were out for this run mic array "*B"was chosen for this run so that additional info could be obtained on tone generation
12	5	1	con	405	in	up	no	B	2	61	88	100	3	0	85								

Engine over area, shut down for bleed modifications

Run	Configuration	Condition	Nozzle area, in.^{2}	Colander	Flap	Case lining	Microphone area§	Engine no.	Outside air temp, °F	Relative humidity, %	Wind azimuth, °	Wind velocity, mph	Wind gusts, mph	N_L, rpm %	N_H, rpm %	T_6	V_j, ft/sec	P_{t8}	Orifice diameter, in.	$N_L\sqrt{T}$	Primary thrust, lb	Configuration description and comments
Configuration Data								Atmospheric						Engine Data								
115	12	1	lobe	290	out	up	yes	B	1	59.8	79.8	0	3	0	–	–	–	–	–	–			
15	12	1	lobe	290	out	up	yes	B	1	60	80	10	3	0	44.8	79.0	390		16.4	3.6			Engine shut down in daft portion of blanket blew off.
15	12	2	lobe	290	out	up	yes	B	1	60	79	30	5	0	69.7	87.1	352	970	19.0	3.6	350.8	1980	Run 17 will be run in mixed up order. Watch the cond.
17	12	1	lobe	290	out	up	yes	B	1	63	71	30	4	0	88.9	94.0	437	1507	25.2	3.6	444.9	4860	to power setting ID. Run 16 aborted-loose blanket
118	11	1	lobe	290	out	up	no	B	1	66	71	0	6							3.6			
18	11	1	lobe	290	out	up	no	B	1	65	71	0	5		44.9	79.1	386		16.5	3.6			
18	11	2	lobe	290	out	up	no	B	1	65	71	0	6		70.2	88.0	355	976	19.2	3.6	352.1	2000	118 pre-run amb. Generator truck was
18	11	3	lobe	290	out	up	no	B	1	66	73	20	5		84.0	92.5	400		23.2	3.6		3970	moved further away from mics than for
18	11	4	lobe	290	out	up	no	B	1	65	71	0	7		88.9	94.2	433	1507	25.2	3.6	444.7	4870	previous runs.
18	11	5	lobe	290	out	up	no	B	1	64	71	0	3		97.7	98.1	490	1772	29.0	3.6	489.2	6530	
19	6	1	con	455	in	up	no	A	2	59	81	100	2	0	71.1	86.8	340	–	15.8	none			Nozzle was at a 12 down angle instead of normal 6 for
19	6	2	con	455	in	up	no	A	2	58	81	100	3	0	82.5	90.4	380	–	16.7	*			this run. Shut down due to engine match.
19	6	3	con	455	in	up	no	A	2	59	81	80	3	0	89.0	92.8	430	–	17.9				*Body blowing ducts on
120	6	1	con	455	in	up	no	A	2	59	83	280	3	0									
20	6	1	con	455	in	up	no	A	2	59	83	0	2	0	82.2	90.6	380	932	16.4	4.2	409.8	2330	Body blowing duct disconnected and fan
20	6	2	con	455	in	up	no	A	2	59	83	50	2	0	89.0	92.9	425	1144	17.8	4.2	443.8	3450	bleed installed with 4.2" dia orifice
20	6	3	con	455	in	up	no	A	2	58	83	0	0	0	97.9	97.5	520	1150	20.0	4.2	487.1	5060	
21	5	1	con	409	in	up	no	A	2	60	83	250	2	0	82.2	90.9	395	1008	17.0	4.2	410	2590	
21	5	2	con	409	in	up	no	A	2	59	83	250	2	0	89.0	93.1	435	1215	18.5	4.2	443.4	3690	
21	5	3	con	409	in	up	no	A	2	60	83	250	3	0	97.9	97.5	320	1524	21.0	4.2	486	5320	
121	5	1	con	409	in	up	no	A	2	60	83	250	4	0	–	–	–						Ambient
22	7	1	lobe	355	in	up	no	A	2	62	70	300	2	1	82.2	91.4	420	1198	19.0	2.99	401.8	2600	
22	7	2	lobe	355	in	up	no	A	2	62	70	250	4	0	89.1	93.8	470	1433	21.3	2.99	436.5	3970	
22	7	3	lobe	355	in	up	no	A	2	62	70	280	3	1	94.7	96.4	520	1618	23.3	2.99	4632	5150	
22	7	4	lobe	355	in	up	no	A	2	63	70	250	5	0	97.6	98.6	550	1707	25.3	2.99	478	6010	
122	7	1	lobe	355	in	up	no	A	2	63	70	200	7	0	–	–	–		–	–			
23	14	1	con	355	out	up	no	A	1	65	76	340	4	1	45.1	79.2	380		16.0	5.51			
23	14	2	con	355	out	up	no	A	1	66	76	20	8	0	60.2	86.0	340		18.7	5.51			
23	14	3	con	355	out	up	no	A	1	67	76	0	8	0	70.0	87.0	330		17.5	5.51			
23	14	4	con	355	out	up	no	A	1	67	76	40	4	0	82.0	90.7	353	970	19.1	5.51	409.8	2420	Bleed valve still open
23	14	5	con	355	out	up	no	A	1	66	76	350	8	0	88.8	92.9	375	1155	20.8	5.51	443	3550	
23	14	6	con	355	out	up	no	A	1	66	76	20	8	1	97.5	98.7	408	1410	23.5	5.51	486.6	4900	
123	14	1	con	355	out	up	no	A	1	66	76	0	8	0	–	–	–		–	–			
																							Ambient

APPENDIX B

ORIGINAL TEST PLAN

The Boeing Airplane Company will conduct a static acoustic test program on the Buffalo/Spey MK 801 SF engine installation on the Modified C8A AWJSRA (Augmentor Wing Jet STOL Research Aircraft). The test program will combine the objectives of acquiring full scale exploratory noise data, with and without the colander plate, along with examining the noise reduction potential by engine derating (hot nozzle area increase) and the use of lobe-type suppressor nozzles. The output will be to determine the noise reduction potential and cost trades for this experimental airplane (AWJSRA). This program will be closely coordinated with deHavilland Aircraft Limited of Canada.

Testing will be accomplished at NASA Ames on the C8A Buffalo airplane. The aircraft will be situated to minimize wind effects, and such that no buildings or large structures are within 500 ft.

The acoustic microphone array will consist of 12 one-half inch microphones located along a 100-ft sideline from the engine centerline, and one-half inch above the ground surface (see figs. B-1 and B-2). Two one-half inch microphones will be located 10 ft from the engine centerline, as shown on figure B-1, for a close-in evaluation of the engine case blanket. An IRIG time code will be recorded on the tape simultaneously with the acoustic data.

Microphone calibration on-site will consist of piston phone calibrations prior to and following each test run. The complete acoustic data recording system will have laboratory calibration consistent with existing procedures, and traceable to the National Bureau of Standards.

The acoustic data reduction will be accomplished in 1/3 octave bands with center frequencies of 50 Hz through 10 kHz. Data presentation will be in 1/3 octave, OASPL, PNL, PNLT with selected configurations analyzed with narrow band data. The PNL and PNLT values will be shown for the sideline distances necessary to evaluate the result of the noise suppression on the community. The data reduction instrumentation will be calibrated per existing procedures and traceable to the National Bureau of Standards.

Prior to recording data, the wind, temperature, and humidity must be within the limits shown on figure B-3. Regular checks of these parameters are required during a test run.

The data will be recorded on 1 in. magnetic tape, FM mode at a record speed of 30 in. per second. All gain settings will be verbally recorded on the tape as well as written in the run log. Forty-five seconds of data will be recorded at each engine power condition.

TEST PROCEDURE

1. Start the engine and allow warm-up time as required.

2. Advance throttle until test condition 1 is reached, at which time a clock will be started and no further changes in the throttle position will be made.

3. At 1 minute on the clock, acoustic recording will begin. (Gain settings will have been established during the 1-minute stabilization period.) A total record time of 45 seconds is required. Propulsion data (engine parameters) will be recorded during the same time period.

   Having received a "Data Complete" from both acoustics and propulsion, the throttle will be advanced to the second condition and the same procedures followed. Condition 3 will also follow the same procedure.

4. Atmospheric conditions (wind speed, direction, relative humidity, and outside air temperature) will be recorded manually during the period from 1 minute to 1 minute and 45 seconds.

5. Engine power settings will be controlled to target N_H (high pressure compressor rotor speed, uncorrected) for nozzle configurations producing matched operating conditions.

   For over-area nozzle configurations producing unmatched operating conditions, N_L (low pressure compressor rotor speed) will be used. The N_L for the over-area nozzles will be set to the same value as that which occurred during match nozzle testing.

   For over-area testing, the throttle must be advanced slowly and constant monitoring of the vital engine parameters maintained so that no operating limits are exceeded.

6. Figure B-4 shows the case lining installation for the case radiated noise evaluation.

   Table B-1 lists the test configurations, microphone location requirements for the test program.

   This test plan has been developed using the ground rule of expending the very minimum amount of engine run time.

TEST HARDWARE

The lobe nozzle (BNS-1, see fig. B-5) for this test will be a 13 lobe, array area ratio of 2.2. One engine set of lobe nozzles will be constructed with a geometric exit area of 2387 cm^2 (370 $in.^2$). This area is designed oversize and will be blocked to provide a match flow area with the colander plate installed.

When tests without the colander plate are run, approximately 516 cm^2 (80 $in.^2$) of the nozzle exit plane will be blocked off.

Engine matching procedures, operating limits, and instrumentation will be established at a later date, following contacts with deHavilland, Rolls Royce, and NASA.

The engine case treatment (fig. B-4) consists of two layers of lead-loaded vinyl (0.48 lb/ft^2) with 1.5-in. fiberglass blanket (1.5 lb/ft^3) sandwiched between the lead vinyl.

Boeing will design and fabricate the lobed nozzles, as well as the engine case treatment. Specifications for the nozzle design have been transmitted to the Propulsion Laboratory Design Group.

Specifications for the engine case treatment are shown below and the materials will be ordered by the Propulsion Laboratory. This is a preliminary test plan, updating, as required, will be accomplished following contacts with deHavilland, Rolls Royce, and NASA.

Engine Case Treatment Specifications

Lead Vinyl (Lead-Loaded Vinyl)

Manufacturer: Ferro Composites Corporation
Weight: Approximately 0.5 lb/ft^2
Required: 600 ft^2

Fiberglass Filled Blankets

Fiberglass BMS 8-48 1.5-in. thick at 1.5 lb/ft^3
Blanket covering: Orcon fabric BMS 8-142 Type I
Make blankets in Boeing interior shop per sketch.

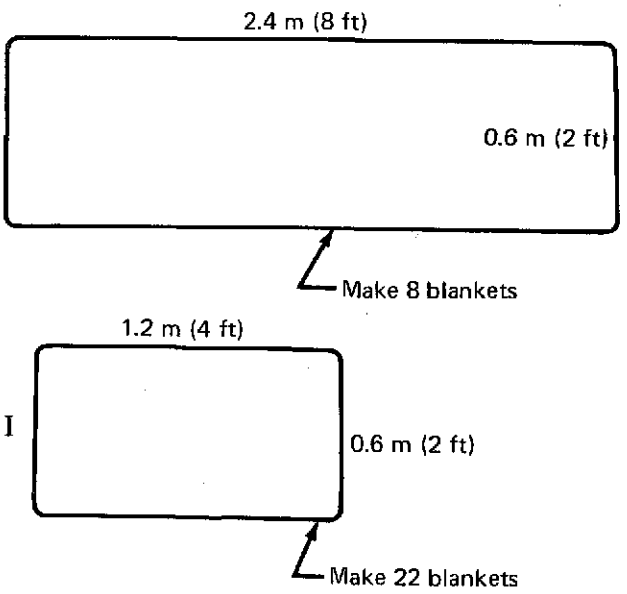

TABLE B-1—CONFIGURATIONS FOR TEST PROGRAM

Config	Primary nozzle	Approx geometric exit area cm^2 ($in.^2$)	Case lining installed	Microphone array	Colander plate installed	Augmentor flap position
1	conical	2290 (355)	no	B	yes	up
2	conical	2290 (355)	no	A	yes	30
3	conical	2290 (355)	no	A	yes	60
4	conical	2290 (355)	yes	B	Yes	up
5	conical	2613 (405)	no	A	yes	up
6	conical	2936 (455)	no	A	yes	up
7	lobe	2290 (355)	no	B	yes	up
8	lobe	2290 (355)	yes	B	yes	up
9	conical	1807 (280)	no	A	no	up
10	conical	2290 (355)	no	A	no	up
11	lobe	1871 (290)	no	B	no	up
12	lobe	1871 (290)	yes	B	no	up

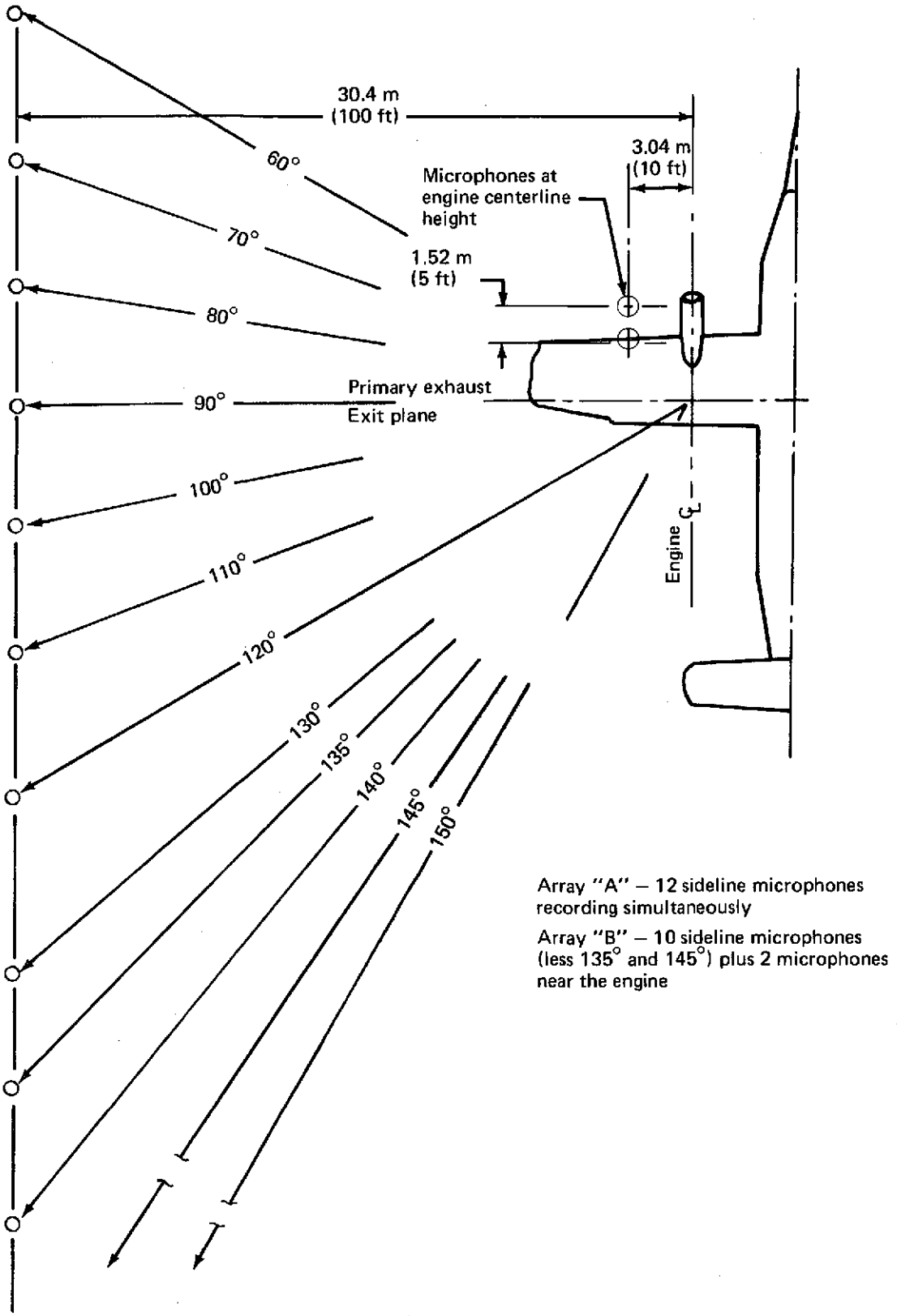

FIGURE B-1.–MICROPHONE ARRAYS

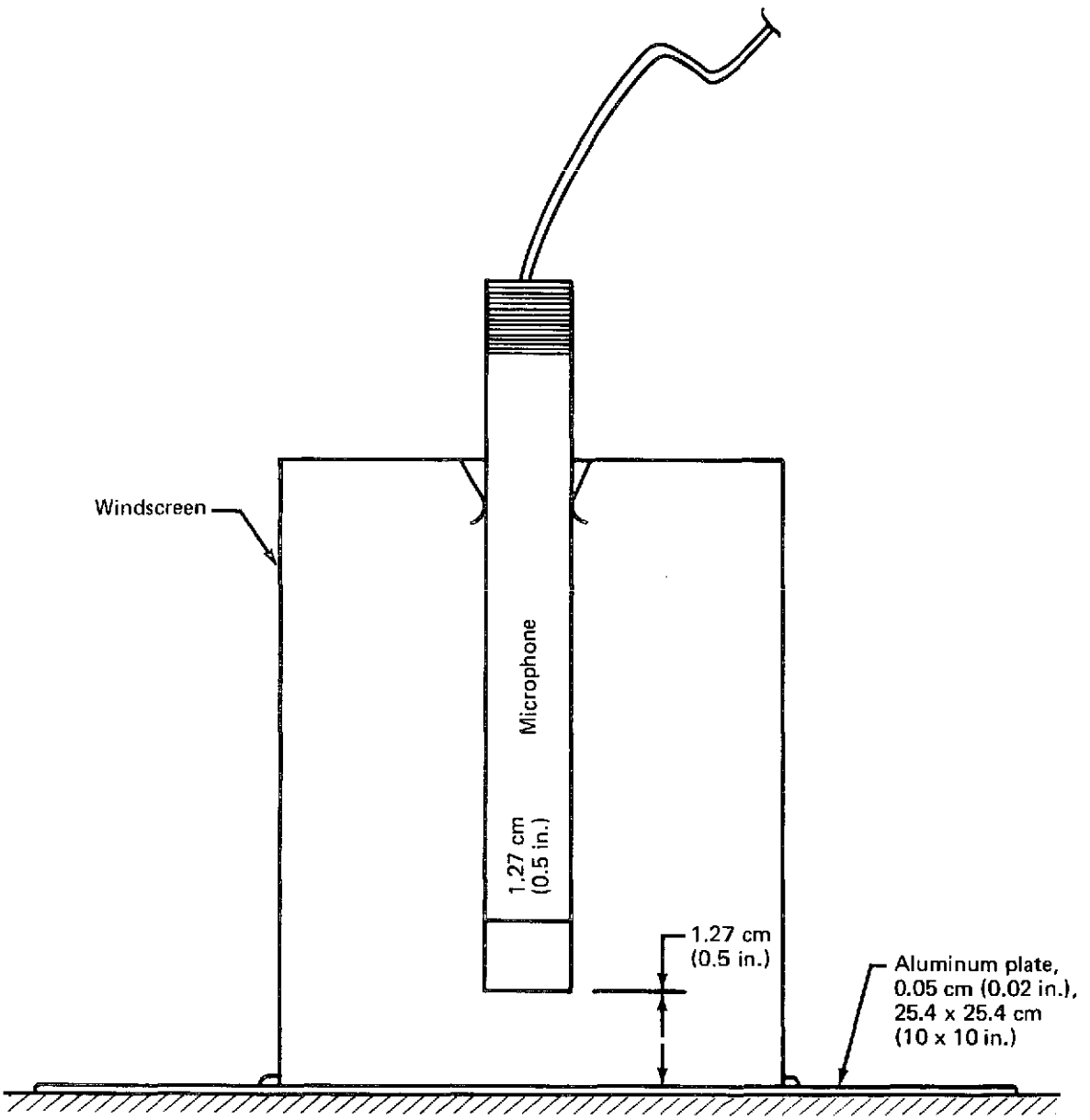

Use of ground microphones per Boeing document D6-40330, *Use of Ground Level Microphones to Acquire Static Free Field Data.*

FIGURE B-2.—TYPICAL MICROPHONE INSTALLATION

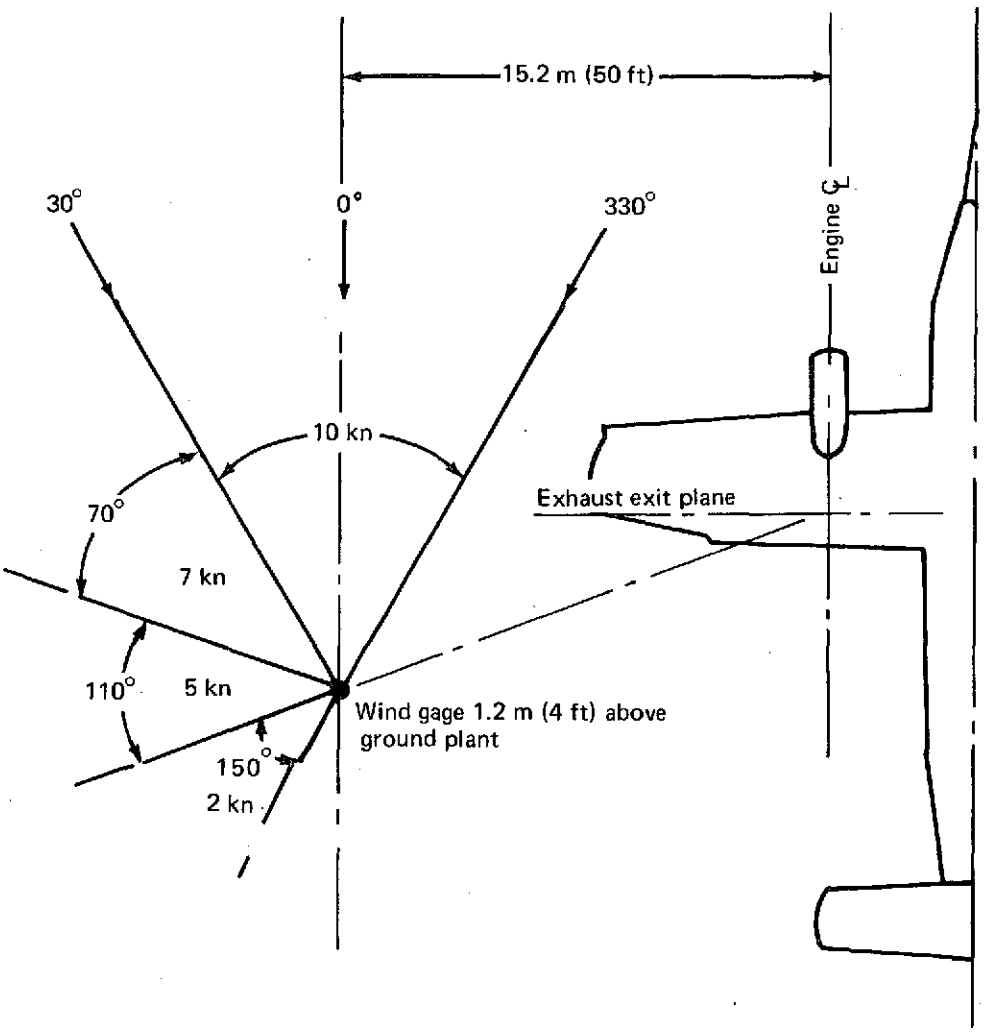

Wind vector as shown
Humidity, 30% to 90%
Temperature, 0° to 32.2° C (32° to 90° F)

FIGURE B-3.–TEST LIMITS, WEATHER

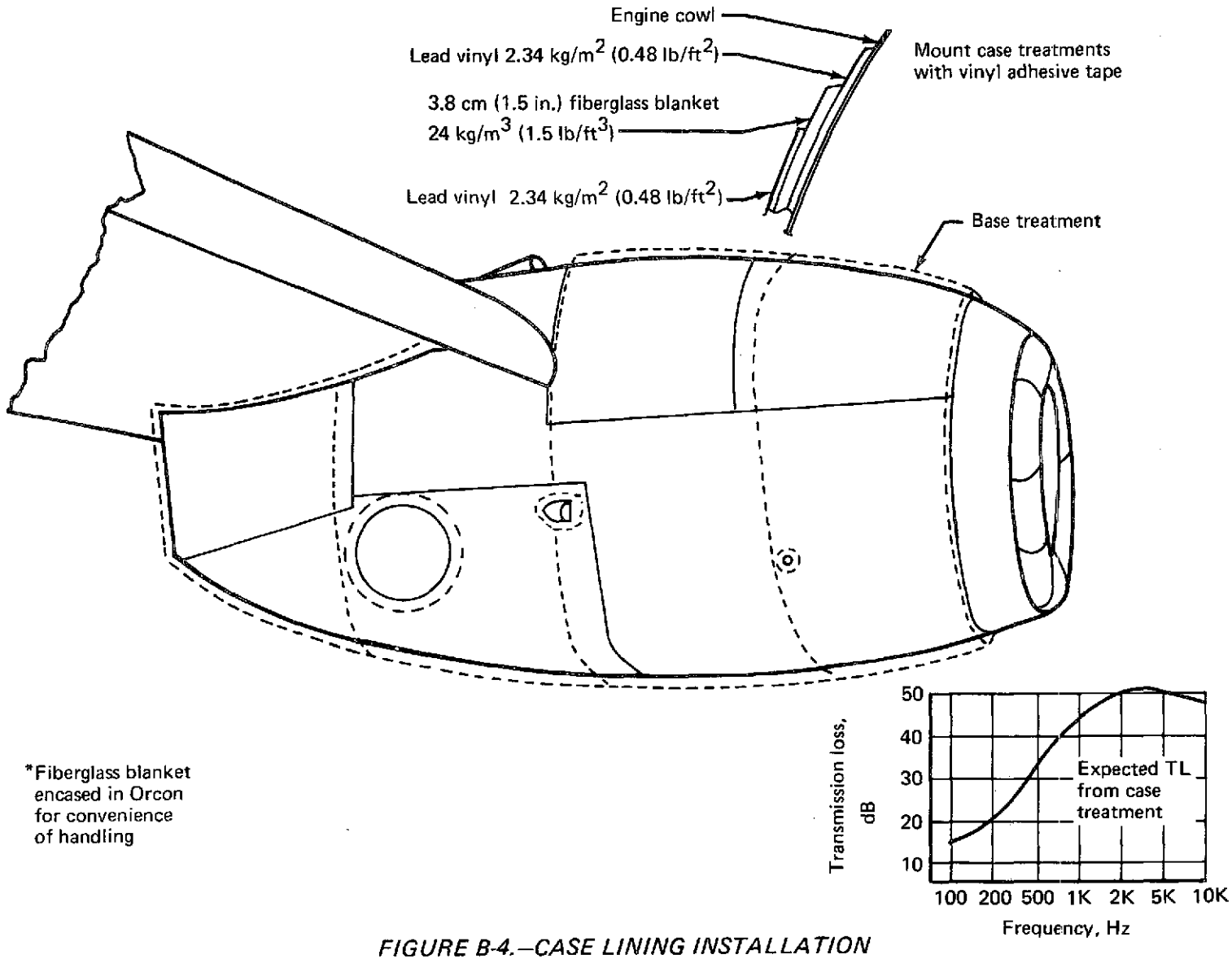

FIGURE B-4.—CASE LINING INSTALLATION

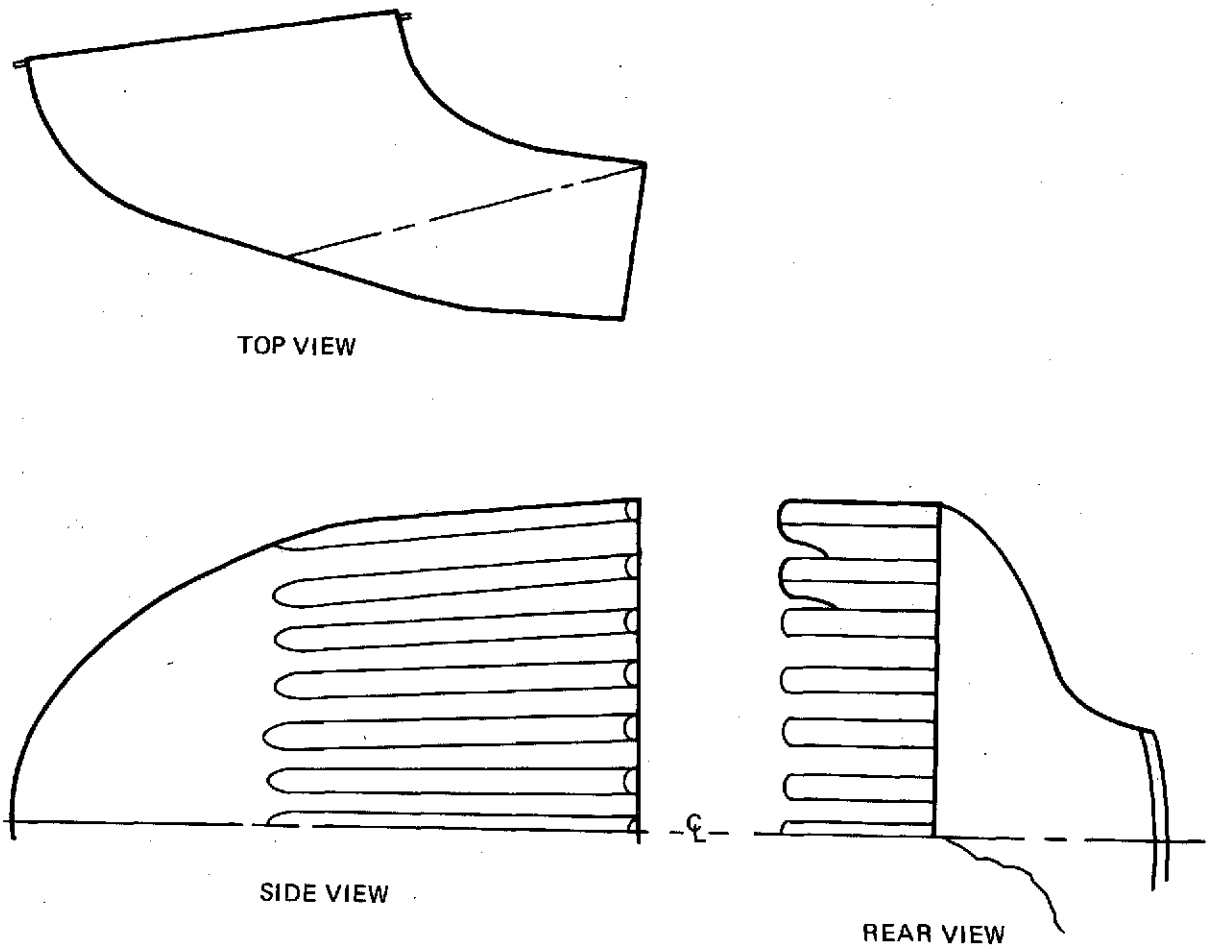

FIGURE B-5.–13 LOBE NOZZLE BNS-1

APPENDIX C

ACOUSTIC DATA RECORDING AND REDUCTION SYSTEMS

ACQUISITION SYSTEM CALIBRATION

Two types of calibration are performed on the data acquisition system prior to recording test data. The first determines the frequency response of the microphone, preamplifier, cables, and signal conditioning equipment. This is performed before and after each test, using the electrostatic actuator method illustrated in figure C-1. The sweep oscillator frequency is referenced to an electronic counter, certified and calibrated by the Boeing Flight Test Laboratory. Said laboratory maintains test standards, references, and equipment with calibration accuracy traceable to the U.S. Bureau of Standards. When the frequency response of the system relative to 250 Hz has been determined, corrections are computed for each 1/3 octave band and applied to the data during reduction to obtain true SPL in dB.

The second calibration is an end-to-end sensitivity check performed each day before and after a test. An acoustic piston phone calibrator with a constant, known SPL at 250 Hz is applied to each microphone, and the calibrator signal is recorded on magnetic tape. This reference is used during the data reduction process to determine system sensitivity. The device used, a Bruel & Kjaer model 4220 piston phone, has a certification traceable to the U.S. Bureau of Standards through a secondary standard maintained by the Boeing Metrology Laboratory.

The tape recorder and reproducer is not included in frequency response calibrations performed in the field. The tape machines are tested and certified by the Boeing Flight Test Laboratory for a flat frequency response when operated in the FM mode. Response at 30 in./sec is flat from dc to 10 kHz.

ACQUISITION PROCEDURES

All microphones are calibrated for sensitivity after they have been placed in the physical configuration that is to be used for data acquisition. The noise floor of each channel is then determined and recordings made prior to the engine test runs. The noise floor of the B & K 1/2-in. microphone systems used for this test are on the order of 10 to 15 μV electrical output, equivalent to 32 to 37 dB SPL overall. The recorded noise floor, however, contains both electrical noise floor and acoustic ambient background noise. The latter usually dominates the noise floor recordings, particularly at frequencies below 1000 Hz.

Data recordings are made for 45 seconds during a stabilized engine thrust setting. The tape-recorded sample includes voice identification and an IRIG 'B' time code reference on track 14. A written tape log includes:

Run identification
Gain settings used for recording each condition
Time code at the start of the recording
Equivalent SPL of the calibration signal
Date, engineer, and serial numbers of recording equipment and microphones.

Figure C-2 shows a typical data channel used to record engine noise for the Jet STOL Static Noise Test.

TEST DATA

Forty-six test conditions were recorded at NASA Ames Research Center, Mountain View, California during the period of July 20, 1973 to August 2, 1973. Tapes were transported to Seattle to the Acoustics Laboratory Data Reduction Facility for processing. All data were analyzed in 1/3 octave bands from 50 Hz to 10 kHz with a 16-second integration time. Corrected SPL values for each 1/3 octave band were output on IBM cards for entry into the CDC 6600 computer for further processing.

DATA REDUCTION SYSTEM

The basic data reduction system consists of an analog tape recorder, a 1/3 octave spectrum analyzer, card punch, time code reader, and associated control and interface circuitry.

The basic equipment is identified in figure C-3 and listed below.

Item	Manufacturer/model
Analog magnetic tape recorder	Ampex/1800L
Spectrum analyzer	General Radio/1921
Card punch	IBM/526
Time code reader	EECO/851A
Card punch interface	Boeing
Oscilloscope	Tektronix/RM503

Item	Manufacturer/model
RMS voltmeter	Fluke/910AR/Z
Noise generator	Allison/650-R
Oscillator	Bruel & Kjaer/1014

Previously recorded data tapes are reproduced on an analog magnetic tape recorder in the FM mode and fed to the system input. The analyzer breaks the overall signal down into a 1/3 octave band spectrum from 50 Hz to 10 kHz, converting each 1/3 octave level into SPL dB in a digital form. This value is transferred to the IBM card punch through the card punch interface. The punched cards are used in the CDC-6600 computer for follow-on computations.

The operator controls the calibration process, start time, sample length, and record gain compensation. Run identification, microphone location, and test condition are entered through the card punch keyboard. System response corrections are entered in the CDC-6600 program.

The General Radio 1921 spectrum analyzer includes a bank of 24 parallel 1/3 octave band filters. These filters meet the requirements of International Standard IEC 225 and USA Standard S1.11-1966 Class III, and have center frequencies of 50 Hz to 10 kHz.

The output of each filter is fed into a digital detector whose output is the true RMS value of the input signal. The resolution of the analyzer is 0.25 dB.

REDUCTION SYSTEM CALIBRATION

Electrical checkout is accomplished by inserting sine wave frequencies and voltages from the B&K oscillator, and random noise from the Allison generator. Output data are compared with the known input levels and used as a guide for correction action.

The square law characteristics of the G.R. analyzer were verified by inserting two sine waves as per IEC 179, Para. 8.5. The required 3 dB attenuation was read out on an H.P. 3400 RMS voltmeter.

All components of the reduction system were certified to manufacturer's specifications by the Flight Test Calibration Laboratory.

DATA REDUCTION PROCEDURE

Prior to actual data reduction of acoustic recordings, the following checks were performed:

a) All equipment was visually inspected.

b) Random noise was used for functional checkout of the analog tape playback, analyzer, and card punch.

Actual data reduction was performed in the following manner:

a) An end-to-end calibration signal on the analog tape was played back and the analyzer system adjusted for direct reading in SPL.

b) All identification information was entered on the cards through the keyboard.

c) The desired data sample to be analyzed was located on the analog tape using the IRIG time signals and voice announcements.

d) After entering the record gain into the card interface, the operator started the analog tape and initiated the start of a 32-second integration of the data sample.

The G.R. analyzer, after completing the analysis, automatically transferred the stored data through the interface onto IBM cards.

e) The completed data was sorted by condition and processed through the CDC-6600 computer for further computations.

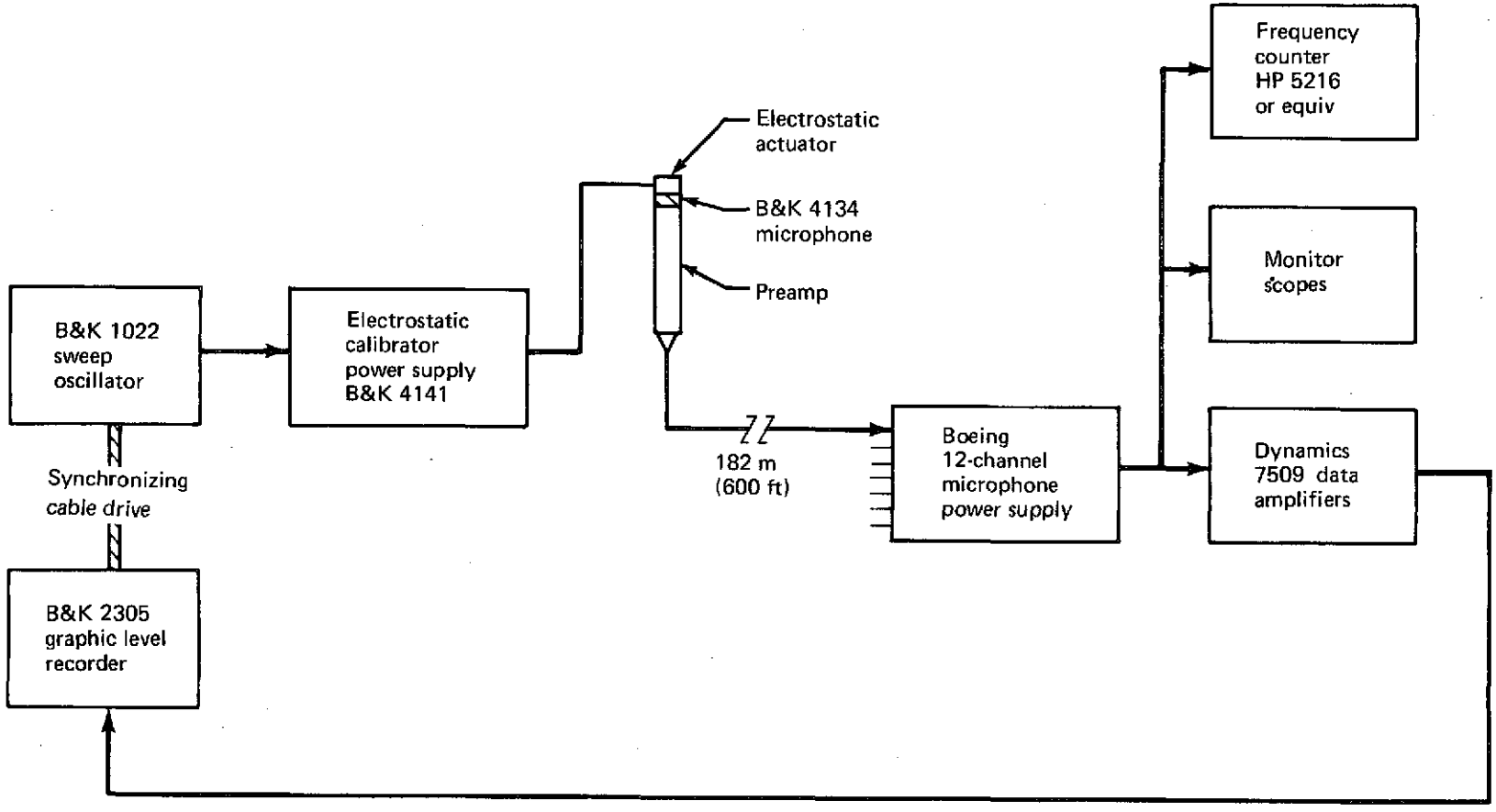

FIGURE C-1.–STATIC NOISE TEST CALIBRATION METHOD, AUGMENTOR WING-JET STOL

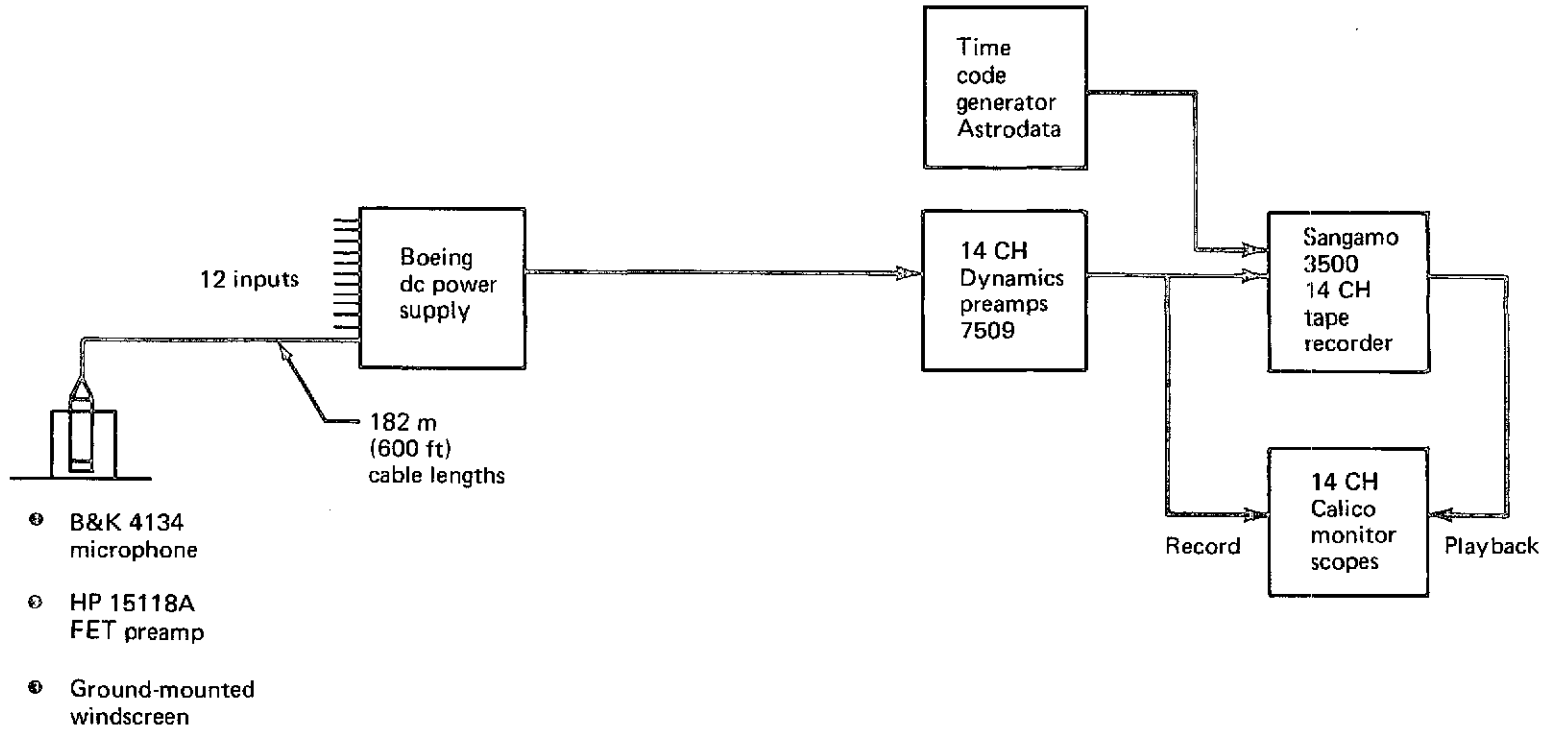

FIGURE C-2.—TYPICAL ENGINE-NOISE DATA CHANNEL

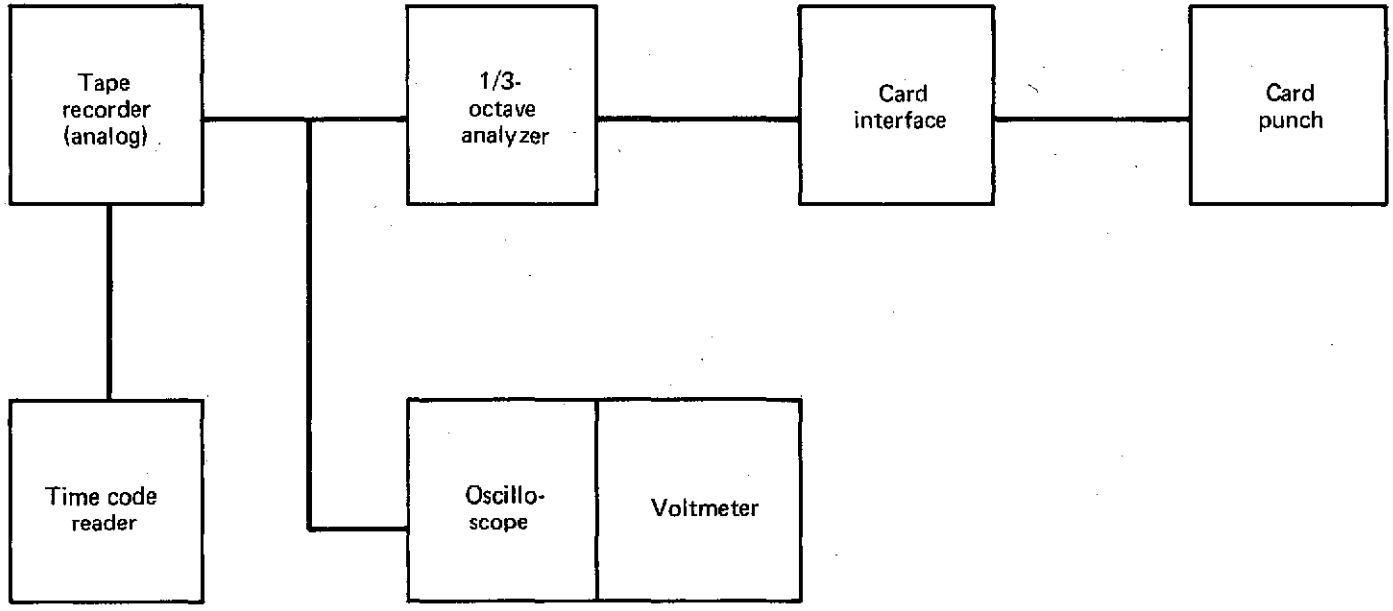

FIGURE C-3.–ACOUSTIC DATA REDUCTION SYSTEM

REFERENCES

1. Tyler, John M.; Sofrin, Thomas G.; and Davis, Jack W.: Rectangular Nozzles for Jet Noise Suppression. Presented at SAE National Aeronautic Meeting, March 1959.

2. Thornock, R.L.: Experimental Investigation of Flow Through Convergent Conical Nozzles. Boeing document D6-20375, March 1968.

3. McClung, C. D.: Parametric Test of Conical Convergent Nozzles. Boeing document T6-5614-1, June 1970.

4. Postlewaite, J. E.: Thrust Performance of Suppressor Nozzles. Journal of Aircraft, 1966.

TABLE 1—LOBE NOZZLE OVERAREA EVALUATION

Colander	Primary area, m (in.^{2})	Approach						Takeoff					
					PNLT, dB						PNLT, dB		
		F_g, kg (lb)		$N_L/\sqrt{T}$ $N_H/\sqrt{T}$	Alt 76 m (250 ft)[a] SL 152 m (500 ft)[b]	304 m (1000 ft)[c]	1216 m (4000 ft)[c]	F_g, kg (lb)		$N_L/\sqrt{T}$ $N_H/\sqrt{T}$	Alt 76 m (250 ft)[a] SL 152 m (500 ft)[b]	304 m (1000 ft)[c]	1216 m (4000 ft)[c]
		Hot	Cold					Hot	Cold				
In[d]	2290 (355)	1780 (3930)	1223 (2700)	433 655 (A1)	120.8	114.4	95.5	2818 (6220)	1536 (3390)	488 708 (T1)	127.2	121.2	102.2
Out	1807 (280)	2061 (4550)	1110 (2450)	433 (A2) 665	122.0	116.6	94.2	3307 (7300)	1404 (3100)	489 (T2) 708	–	–	–
Out	1807 (280)	–	–	–	–	–	–	3035 (6700)	1336 (2950)	467 696 (T3)	123.7 Throttle back	117.0	97.0
Out	1936 (300)	1866 (4120)	1246 (2750)	438 (A3) 665	120.5	115.0	93.0	3099 (6840)	1631 (3600)	500 (T4) 705	123.5	117.0	97.0
Out	1936 (300)	–	–	–	–	–	–	2822 (6230)	1540 (3400)	488 695 (T5)	124.3 Throttle back	118.0	97.0
Out	2194 (340)	1758 (3880)	1309 (2890)	445 (A4) 665	119.4	113.7	92.0	2673 (5900)	1690 (3730)	500 (T6) 637	124.3	118.2	96.8
Out	2194 (340)	1608 (3550)	1246 (2750)	435 660 (A5)	118.0 Throttle back	112.0	90.8	–	–	–	–	–	–
Out	2290 (355)	1667 (3680)	1382 (3050)	452 (A6) 665	118.5	112.8	91.2	2437 (5380)	1735 (3830)	500 (T7) 692	124.0	118.3	96.0
Out	2290 (355)	1486 (3280)	1291 (2850)	439 659 (A7)	117.1 Throttle back	110.6	89.3	–	–	–	–	–	–

Note: Numbers in circles correspond to data in figures 49-51.

[a] Altitude
[b] Sideline
[c] Overhead
[d] Conical nozzle

TABLE 2–CONICAL NOZZLE OVERAREA EVALUATION

Colander	Primary area m (in.^{2})	Approach						Takeoff					
					PNLT, dB						PNLT, dB		
		$F_{g'}$ kg (lb)		$N_L/\sqrt{T}$ $N_H/\sqrt{T}$	Alt 76 m (250 ft)[a] SL 152 m (500 ft)[b]	304 m (1000 ft)[c]	1216 m (4000 ft)[c]	$F_{g'}$ kg (lb)		$N_L/\sqrt{T}$ $N_H/\sqrt{T}$	Alt 76 m (250 ft)[a] SL 152 m (500 ft)[b]	304 m (1000 ft)[c]	1216 m (4000 ft)[c]
		Hot	Cold					Hot	Cold				
In	2290 (355)	1780 (3930)	1223 (2700)	433 665	120.8	114.4	95.5	2818 (6220)	1536 (3390)	488 708	127.2	121.2	102.2
Out	1807 (280)	2102 (4640)	1110 (2450)	433 665	122.1	116.2	98.2	3370 (7440)	1404 (3100)	489 708	–	–	–
Out	1807 (280)	–	–	–	–	–	–	3094 (6830)	1336 (2950)	467 696	127.2 Throttle back	122.0	104.0
Out	2045 (317)	1930 (4260)	1246 (2750)	438 665	121.0	114.2	95.1	3157 (6570)	1631 (3600)	500 705	127.5	120.6	104.0
Out	2045 (317)	–	–	–	–	–	–	2877 (6350)	1540 (3400)	488 695	126.5 Throttle back	119.8	102.6
Out	2290 (355)	1382 (3050)	1309 (2890)	455 665	119.1	111.7	94.0	2485 (5486)	1735 (3830)	500 692	124.6	118.4	100.2
Out	2290 (355)	1291 (2850)	1246 (2750)	435 660	117.2 Throttle back	110.0	91.8	–	–	–	–	–	–
In	2936 (455)	1450 (3200)	1268 (2800)	435 665	118.3	112.4	93.9	2446 (5400)	1653 (3650)	495	126.2	119.8	101.8
In	2936 (455)	1359 (3000)	1228 (2710)	429 662	117.4 Throttle back	111.6	93.1	–	–	–	–	–	–

[a]Altitude
[b]Sideline
[c]Overhead

TABLE 3–SUMMARY OF NOISE SUPPRESSION INCREMENTS

Baseline: Conical nozzle, 2290 cm^2 (355 $in.^2$), colander in		Noise suppression increments, dB					
		Approach (93% N_H)[a]			Takeoff (99% N_H)[b]		
		Sideline 152 m (500 ft)	Overhead 304 m (1000 ft)	Overhead 1216 m (4000 ft)	Sideline 152 m (500 ft)	Overhead 304 m (1000 ft)	Overhead 1216 m (4000 ft)
Lobe 1807 cm^2 (280 $in.^2$)	Colander out	-1.2	-2.2	1.3	–	–	–
	Throttle back	–	–	–	3.5	4.2	5.2
	High, low freq removed	1.8	0.6	4.7	5.0	6.2	7.0
	Directional effect		2.6	6.7		8.2	9.0
Lobe 1936 cm^2 (300 $in.^2$)	Colander out	0.3	-0.6	2.5	3.7	4.2	5.2
	Throttle back	–	–	–	2.7	3.2	5.2
	High, low freq removed	3.1	2.0	5.9	5.1	6.0	7.6
	Directional effect		4.0	7.9		8.0	9.6
Lobe 2194 cm^2 (340 $in.^2$)	Colander out	1.4	0.7	3.2	2.9	3.0	5.4
	Throttle back	2.8	2.4	4.7	–	–	–
	High, low freq removed	5.2	4.1	8.0	5.5	6.0	7.9
	Directional effect		6.1	10.0		8.0	9.9
Lobe 2290 cm^2 (355 $in.^2$)	Colander out	2.3	1.6	4.3	3.2	2.9	6.0
	Throttle back	3.7	3.8	6.2	–	–	–
	High, low freq removed	6.1	5.4	10.0	6.2	6.0	9.0
	Directional effect		7.4	12.0		8.0	11.0
Conical 1807cm^2(280 $in.^2$)	Colander out	-1.3	-1.8	-2.7	–	–	–
	Throttle back	–	–	–	0	-0.8	-1.8
Conical 2045 cm^2(317 $in.^2$)	Colander out	-0.2	0.2	0.4	-0.3	0.6	-1.8
	Throttle back	–	–	–	0.7	1.4	-0.4
Conical 2290 cm^2(355 $in.^2$)	Colander out	1.7	2.7	1.5	2.6	2.8	2.0
	Throttle back	3.6	4.4	3.7	–	–	–
Conical 2936cm^2(455 $in.^2$)	Colander out	2.5	2.0	1.6	1.0	1.4	0.4
	Throttle back	3.4	2.8	2.4	–	–	–

[a] Based on constant airplane lift
[b] Based on total hot and cold takeoff thrust
[c] Altitude 76 m (259 ft)

TABLE 4.—COMPUTED PERFORMANCE OF TEST NOZZLES

Run	Condition				Configuration		T_6, °K (°R)	Primary flow, kg/sec (lb/sec)	Nozzle total pressure[a] kg/cm² (psi)	P_{T_8}/P_A	V_j,[b] m/sec (ft/sec) $\gamma = 1.34$	$WI\sqrt{T_6}/A_{geo}P_{T_8}$	Ideal flow,[c] kg/sec (lb/sec) kgm/sec $\gamma = 1.34$	Discharge coeff WP/WI	Ideal thrust, kg (lb)	Adj. velocity coeff CV_A	Primary gross thrust, kg (lb)
	% N_L	% N_H	$N_L/\sqrt{T}$	$N_A/\sqrt{T}$	Nozzle geometric area (A)	Col-ander											
18	71.6	88.2	352	627	Lobe suppressor, A_{cold} = 1871 cm² (290 in.²) $A_{not\ est} \cong$ 1900 cm² (300 in.)	Out	638 (1149)	31.85 (70.3)	1.38 (18.96)	1.286	297.92 (980)	0.4498	34.2 (75.49)	0.931	973 (2141)	0.99	963 (2119)
	85.6	92.8	422	660			691 (1245)	43.49 (96.0)	1.64 (23.37)	1.585	414.048 (1362)	0.5140	46.27 (102.15)	0.940	1847 (4064)	0.98	1810 (3982)
	90.4	94.5	444	672			721 (1298)	48.34 (106.7)	1.79 (25.45)	1.726	458.128 (1507)	0.5221	50.12 (110.63)	0.964	2271 (4997)	0.978	2221 (4887)
	99.4	98.6	489	702			791 (1425)	55.67 (122.9)	2.09 (29.7)	2.015	538.69 (1772)	0.524	56.06 (123.75)	0.993	3077 (6769)	0.968	2978 (6552)
22	83.4	92.2	410	656	Lobe suppressor, A_{cold} = 2213 cm² (343 in²) $A_{not\ est} \cong$ 2290 cm² (355 in.²)	In	703 (1267)	37.99 (83.86)	1.46 (20.73)	1.408	363 (1193)	0.4872	45.64 (100.75)	0.832	1243 (2734)	0.968	1382 (3041)
	90.1	94.7	443	673.5			755 (1360)	46.37 (102.36)	1.66 (23.63)	1.605	439 (1443)	0.5158	53.16 (117.34)	0.872	1863 (4098)	0.978	2041 (4490)
	95.5	97.2	470	691.6			808 (1458)	51.53 (113.76)	1.83 (26.0)	1.766	495 (1627)	0.5234	57.35 (126.6)	0.898	2395 (5269)	0.972	2542 (5592)
	98.3	99.2	484	706.2			893 (1517)	53.57 (118.26)	–	–	–	–	–	–	–	–	–
24	625	85.3	305	604	Conical A_{cold} = 2639 cm² (409 in.²) $A_{not\ est}$ = 2665cm² (413 in.²)	In	625 (1125)	24.62 (54.35)	1.14 (16.24)	1.105	187 (616)	0.3203	29.02 (64.06)	0.848	473 (1040)	1.02	482 (1061)
	82.7	91.5	405	649			676 (1218)	36.31 (80.16)	1.31 (18.68)	1.271	299 (985)	0.4435	44.42 (98.05)	0.817	1115 (2454)	0.998	1113 (2449)
	90.0	94.1	442	668			723 (1302)	44.25 (97.68)	1.46 (20.70)	1.408	368 (1210)	0.4874	52.32 (115.49)	0.846	1670 (3673)	1.00	1670 (3673)
	99.5	98.7	488	701			821 (1479)	51.69 (114.1)	1.7 (24.20)	1.464	469 (1542)	0.5187	61.06 (134.8)	0.846	2485 (5468)	0.99	2461 (5414)
	62.7	85.8	306	608	Conical A_{cold} = 2942 cm² (456 in.²) $A_{not\ est}$ = 2968 (460 in.²)	In	630 (1134)	24.72 (54.57)	1.12 (15.93)	1.084	169 (555)	0.292	28.83 (63.64)	0.857	428 (941)	1.02	436 (960)
	82.69	91.8	404	649			677 (1219)	35.97 (79.4)	1.27 (18.0)	1.224	276 (907)	0.419	45.1 (99.56)	0.797	1017 (2238)	0.998	1015 (2234)
	90.2	94.4	441	668			723 (1302)	43.93 (96.88)	1.39 (19.77)	1.345	343 (1129)	0.471	53.77 (118.7)	0.817	1547 (3403)	1.00	1547 (3403)
	98.8	98.7	483	697			813 (1464)	50.87 (112.3)	1.58 (22.5)	1.531	433 (1424)	0.508	62.29 (137.5)	0.817	2259 (4970)	0.992	2241 (4930)

TABLE 4.—Concluded

Run	Condition				Configuration		T_6, °K (°R)	Primary flow kg/sec (lb/sec)	Nozzle total pressure[a] kg/cm² (psi)	P_{T_8}/P_A	V_J[b] m/sec (ft/sec) $\gamma = 1.34$	$\frac{W\sqrt{T_6}}{A_{geo} P_{T_8}}$	Ideal flow,[c] kg/sec (lb/sec) kgm/sec $\gamma = 1.34$	Discharge coeff WP/WI	Ideal thrust kg (lb)	Adj. velocity coeff $C V_A$	Primary gross thrust, kg (lb)
	% N_L	% N_H	$N_L/\sqrt{T}$	$N_A/\sqrt{T}$	Nozzle geometric area (A)	Col-ander											
26	71.6	88.6	350	626	Conical A_{cold} = 1807 cm² (283 in.²) $A_{not\ est}$ = 1826 cm² (283 in.²)	Out	669 (1205)	30.98 (68.39)	1.38 (19.65	1.337	327 (1076)	0.468	34. (75.05)	0.911	1040 (2287)	1.01	1050 (2310)
	83.5	92.9	409	657			721 (1299)	41.4 (91.38)	1.69 (24.03)	1.634	436 (1434)	0.518	44.27 (97.72)	0.935	1851 (4073)	0.998	1850 (4069)
	90.7	95.8	444	677			778 (1402)	47.79 (105.5)	1.97 (28.07)	1.909	515 (1693)	0.524	50.37 (111.2)	0.948	2523 (5551)	0.997	2516 (5535)
	97.4	99.9	476	706			843 (1517)	53.41 (117.9)	2.28 (32.44)	2.207	587 (1932)	0.524	55.95 (123.5)	0.954	3218 (7080)	0.99	3186 (7009)
27	81.5	91.5	399	647	Conical A_{cold} = 2045 cm² (317 in.²) $A_{not\ est}$ = 2065 cm² (320 in.²)	Out	666 (1199)	36.6 (80.8)	1.44 (20.47)	1.392	347 (1142)	0.4839	41.48 (91.56)	0.882	1304 (2868)	0.998	1301 (2862)
	90.5	94.5	443	668			713 (1284)	46.16 (101.9)	1.68 (23.93)	1.628	432 (1421)	0.517	50.1 (110.6)	0.921	2045 (4500)	1.00	2045 (4500)
	97.4	97.2	477	688			769 (1385)	51.76 (114.3)	1.93 (27.93)	1.863	503 (1654)	0.524	55.95 (123.5)	0.925	2671 (5876)	0.992	2650 (5829)
28	72.0	88.6	351	626	Conical A_{cold} = 2290 cm² (355 in.²) $A_{not\ est}$ = 2310 cm² (358 in.²)	In	653 (1177)	31.21 (68.9)	1.24 (17.70)	1.204	260 (856)	0.4076	34.11 (75.29)	0.915	833 (1832)	1.01	841 (1851)
	83.0	92.3	405	652			698 (1257)	38.28 (84.5)	1.43 (20.27)	1.379	351 (1153)	0.4806	44.57 (98.39)	0.859	1376 (3028)	0.996	1371 (3016)
	89.8	94.8	438	668			750 (1351)	43.85 (96.8)	1.58 (22.53)	1.532	416 (1369)	0.508	50.51 (111.5)	0.868	1872 (4119)	1.00	1872 (4119)
	98.7	99.3	483	703			839 (1510)	52.37 (115.6)	1.87 (26.55)	1.806	513 (1687)	0.523	58.03 (128.1)	0.902	2755 (6061)	0.99	2727 (6000)

[a] Average total pressure from probes 1, 2, and 3 for the lobe nozzle and the average from probes 1, and 2 for the conical nozzles.

[b] V_J is the ideal fully expanded jet velocity

[c] Based on estimated hot area (1% increase for the conical nozzles and = 3% increase for the lobe nozzle)

Note: Ambient pressure – 1.035 kg/cm² (14.72 psi)

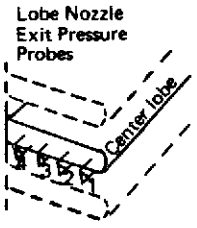

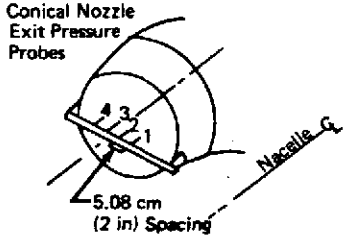

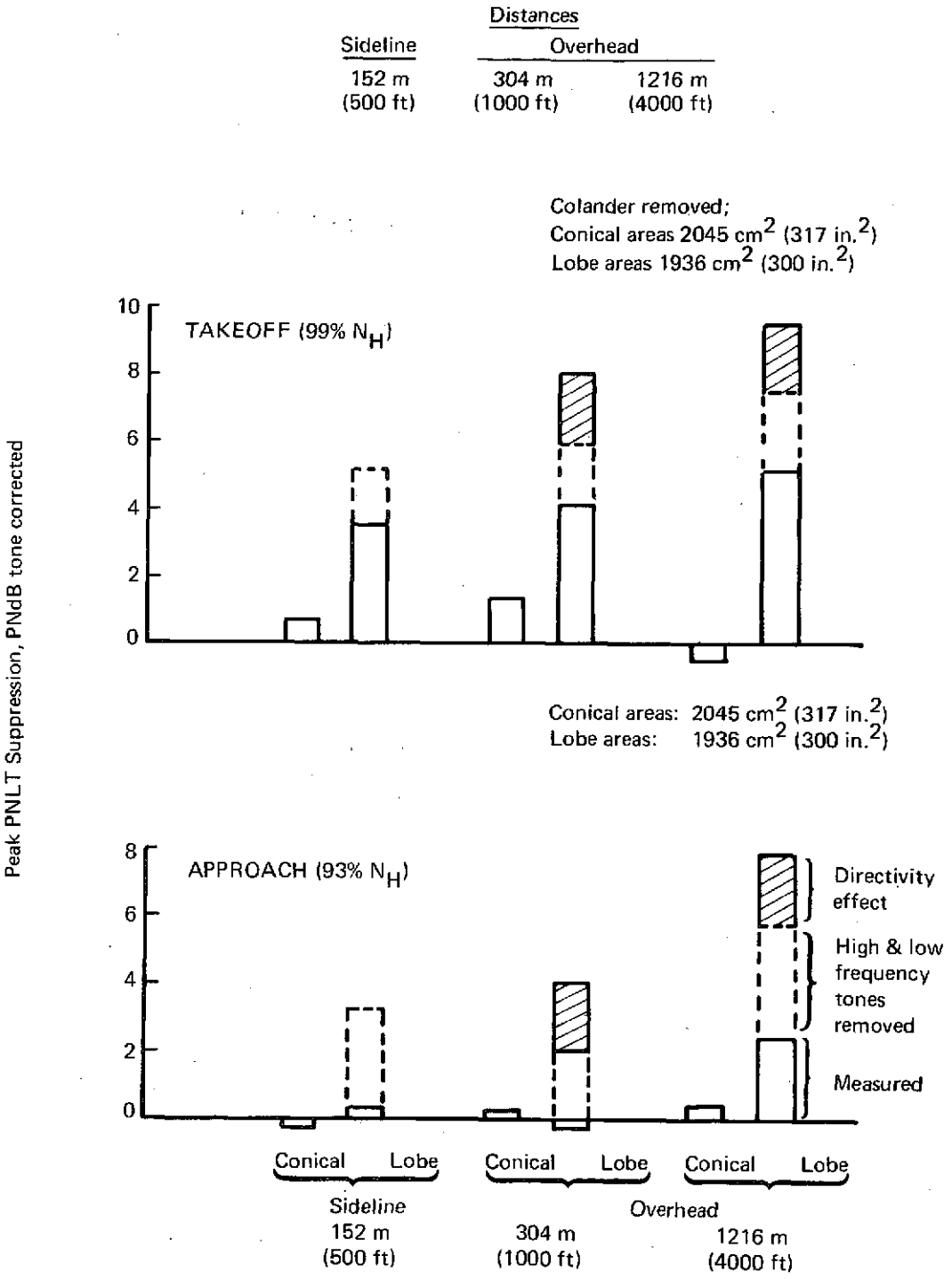

FIGURE 1.–NOISE SUPPRESSION, FIXED AREA NOZZLES

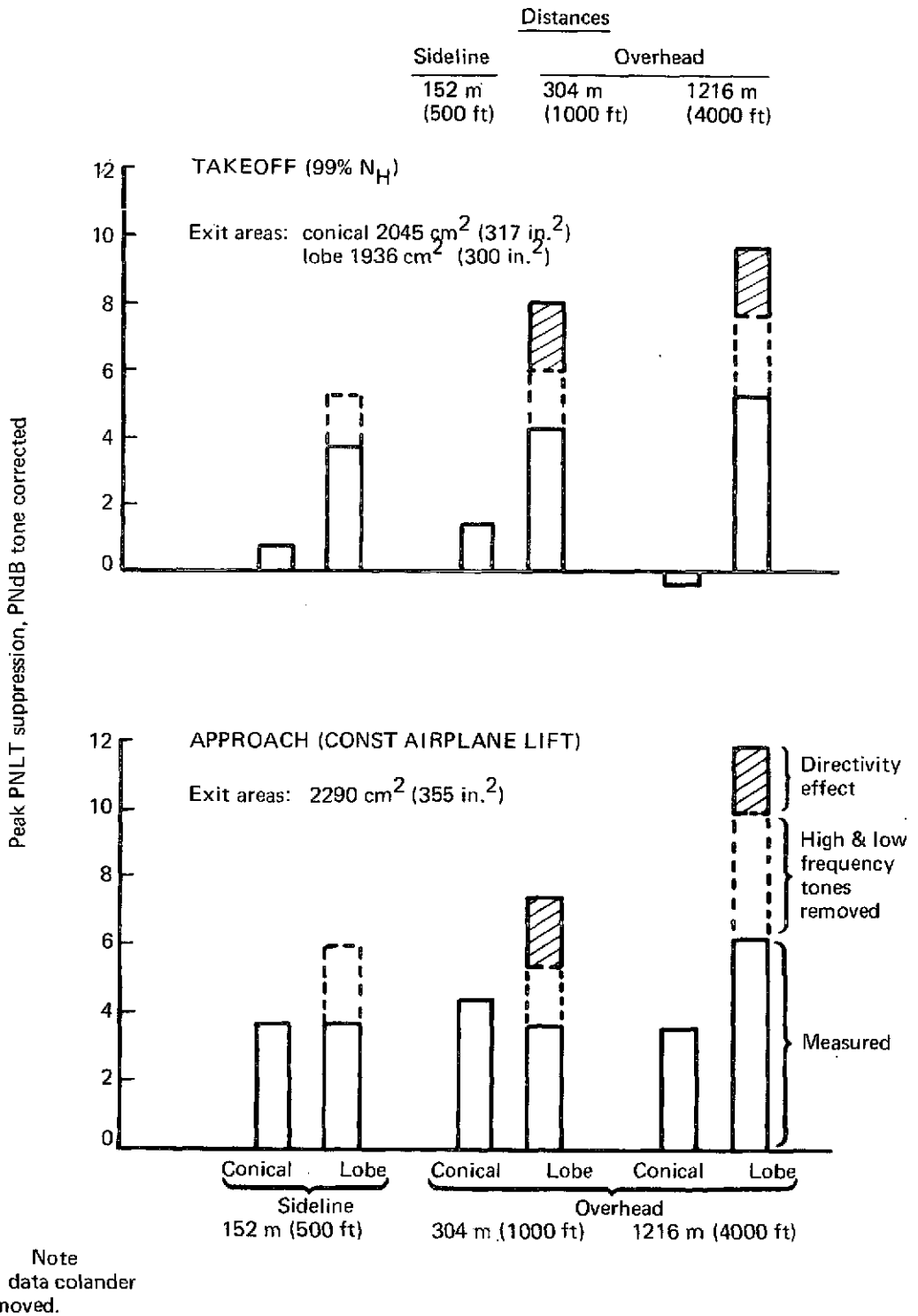

Note
All data colander removed.

FIGURE 2.—NOISE SUPPRESSION, VARIABLE AREA NOZZLES

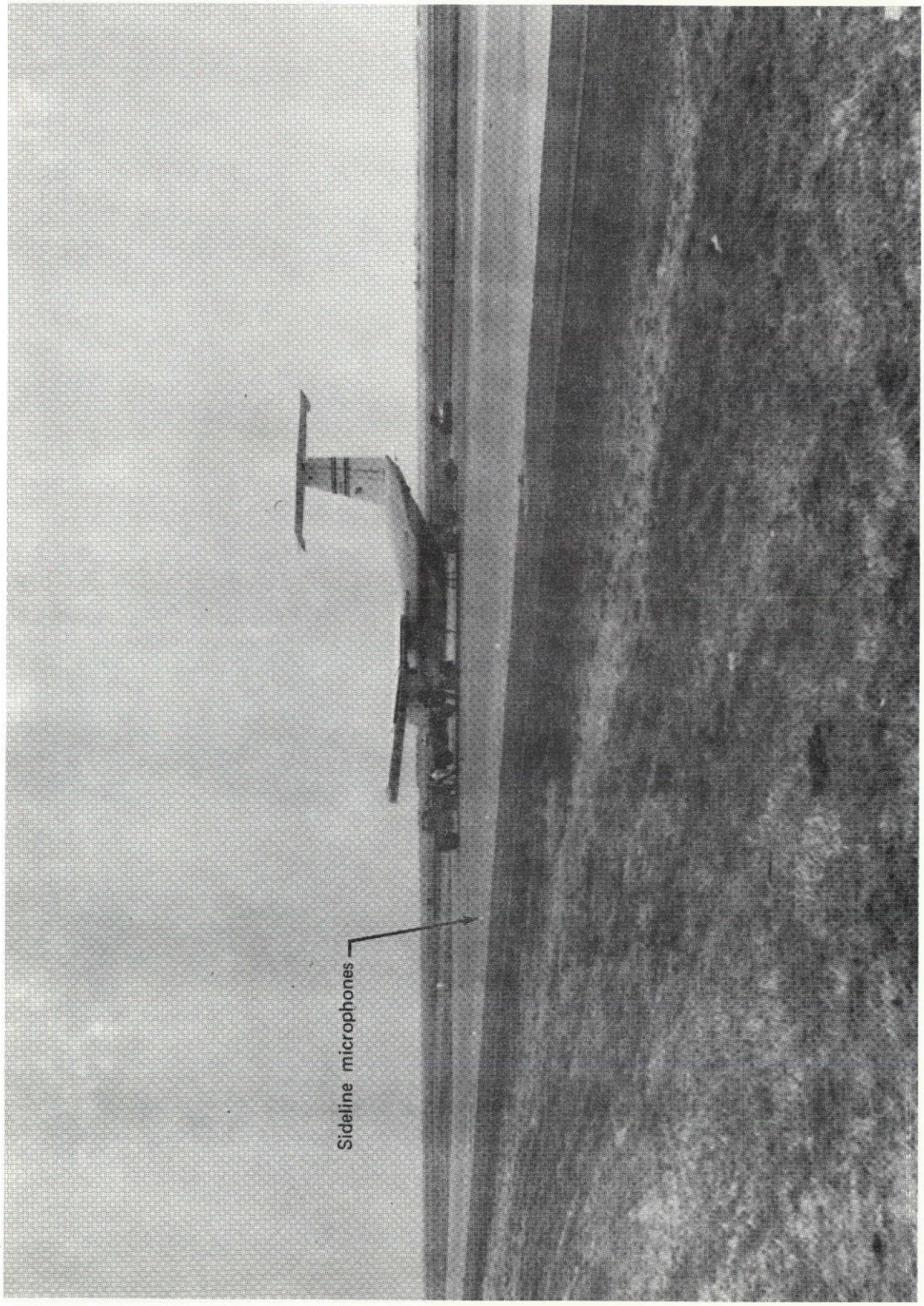

FIGURE 3.–C8A BUFFALO ACOUSTIC TEST SITE

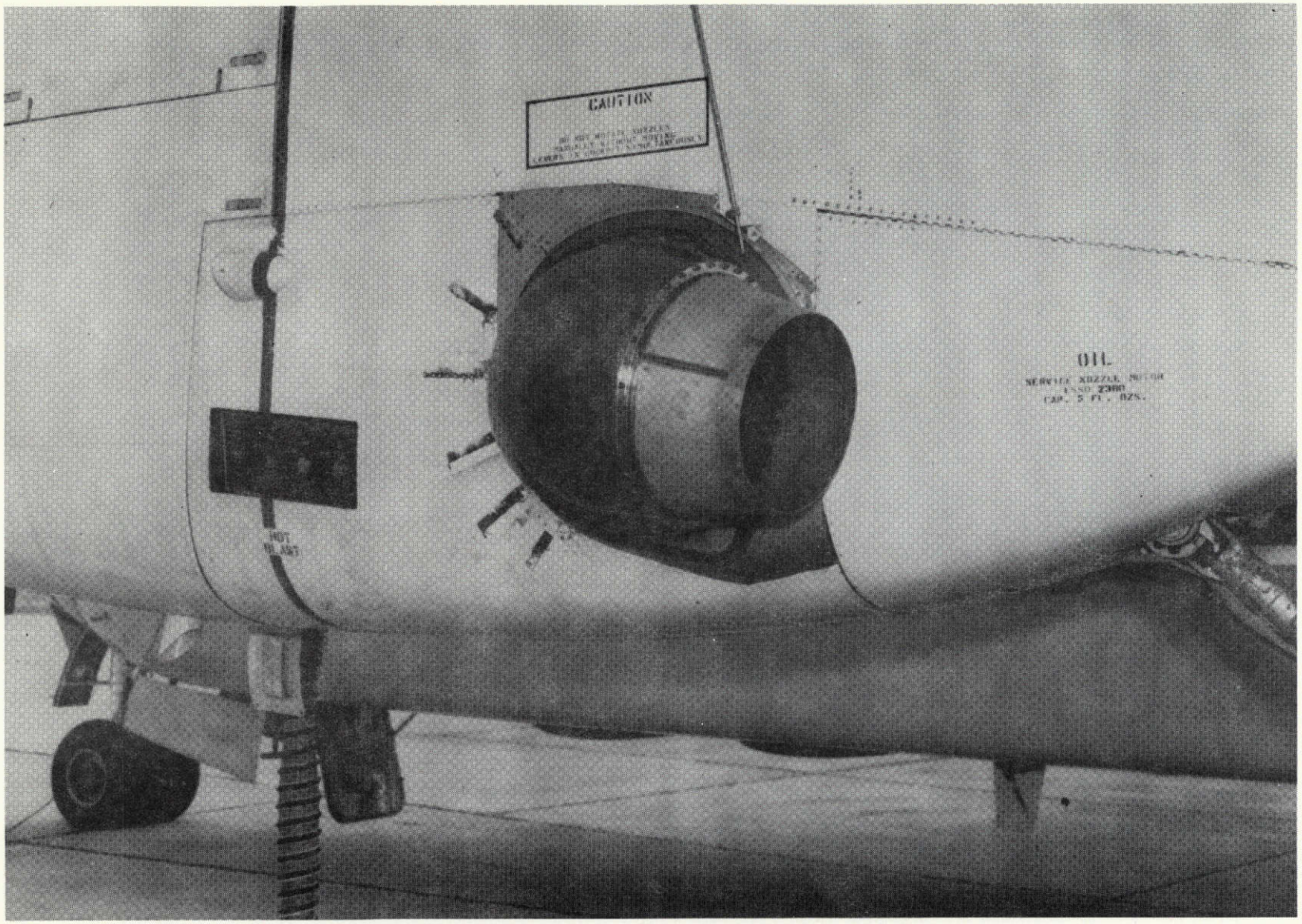

FIGURE 4.—C8A BUFFALO ACOUSTIC TEST BASELINE NOZZLE CONFIGURATION

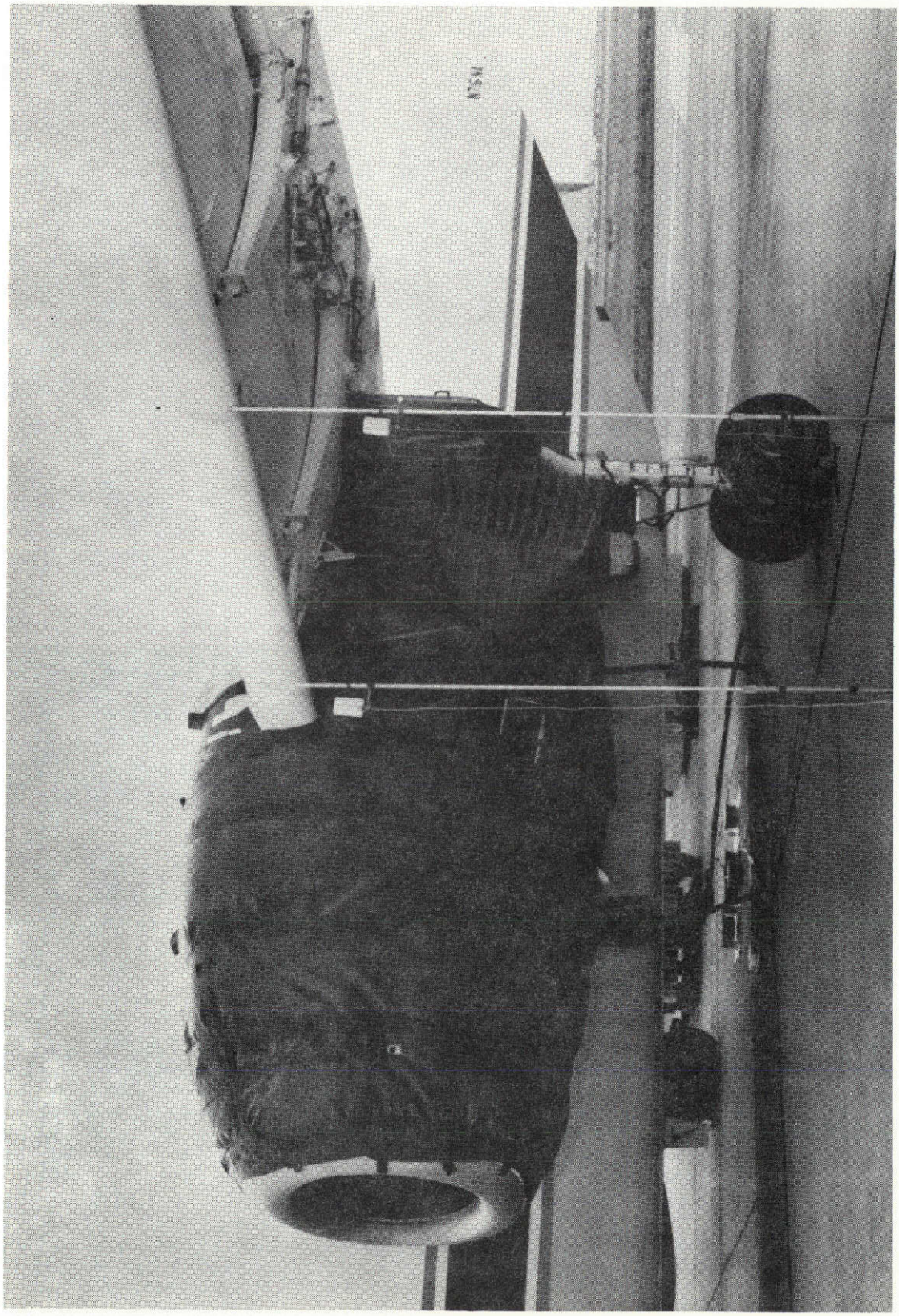

FIGURE 5.—C8A BUFFALO ACOUSTIC TEST LOBE NOZZLE AND ENGINE CASE TREATMENT

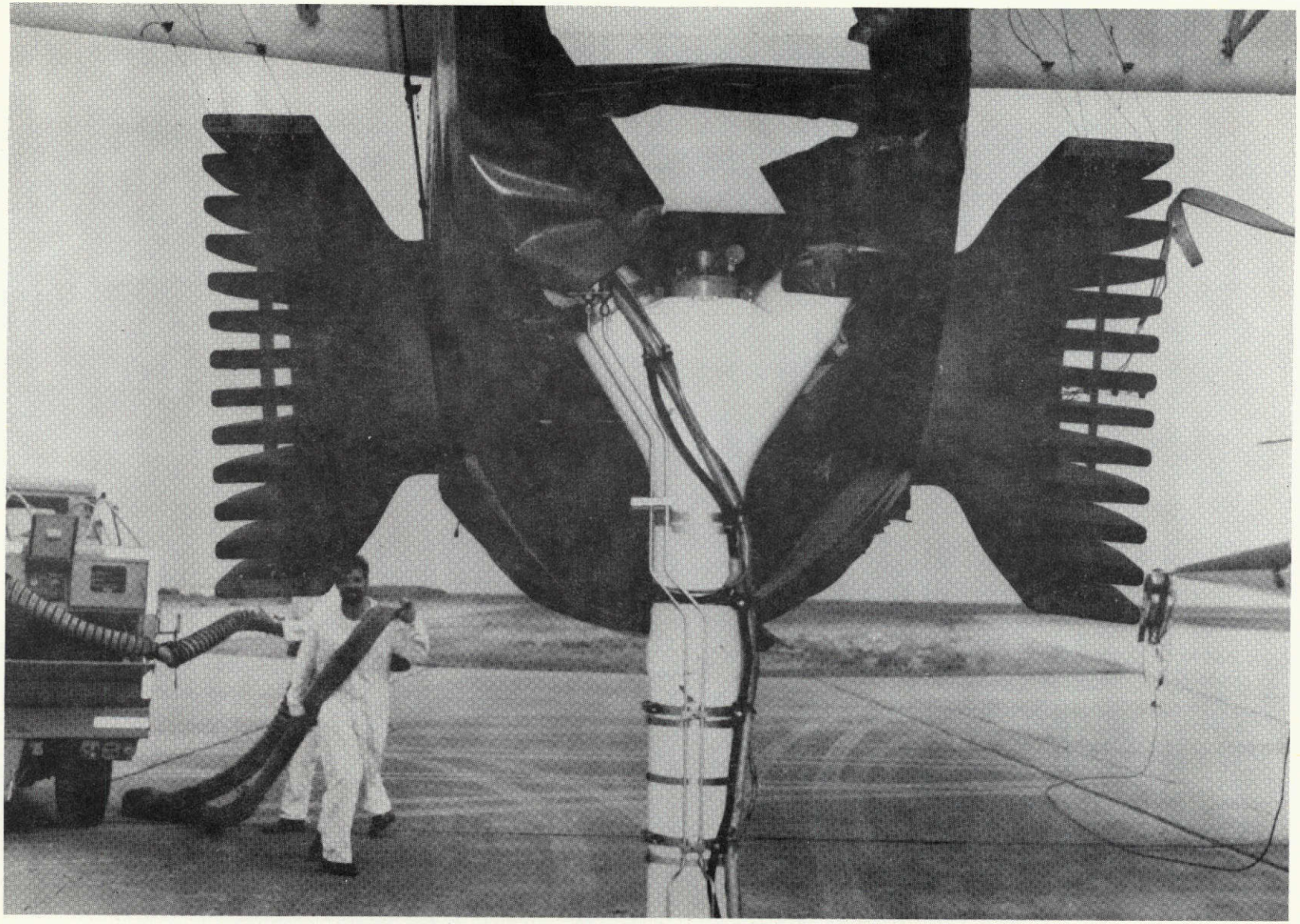

FIGURE 6.—AFT VIEW OF LOBE NOZZLES INSTALLED ON C8A BUFFALO, OUTER LOBES BLOCKED (1871 CM^2 [290 $IN.^2$] AREA)

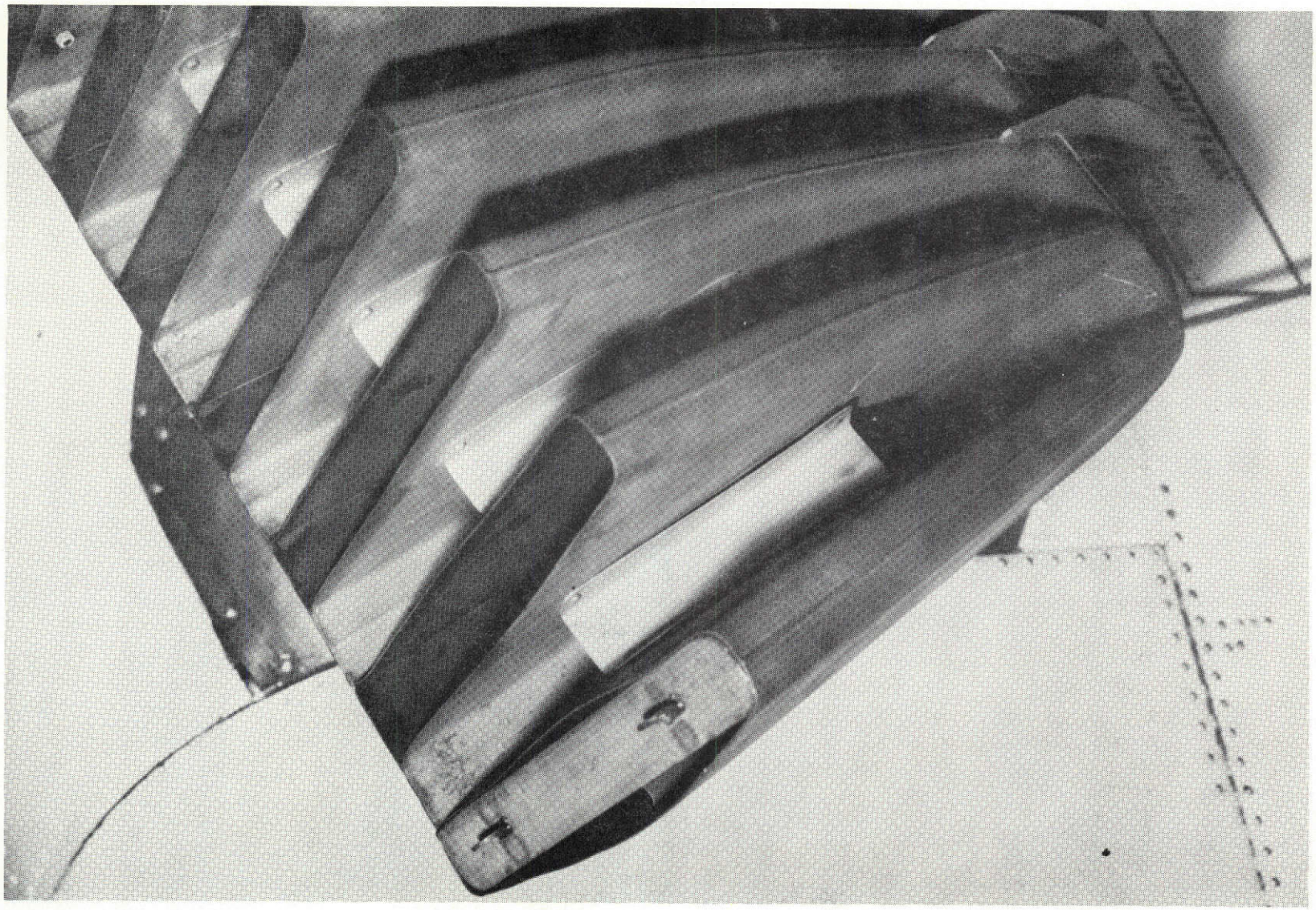

FIGURE 7.—LOBE NOZZLE FOLLOWING FAILURE OF BLOCKED OUTER LOBE

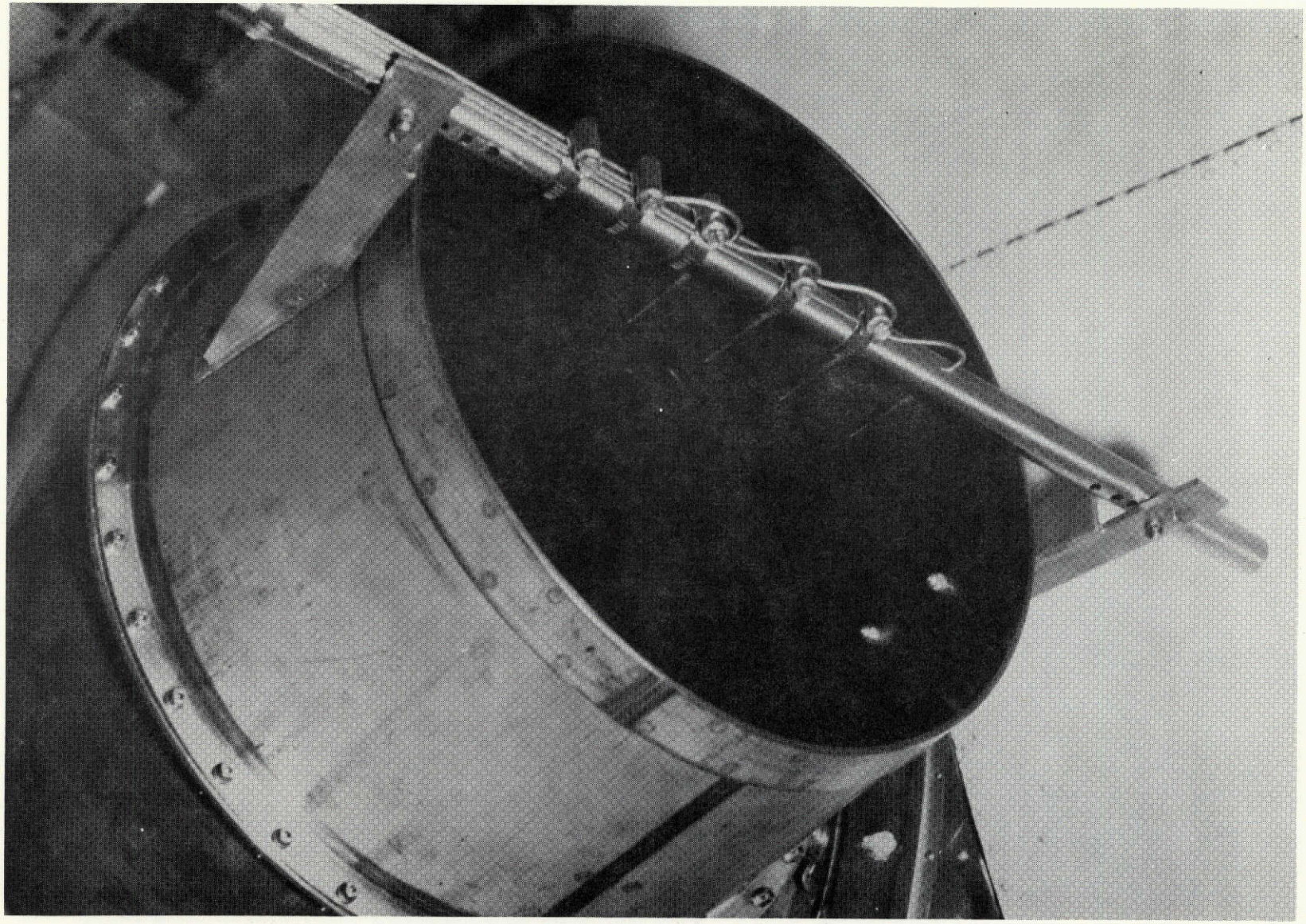

FIGURE 8.–TOTAL PRESSURE RAKE USED WITH CONICAL NOZZLES

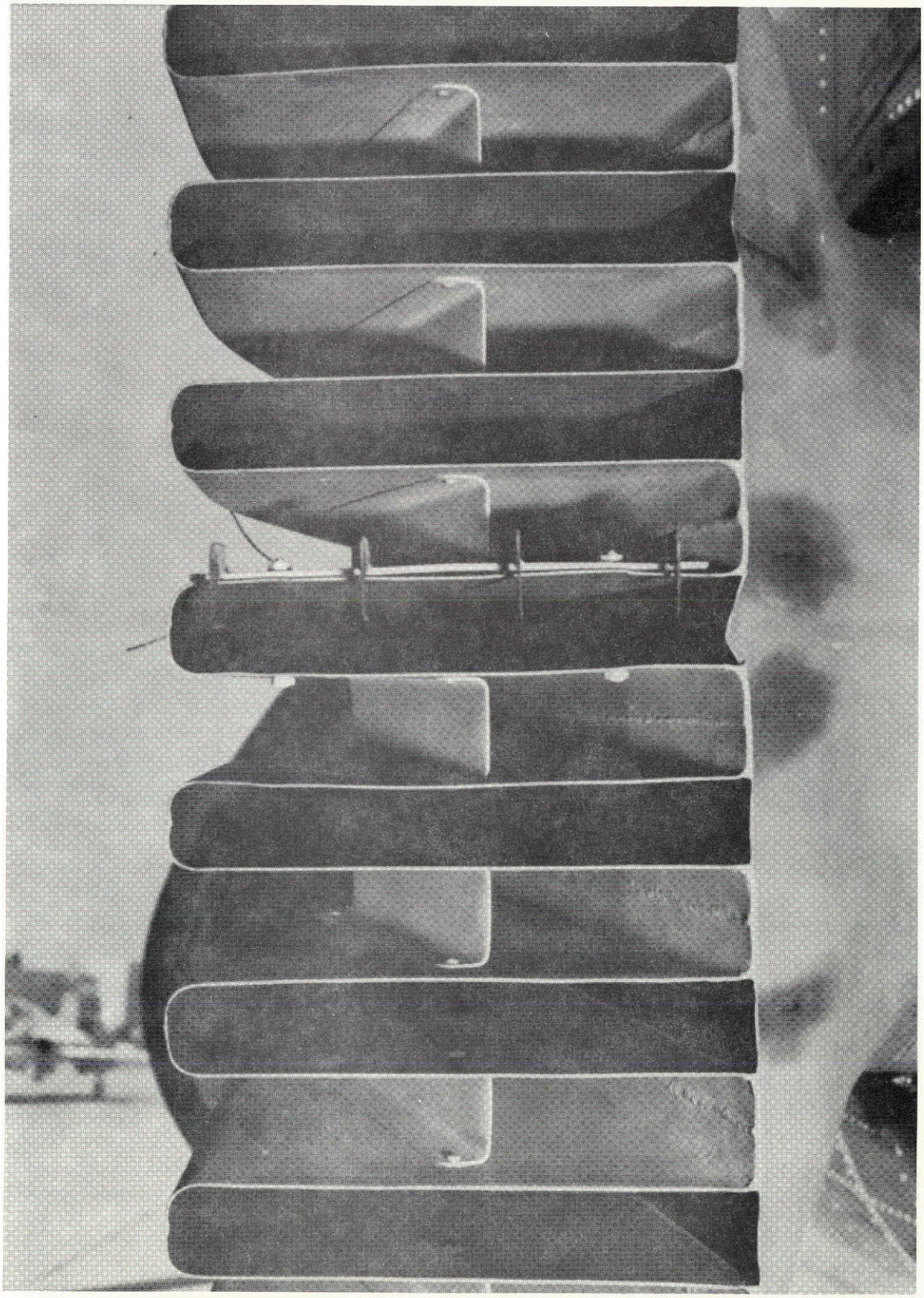

FIGURE 9.—TOTAL PRESSURE RAKE MOUNTED IN CENTER LOBE

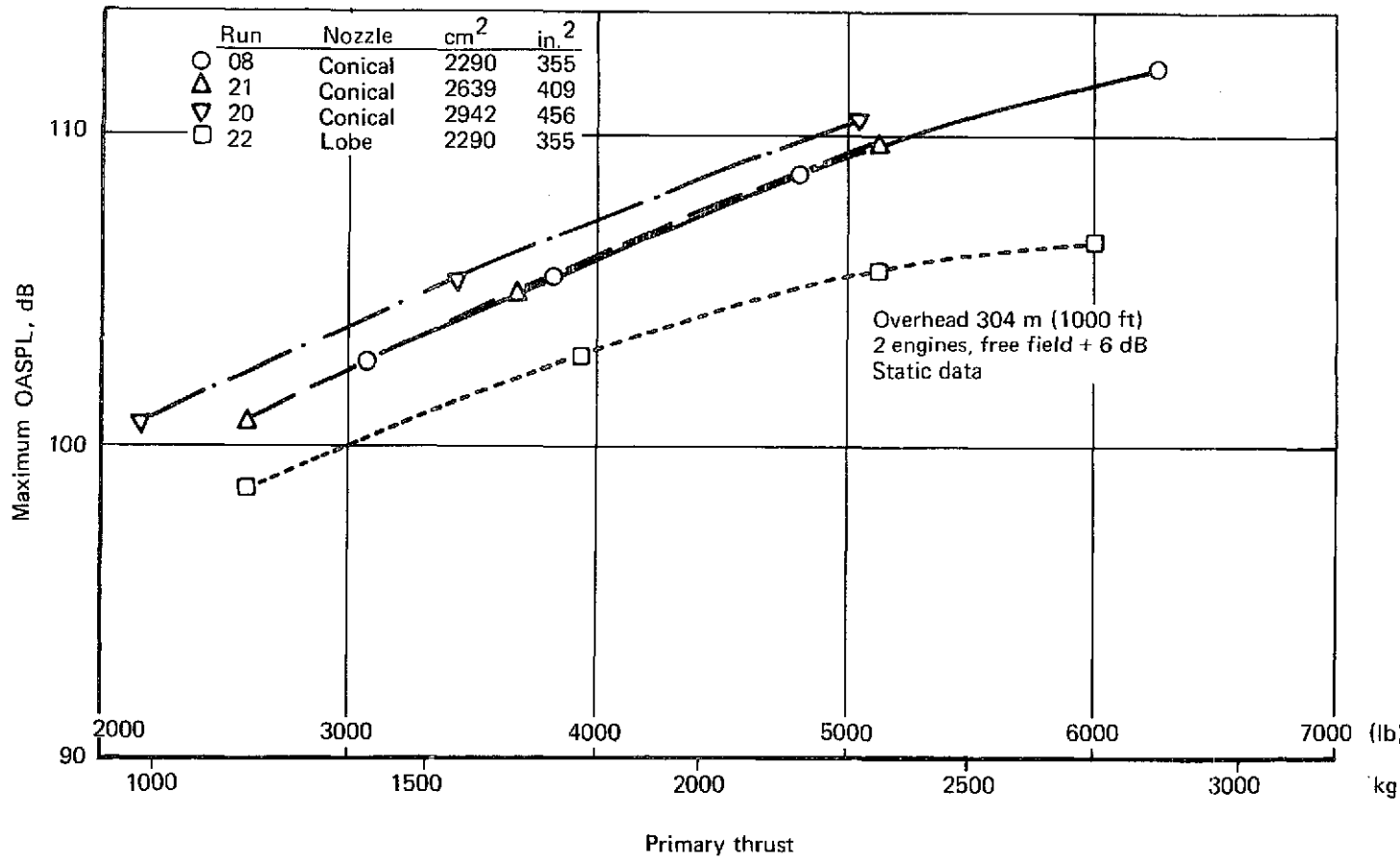

FIGURE 10.—MAXIMUM OASPL VERSUS THRUST, 304 METERS OVERHEAD, COLANDER IN

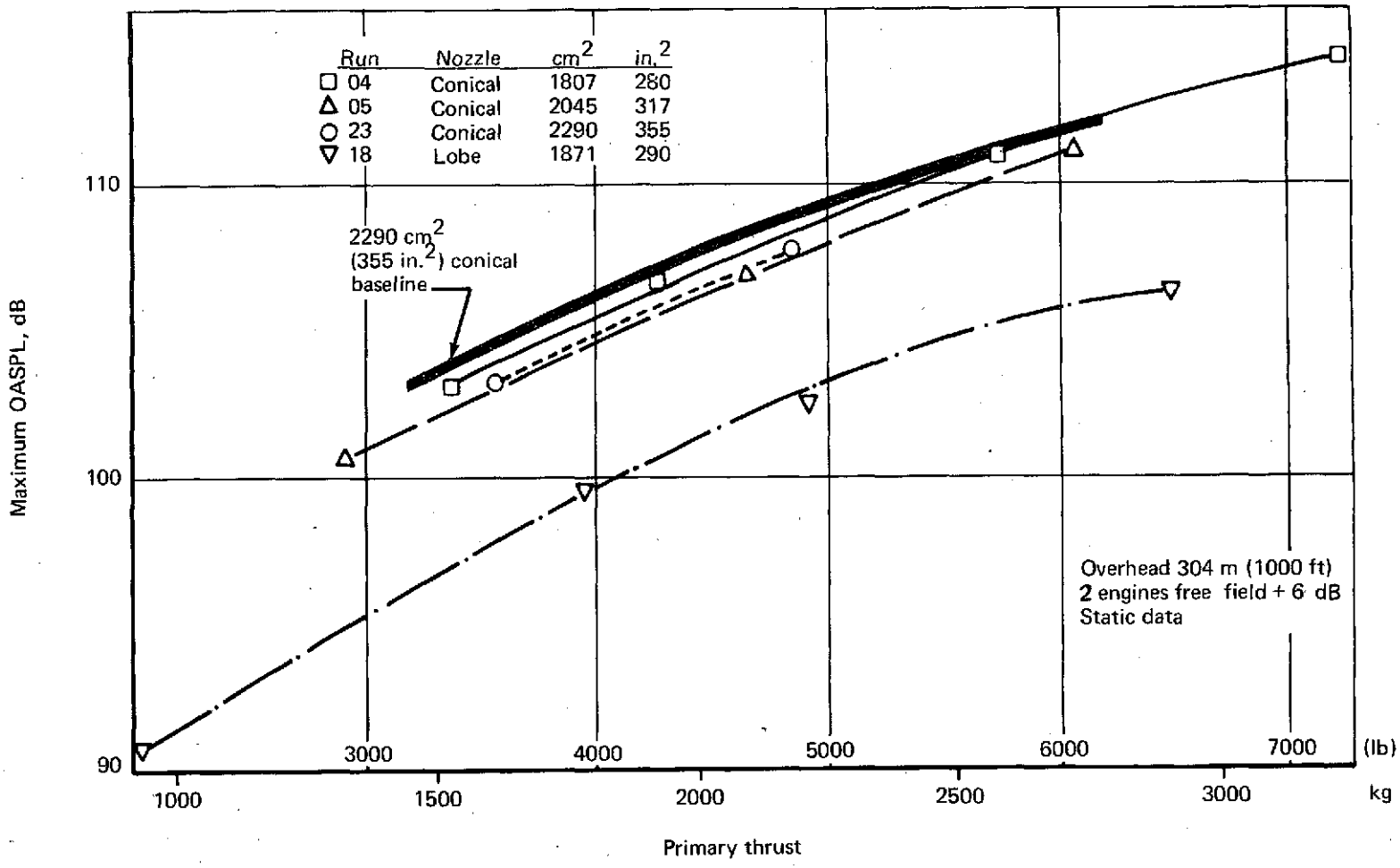

FIGURE 11.–MAXIMUM OASPL VERSUS THRUST, 304 METERS OVERHEAD , COLANDER OUT

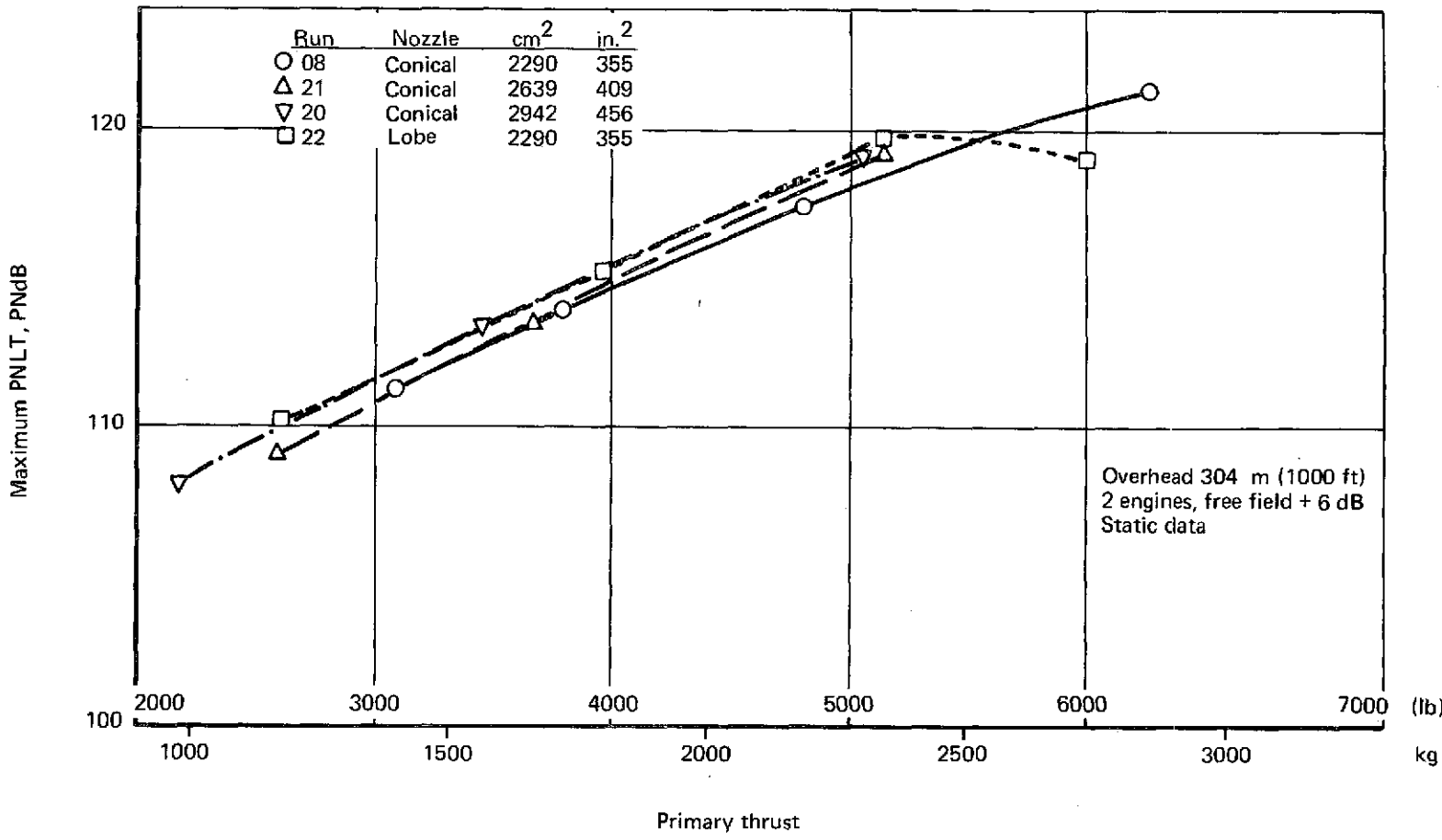

FIGURE 12.—MAXIMUM PNLT VERSUS THRUST, 304 METERS OVERHEAD, COLANDER IN

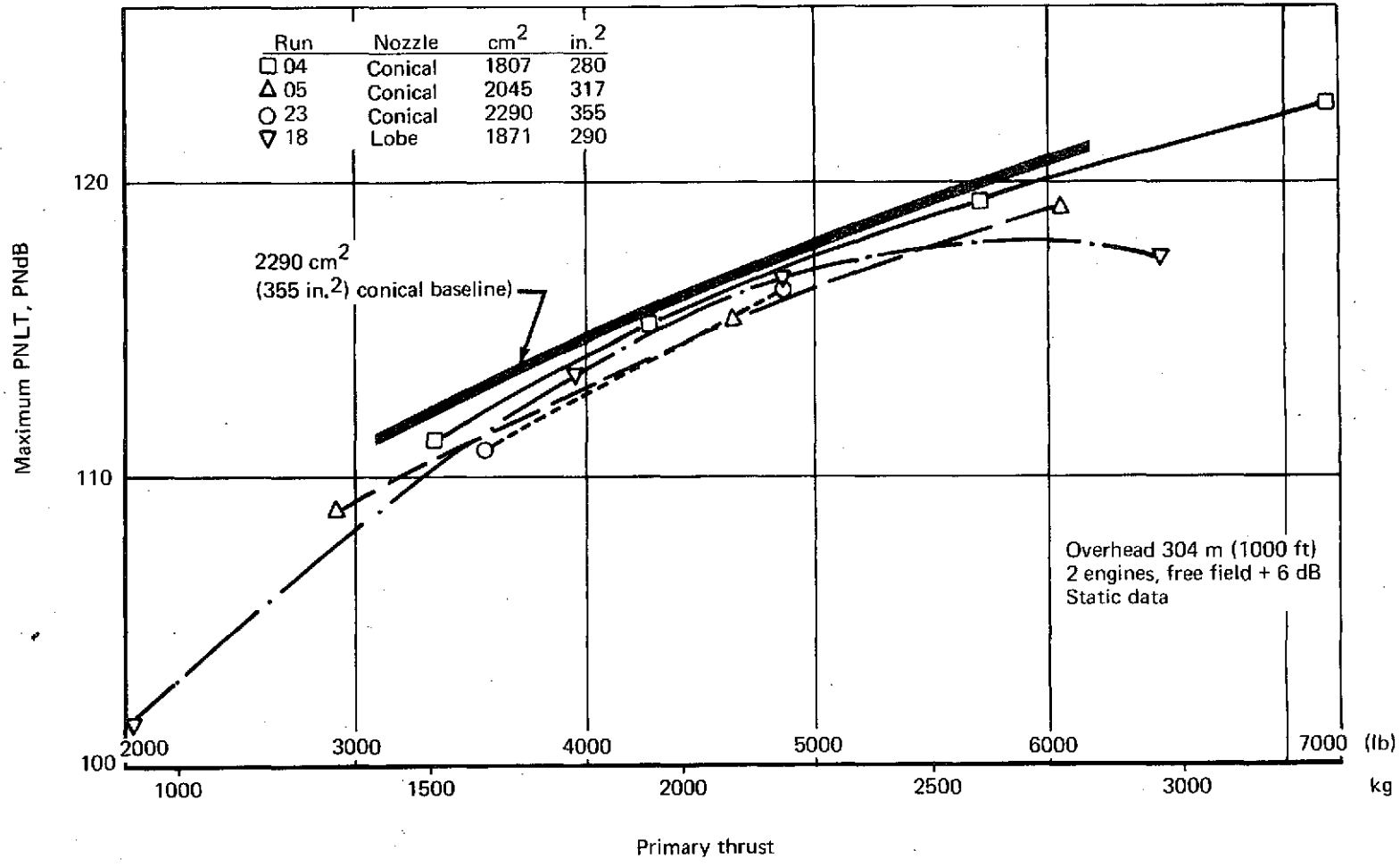

FIGURE 13.–MAXIMUM PNLT VERSUS THRUST, 304 METERS OVERHEAD, COLANDER OUT

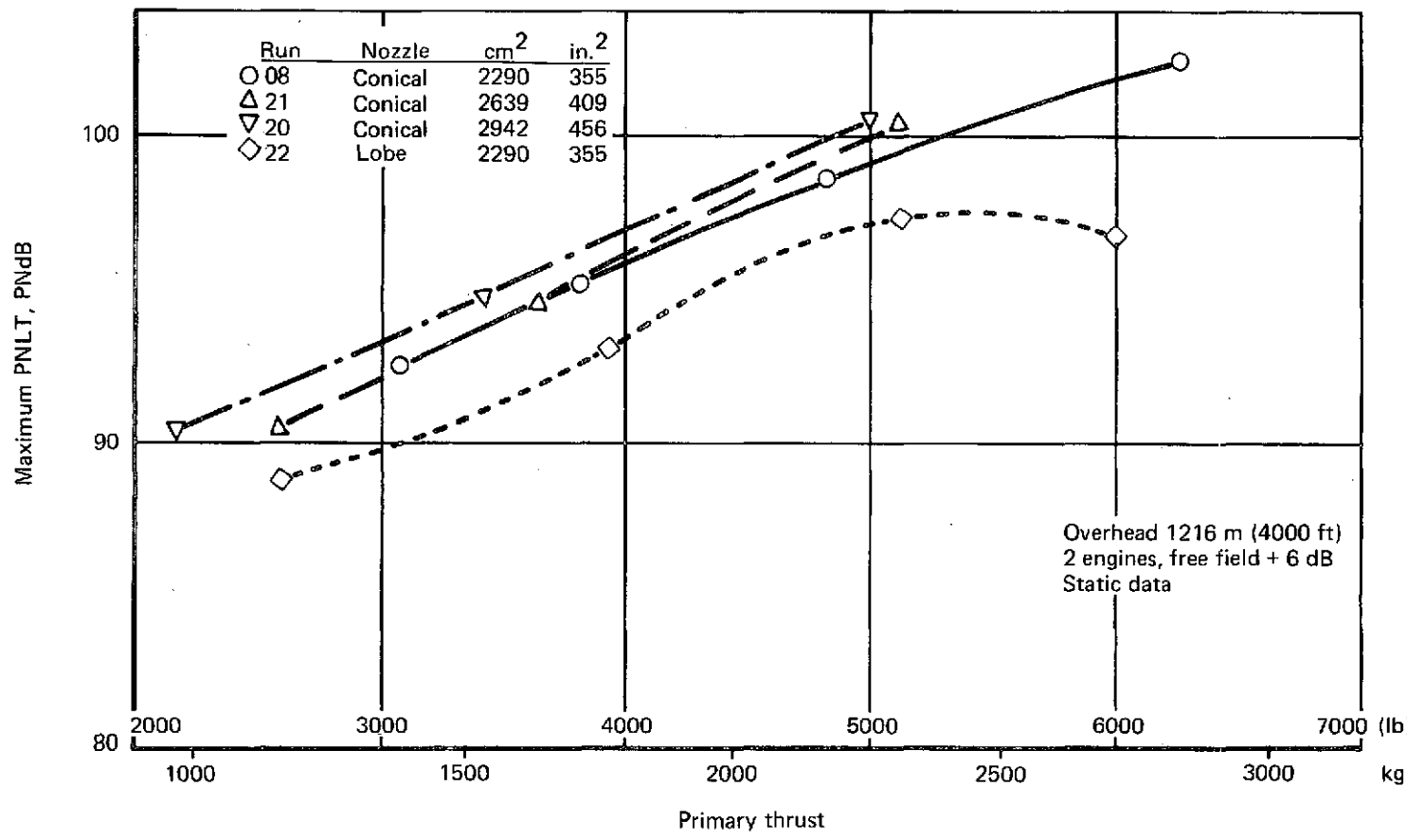

FIGURE 14.–MAXIMUM PNLT VERSUS THRUST, 1216 METERS OVERHEAD, COLANDER IN

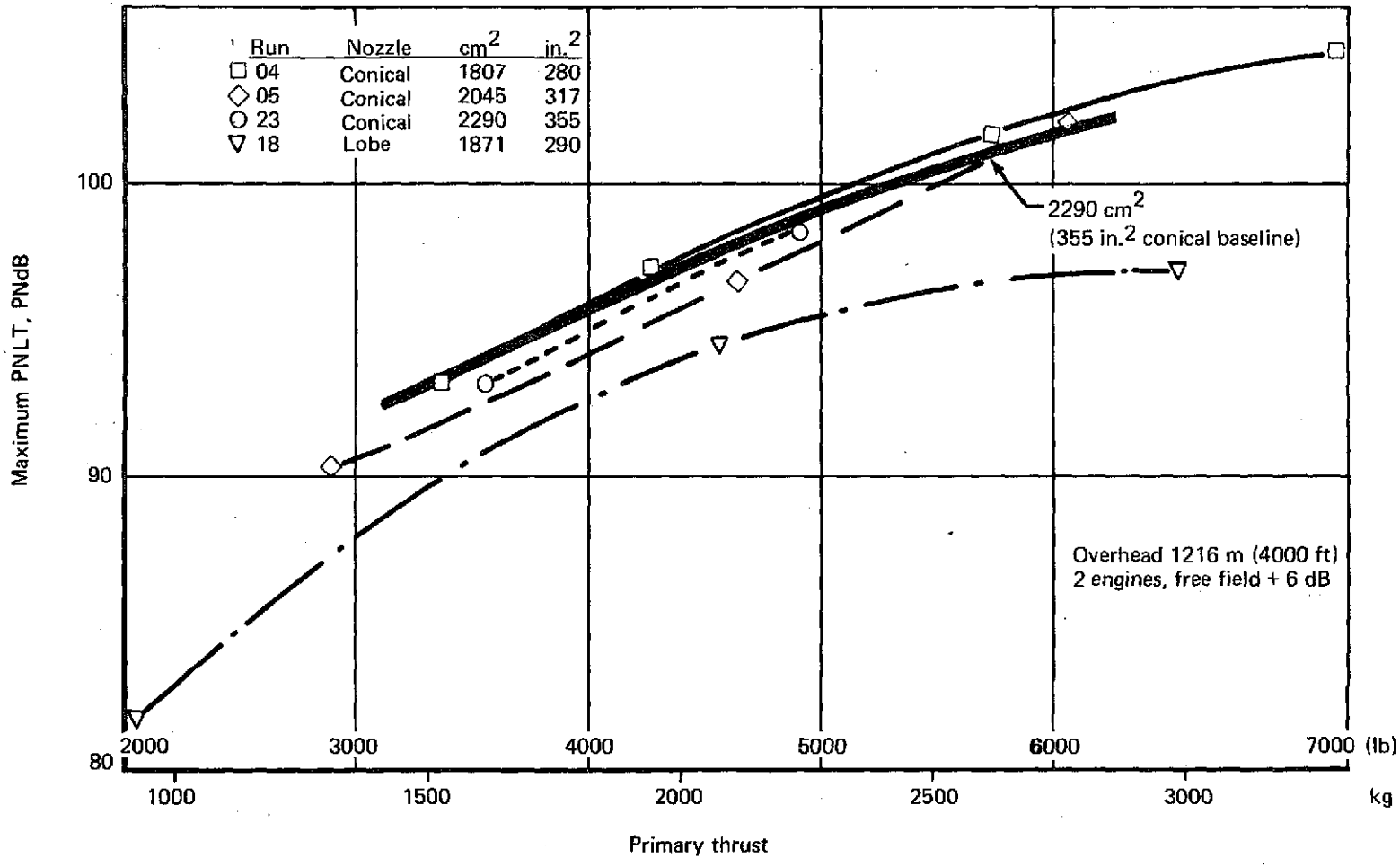

FIGURE 15.—MAXIMUM PNLT VERSUS THRUST, 1216 METERS OVERHEAD, COLANDER OUT

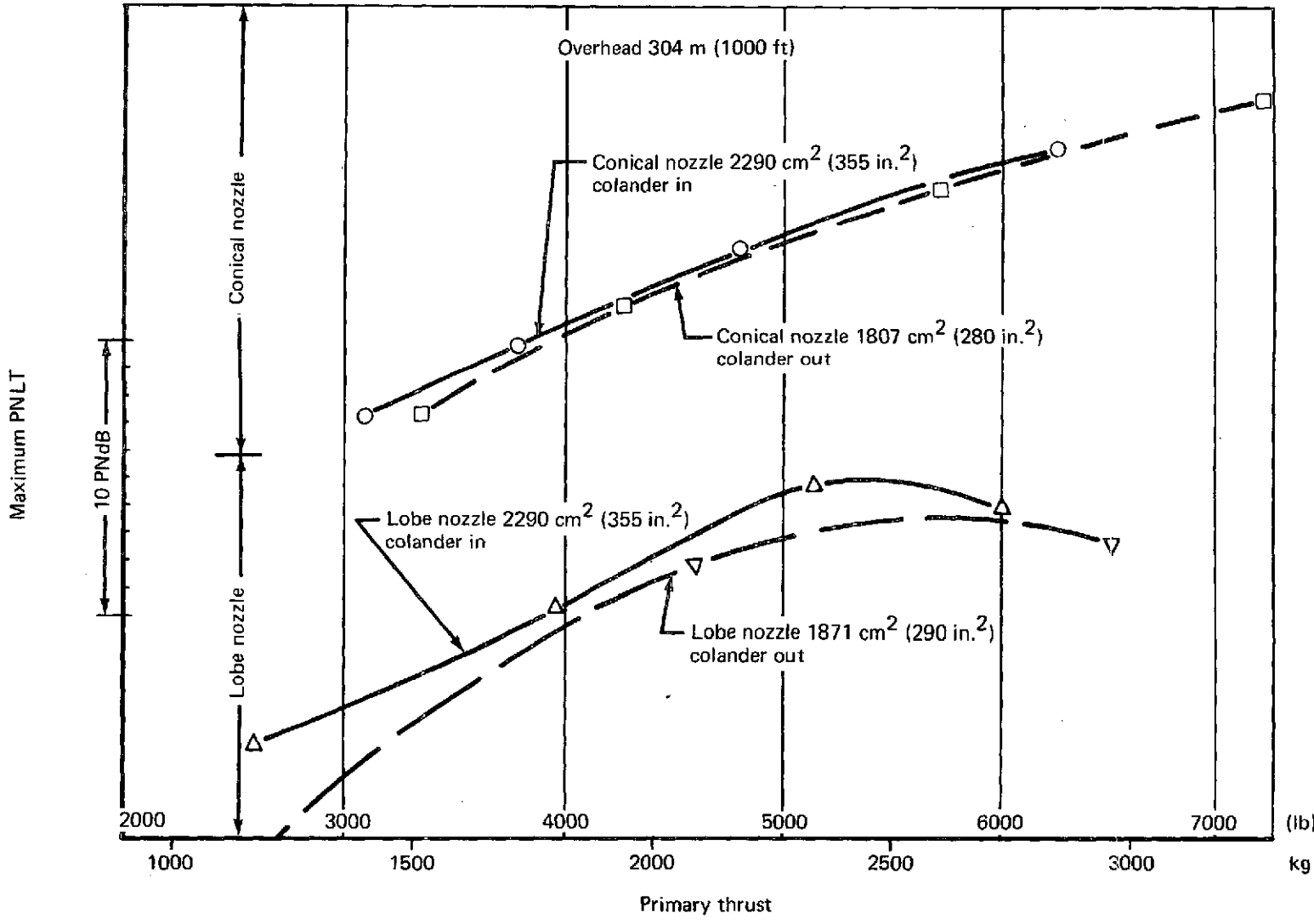

FIGURE 16.—COMPARISON OF MAXIMUM PNLT VERSUS THRUST, COLANDER IN AND OUT

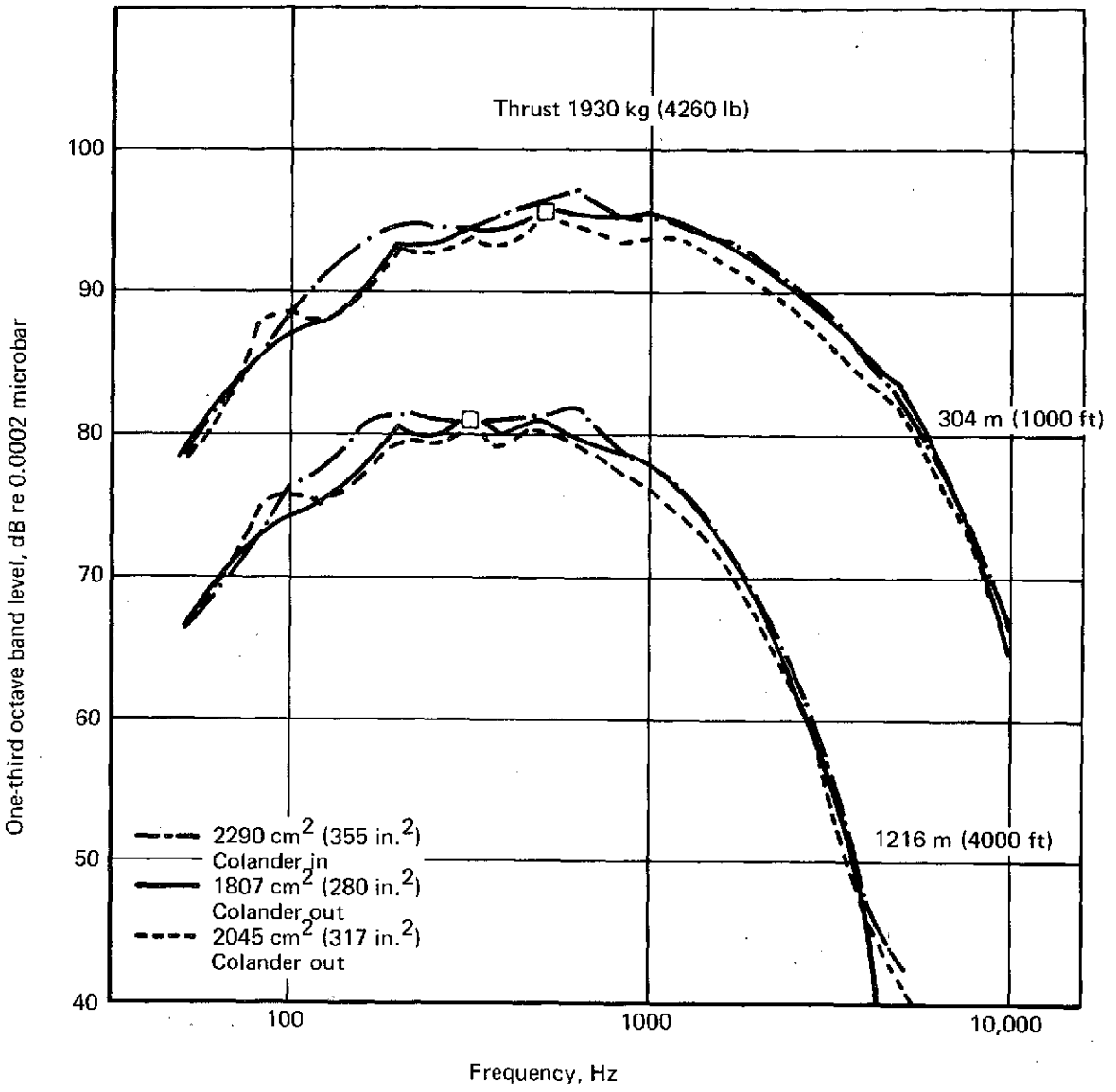

FIGURE 17.–SPL PLOTS, OVERHEAD, CONICAL NOZZLES

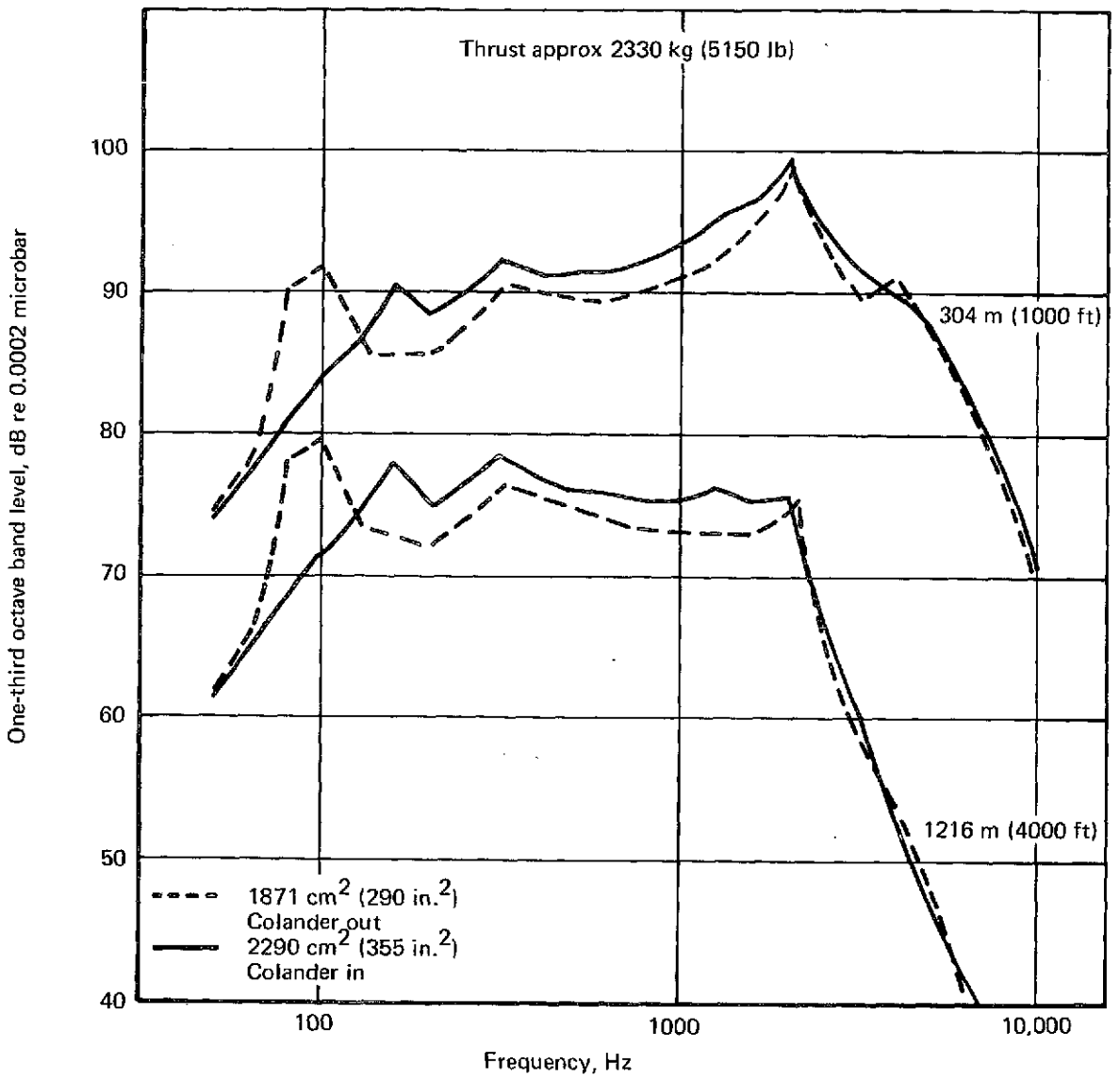

FIGURE 18.–SPL PLOTS, OVERHEAD, LOBE NOZZLES

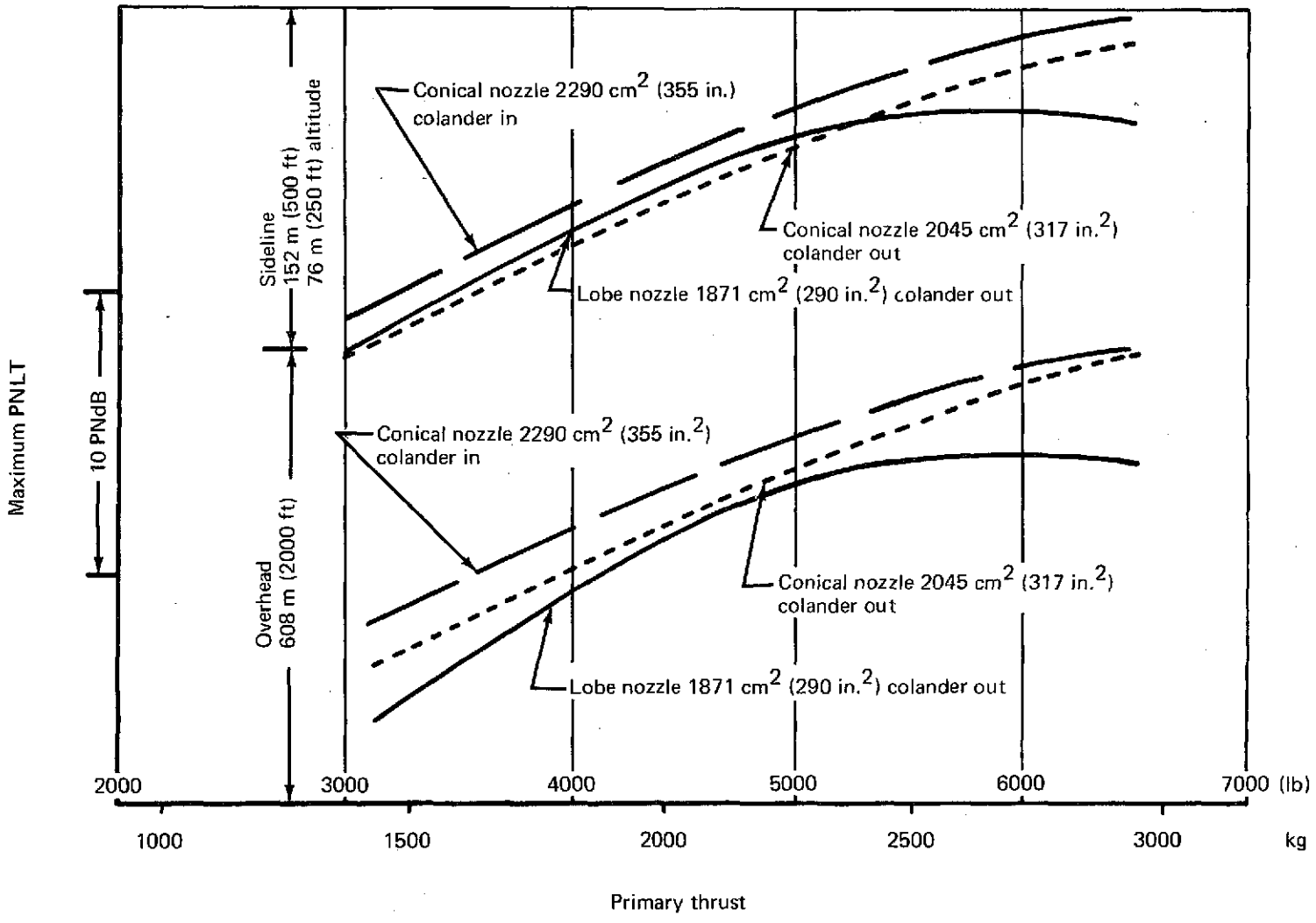

FIGURE 19.—MAXIMUM PNLT VERSUS THRUST, 152 AND 608 METERS DISTANT

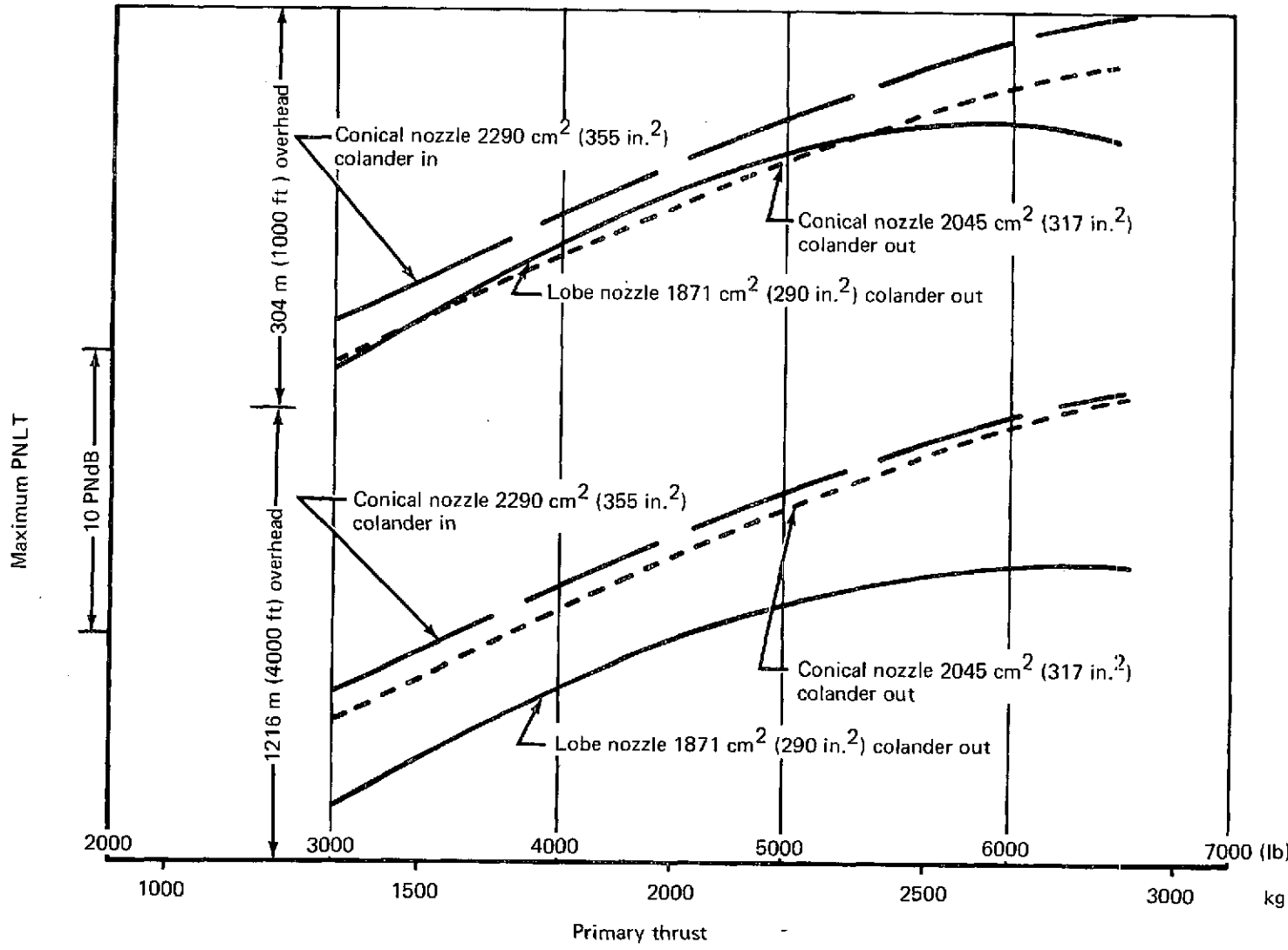

FIGURE 20.–MAXIMUM PNLT VERSUS THRUST, 304 and 1216 METERS OVERHEAD

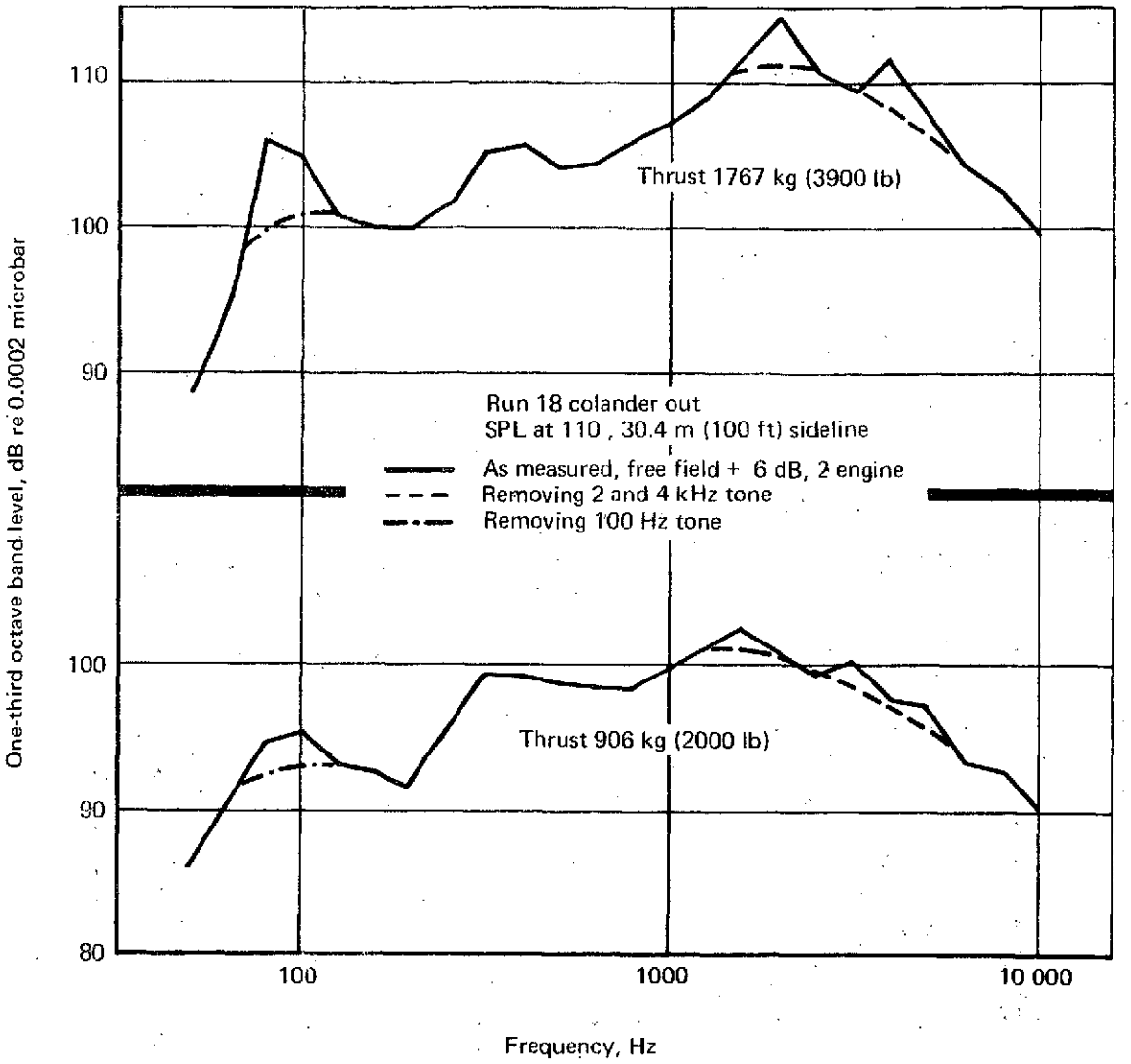

FIGURE 21.—SPL PLOTS, LOBE NOZZLE, AT TWO LOWER-THRUST SETTING'S

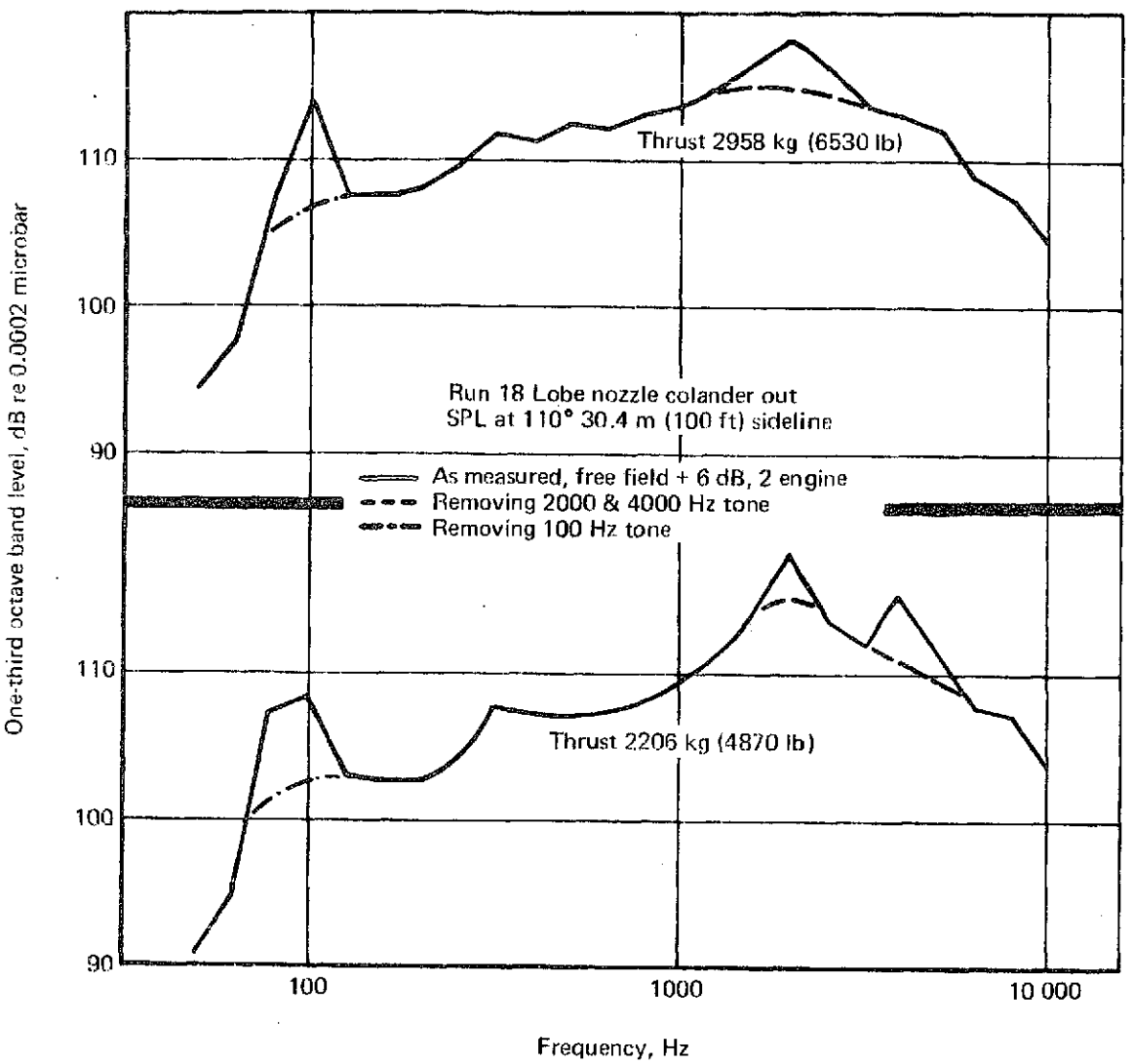

FIGURE 22.–SPL PLOTS, LOBE NOZZLE, AT TWO HIGHER-THRUST SETTINGS

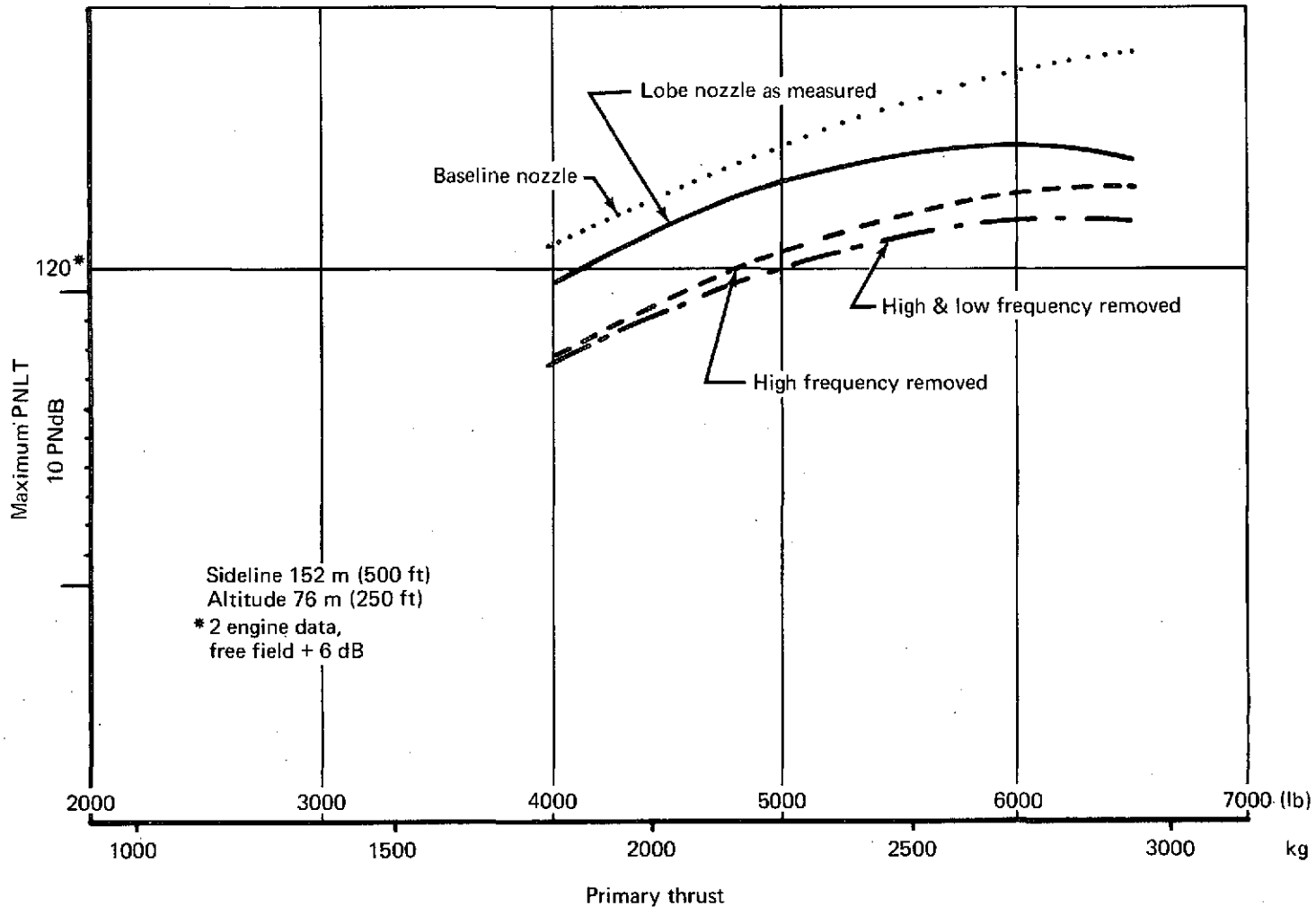

FIGURE 23.—ADDITIONAL SUPPRESSION POTENTIAL, LOBE MOZZLE, AT SIDELINE DISTANCE

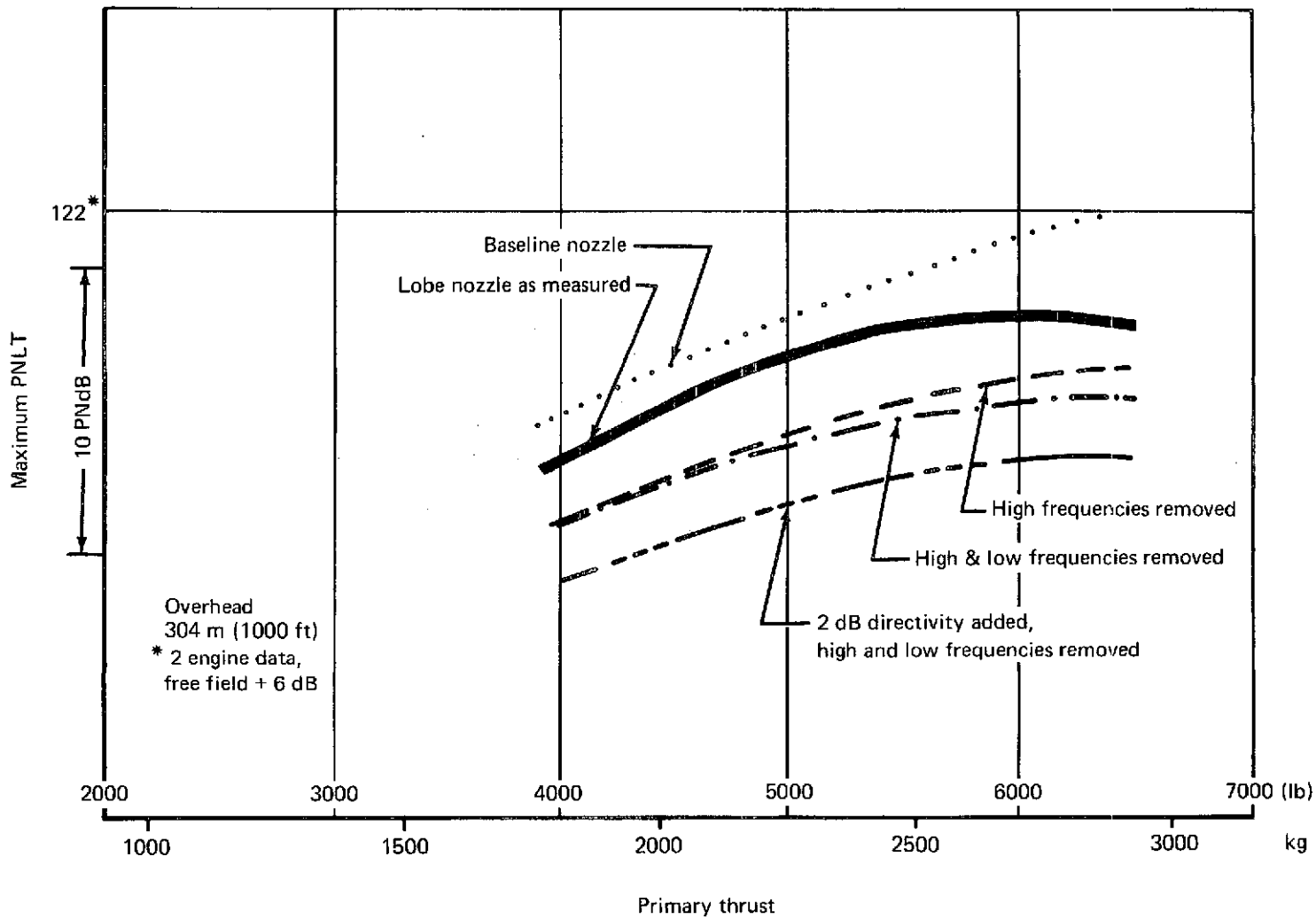

FIGURE 24.—ADDITIONAL SUPPRESSION POTENTIAL, LOBE NOZZLE, 304 METERS OVERHEAD

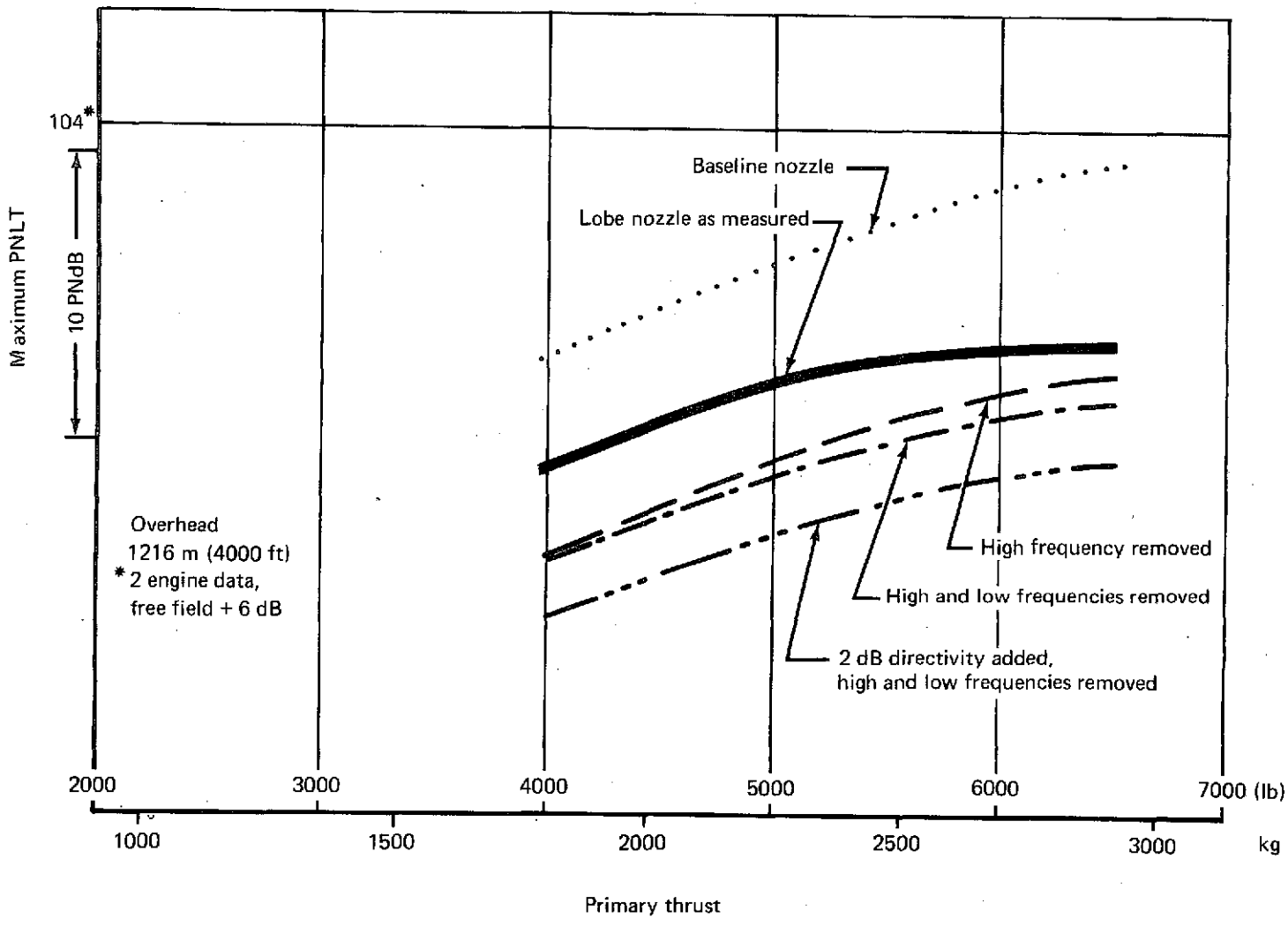

FIGURE 25.—ADDITIONAL SUPPRESSION POTENTIAL, LOBE NOZZLE, 1216 METERS OVERHEAD

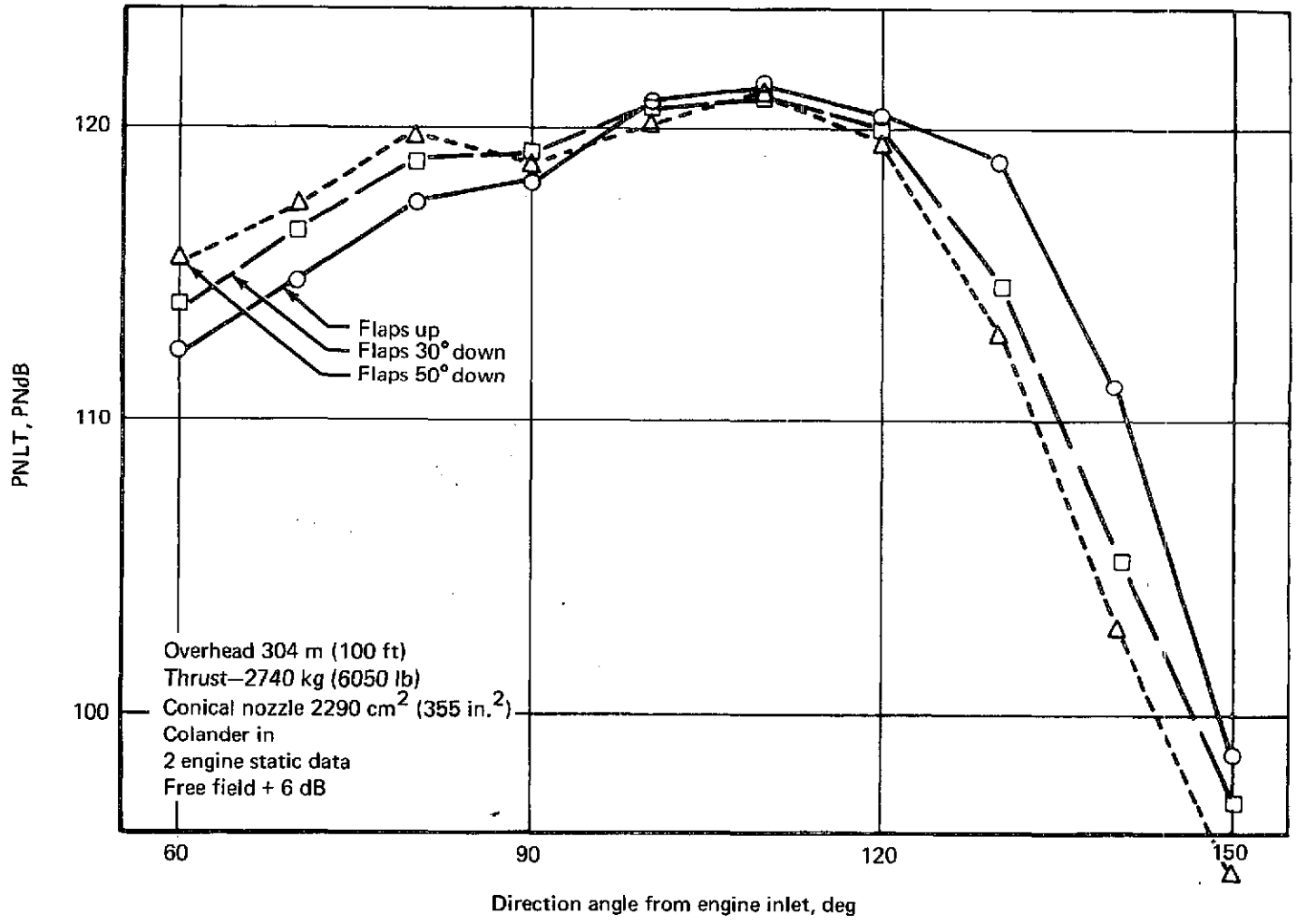

FIGURE 26.—EFFECT OF FLAP ANGLE ON SOUND DIRECTIVITY

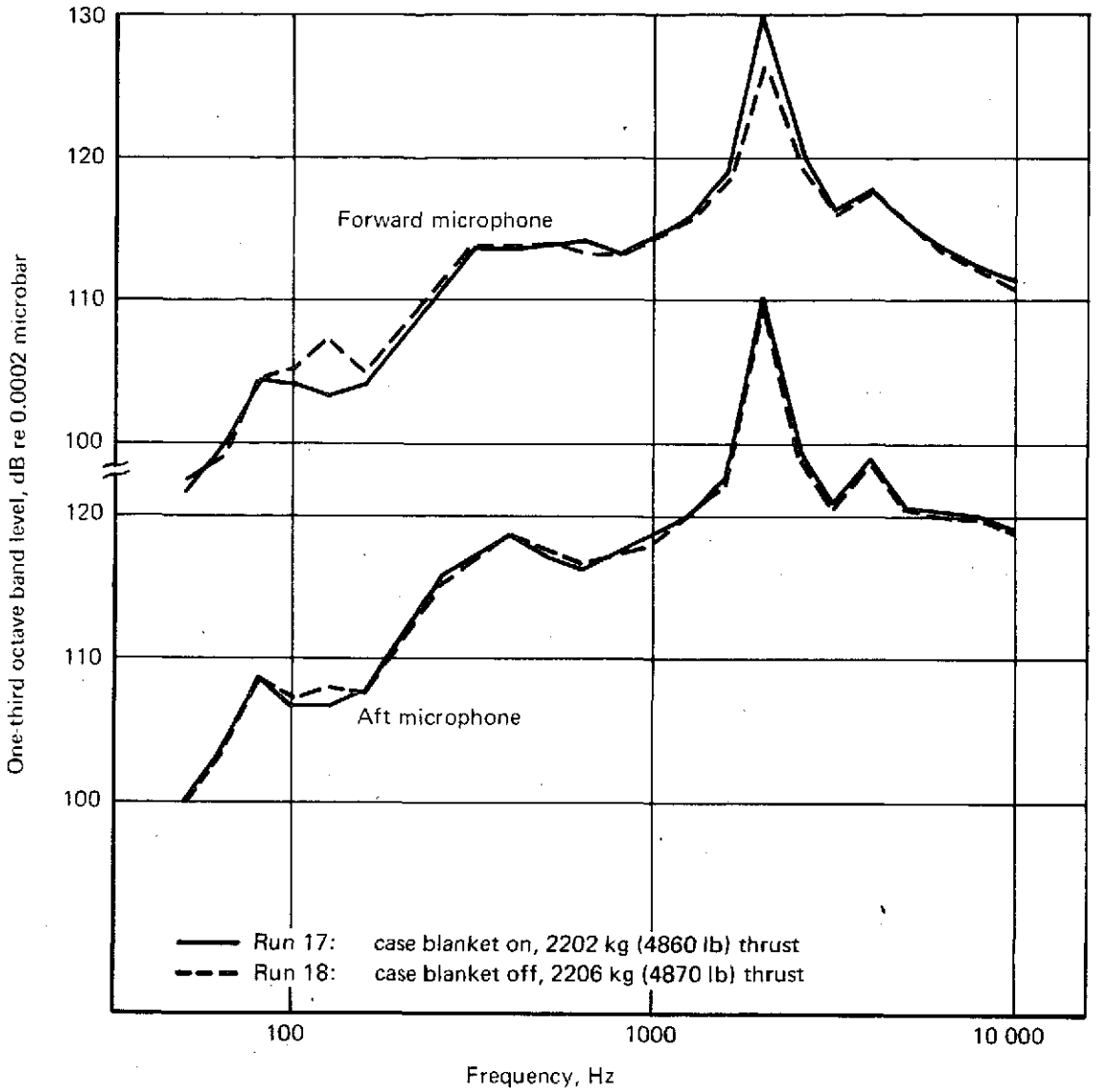

FIGURE 27.–SPL MEASURED CLOSE IN AT HIGHER THRUST

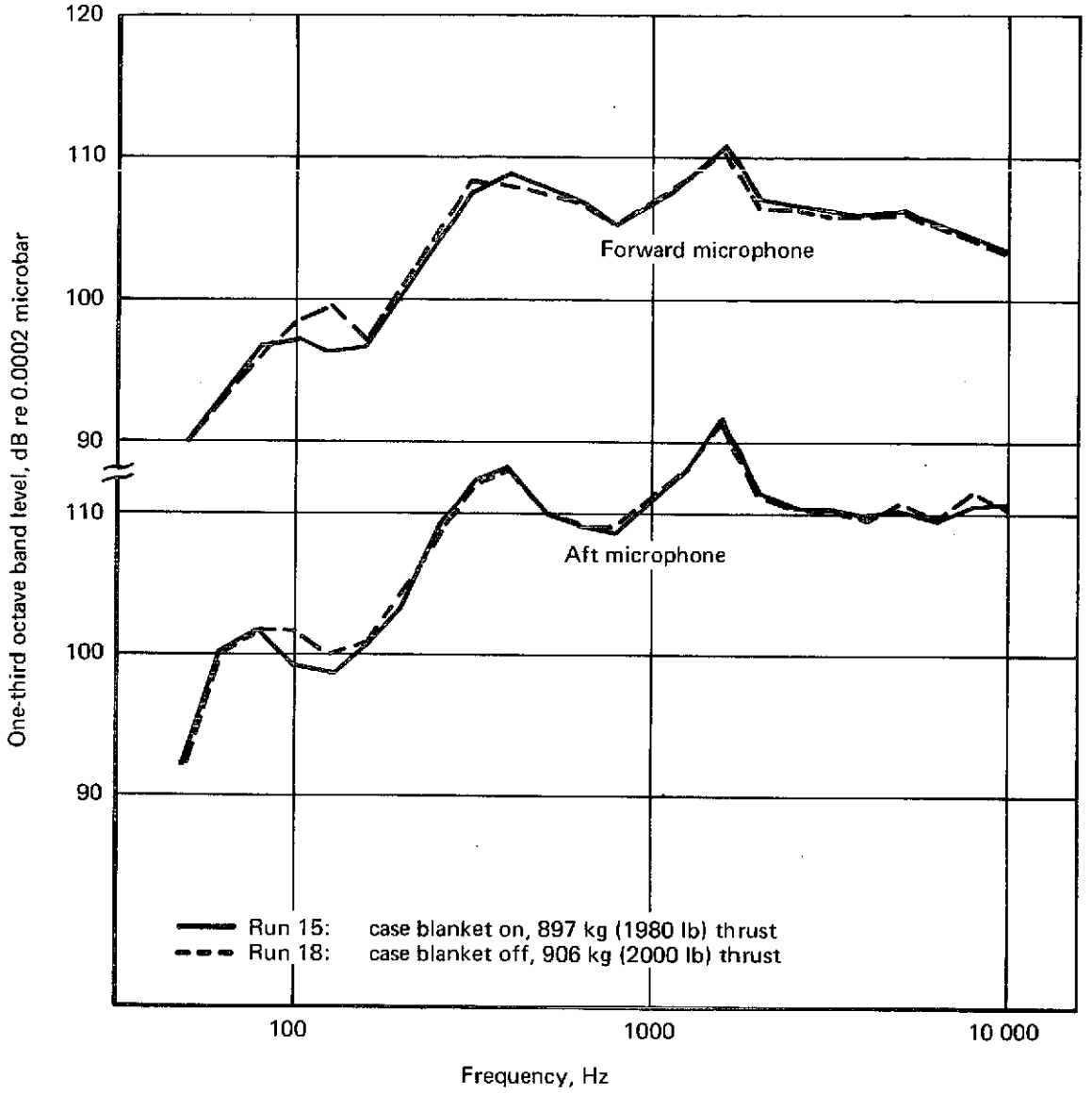

FIGURE 28.–SPL MEASURED CLOSE IN, AT LOW THRUST

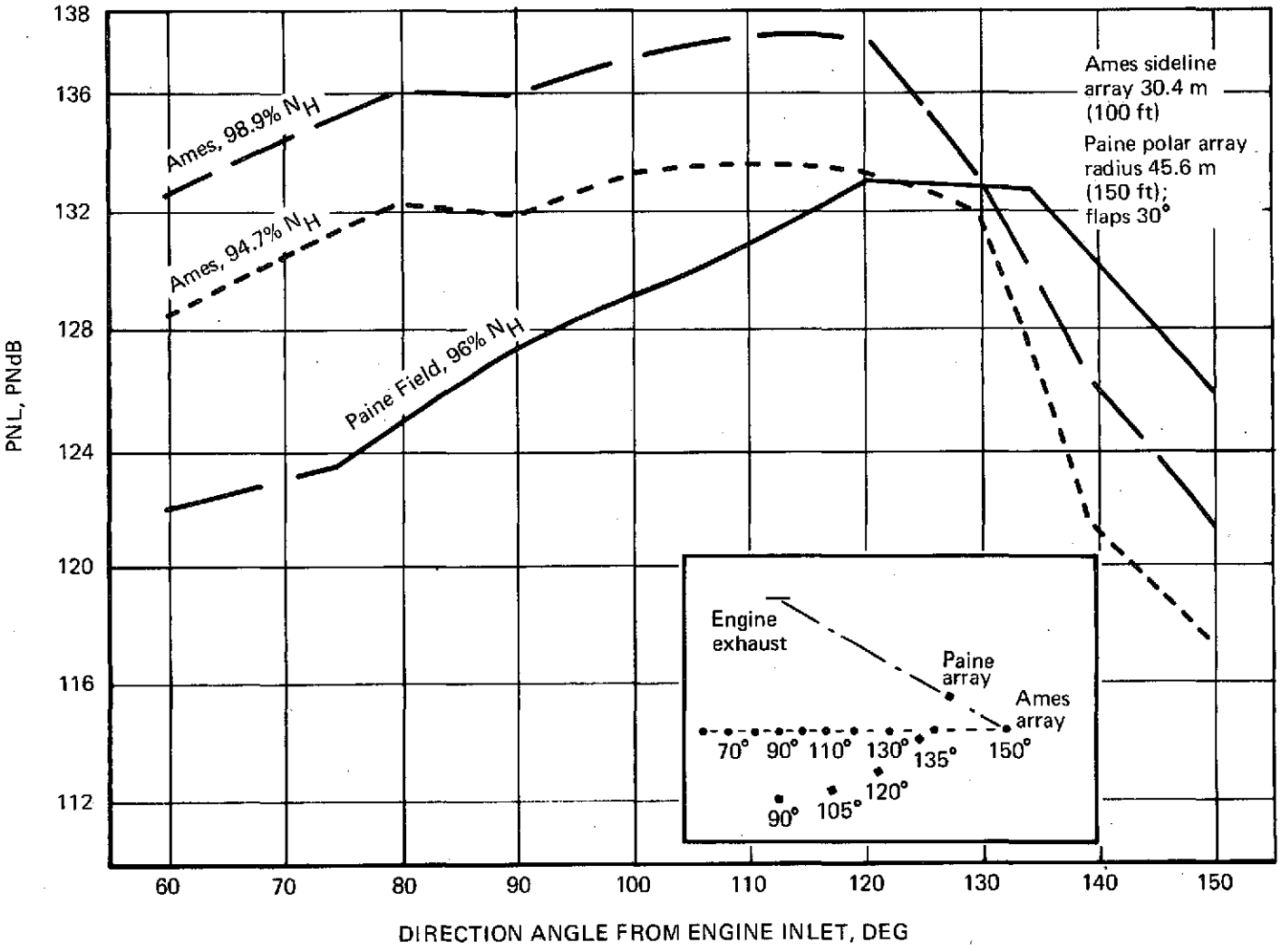

FIGURE 29.—COMPARISON OF AMES AND PAINE FIELD STATIC NOISE DATA

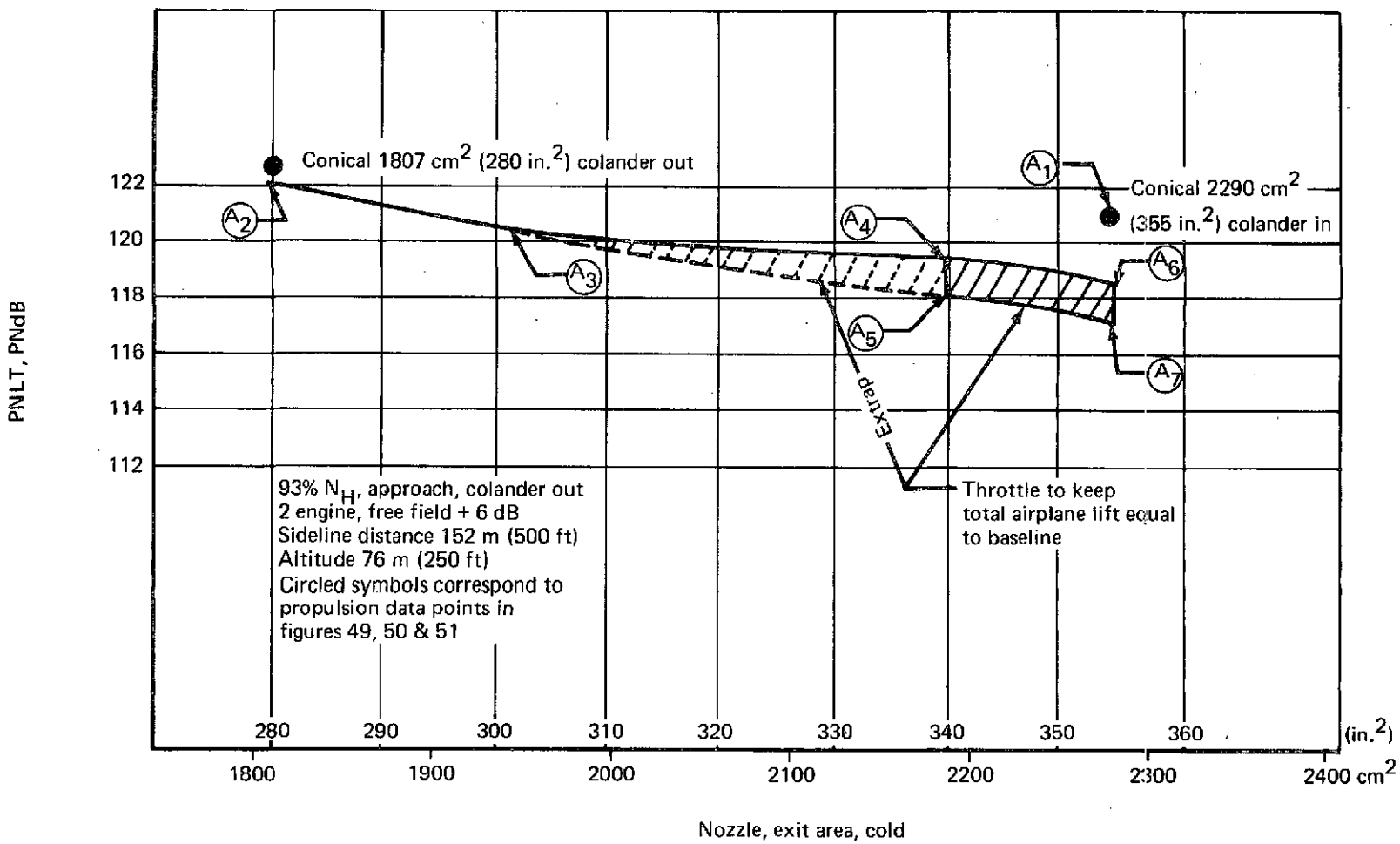

FIGURE 30.—EFFECT OF LOBE NOZZLE AREA ON SIDELINE NOISE

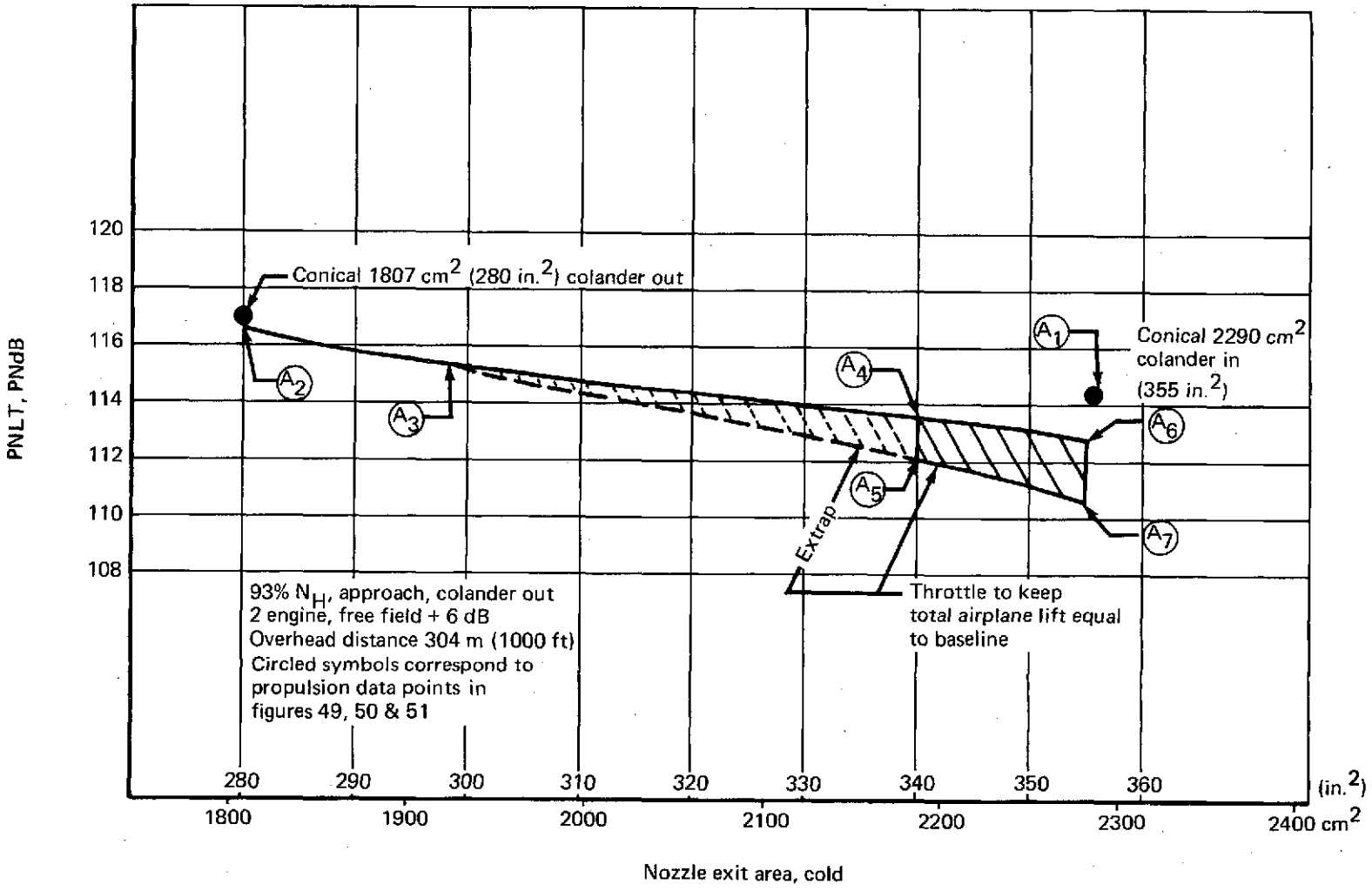

FIGURE 31.–EFFECT OF LOBE NOZZLE AREA ON NOISE 304 METERS OVERHEAD

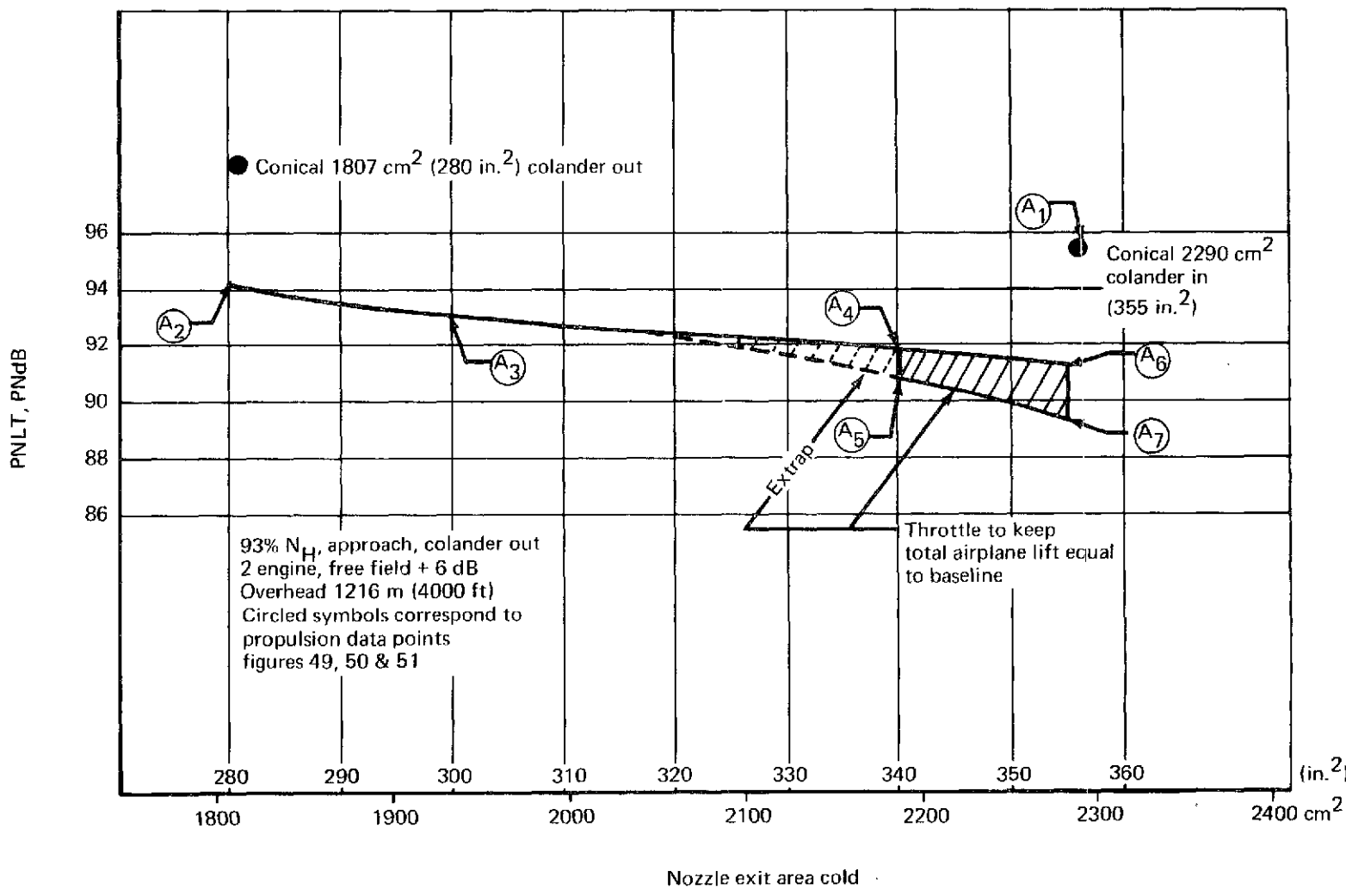

FIGURE 32.–EFFECT OF LOBE NOZZLE AREA ON NOISE 1216 METERS OVERHEAD

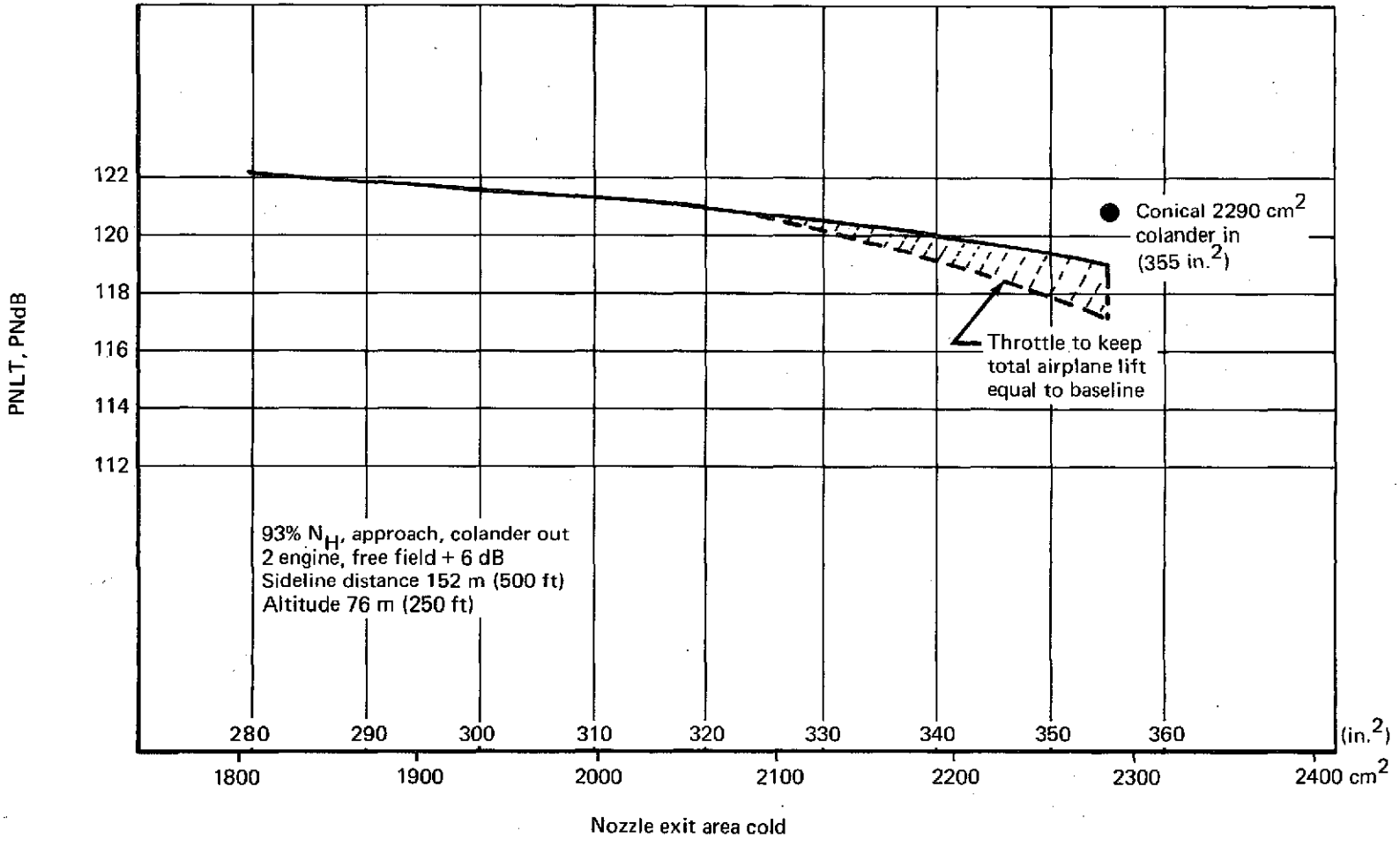

FIGURE 33.–EFFECT OF CONICAL NOZZLE AREA ON SIDELINE NOISE

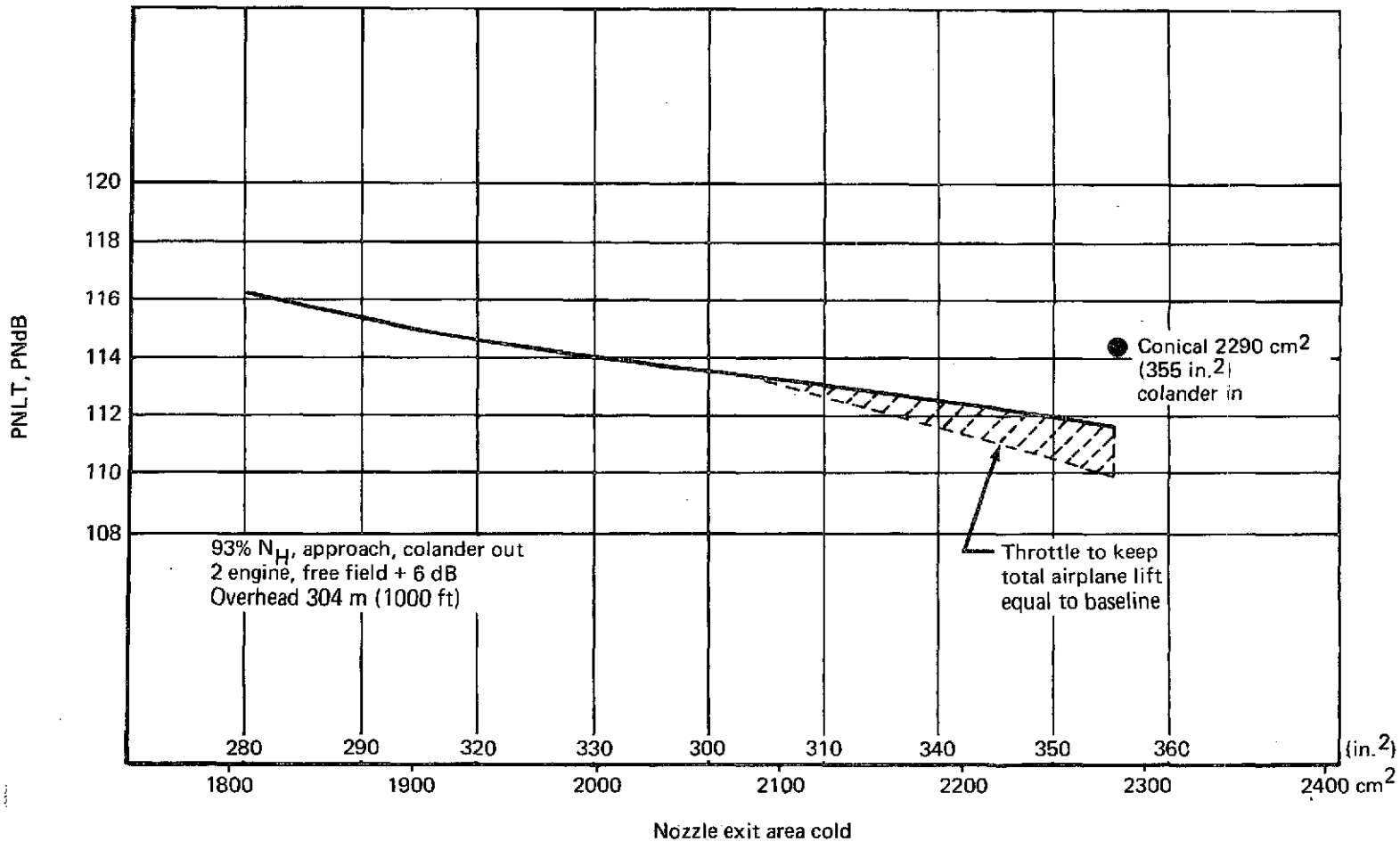

FIGURE 34.—EFFECT OF CONICAL NOZZLE AREA ON NOISE 304 METERS OVERHEAD

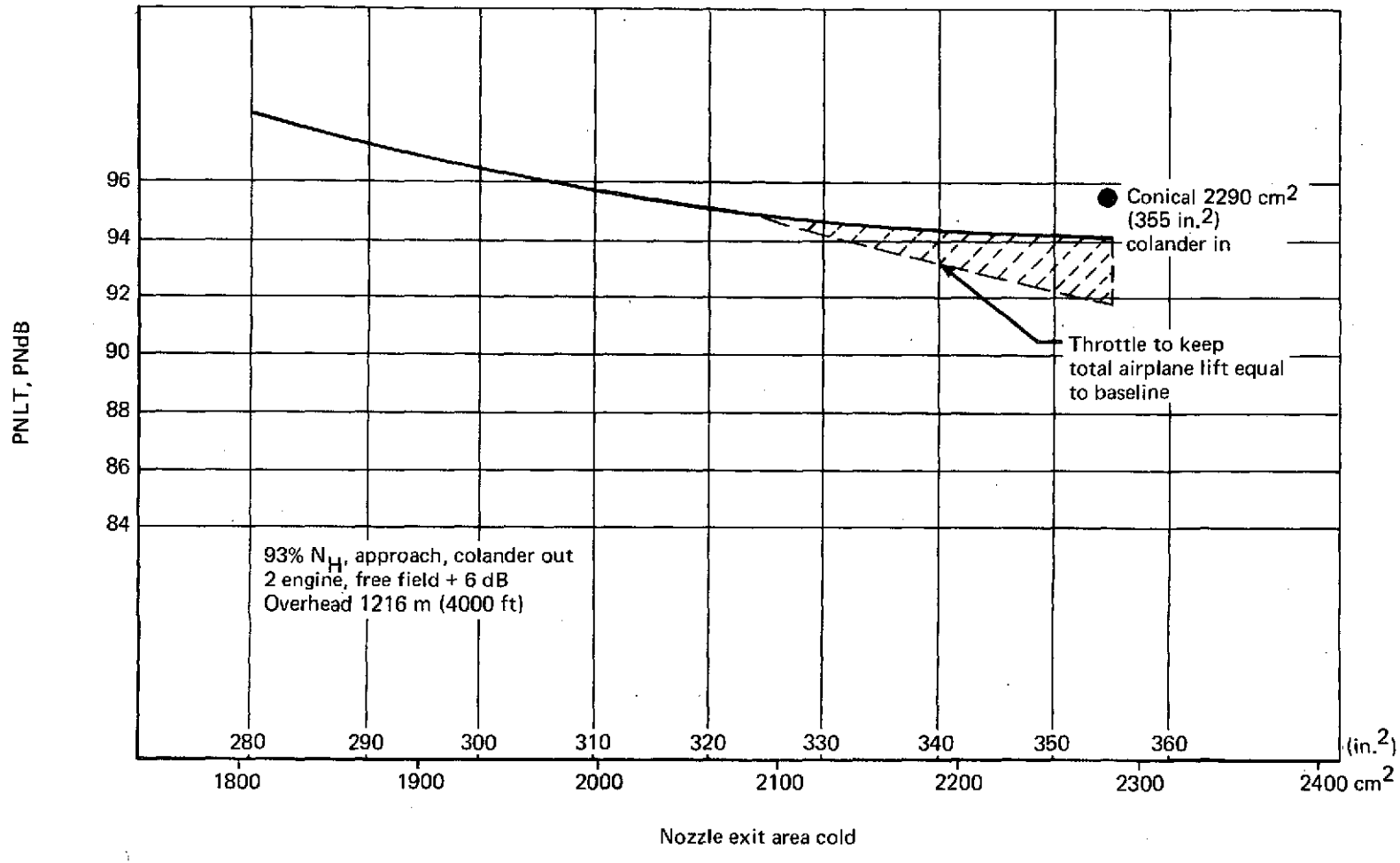

FIGURE 35.–EFFECT OF CONICAL NOZZLE AREA ON NOISE 1216 METERS OVERHEAD

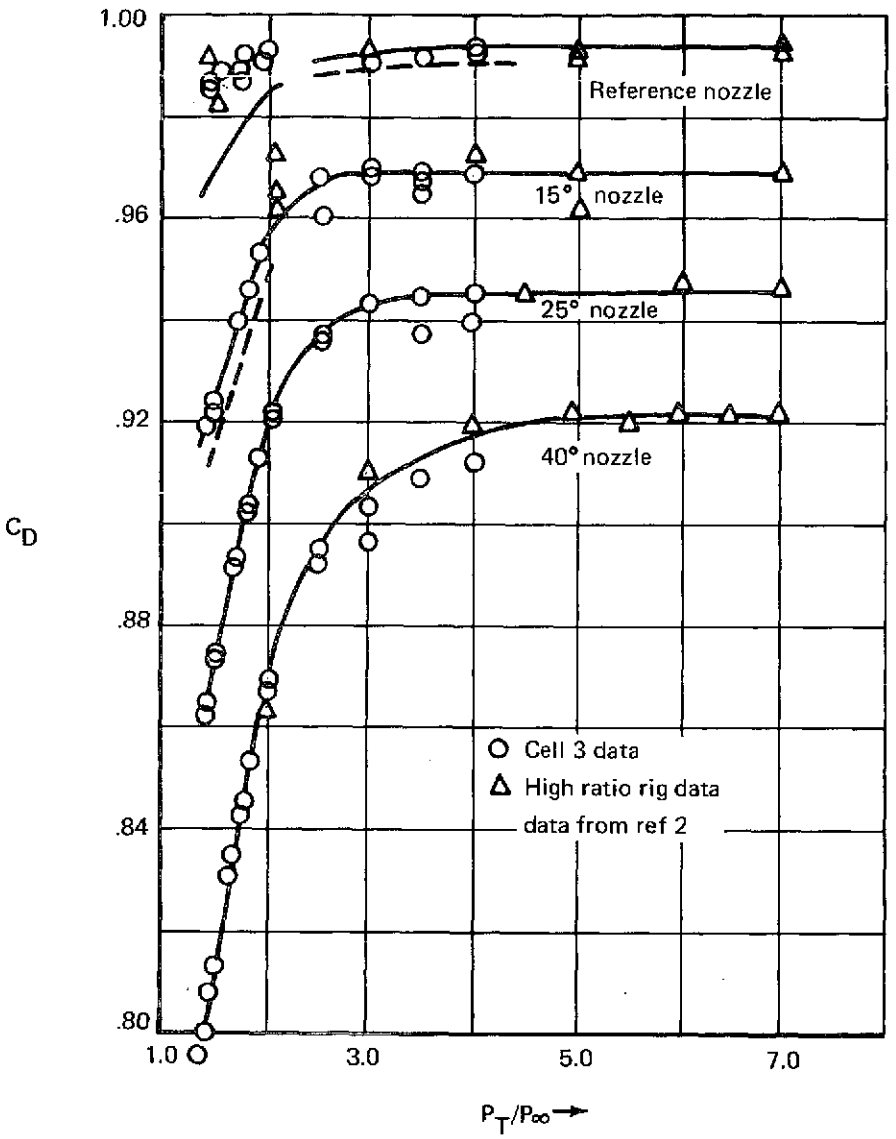

FIGURE 36.–NOZZLE ANGLE AND PRESSURE RATIO EFFECT ON DISCHARGE COEFFICIENTS,CONICAL CONVERGENT NOZZLES

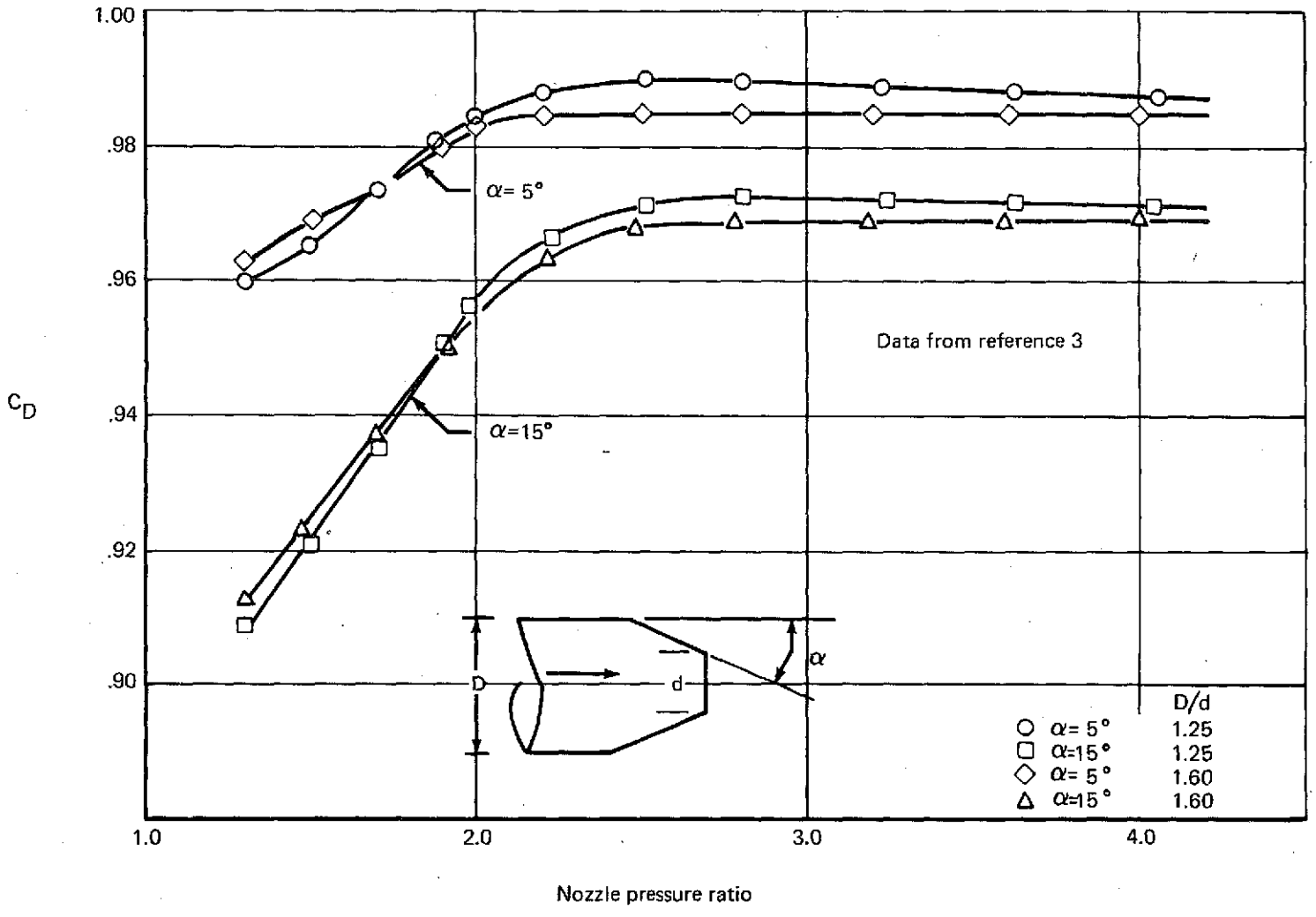

FIGURE 37.—DISCHARGE COEFFICIENTS FOR CONICAL NOZZLES WITH TWO DIFFERENT ONE-HALF ANGLES AND DIAMETER RATIOS

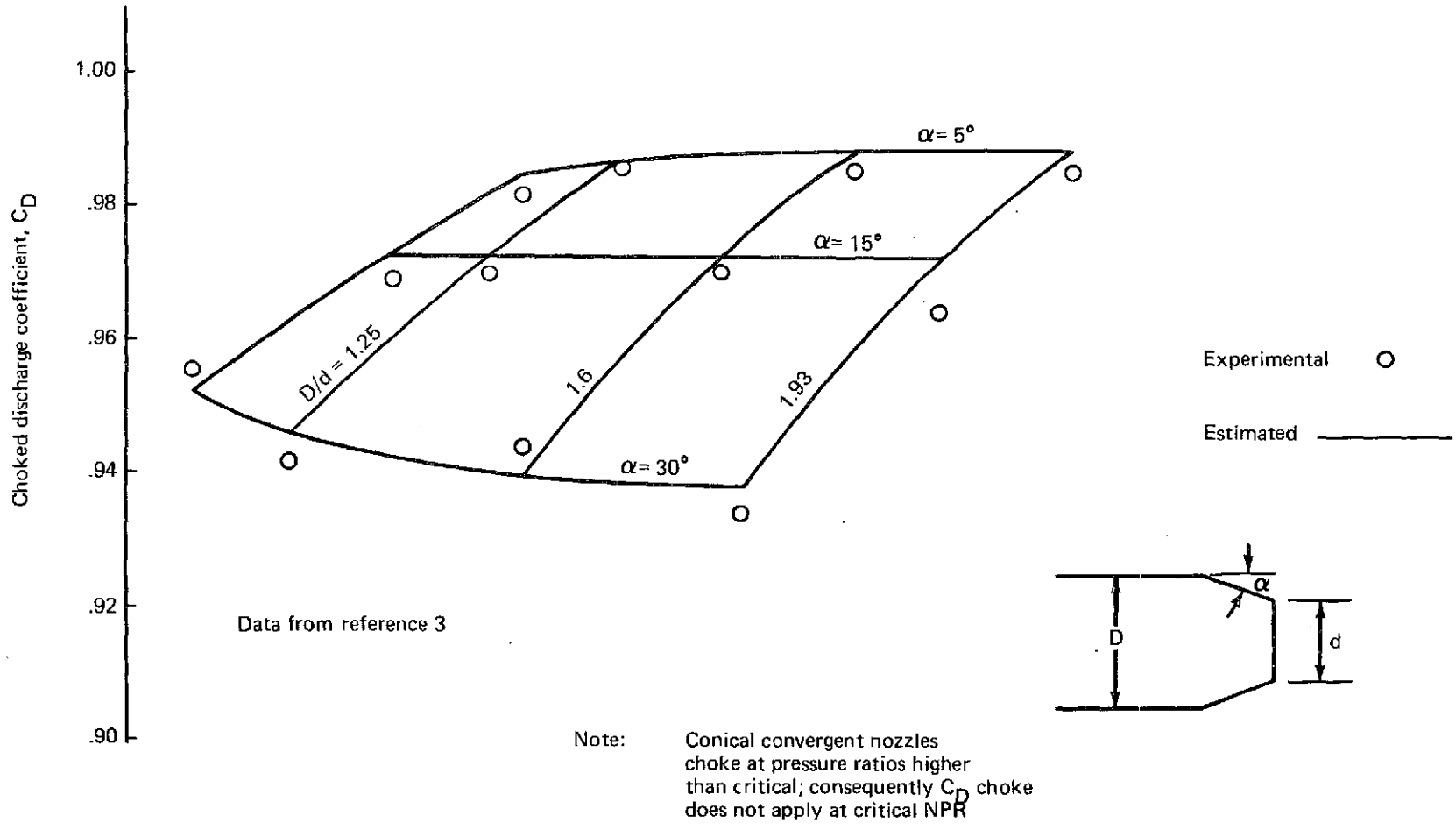

FIGURE 38.—EFFECT OF CONICAL NOZZLE ONE-HALF ANGLE AND DIAMETER RATIO ON CHOKED DISCHARGE COEFFICIENT

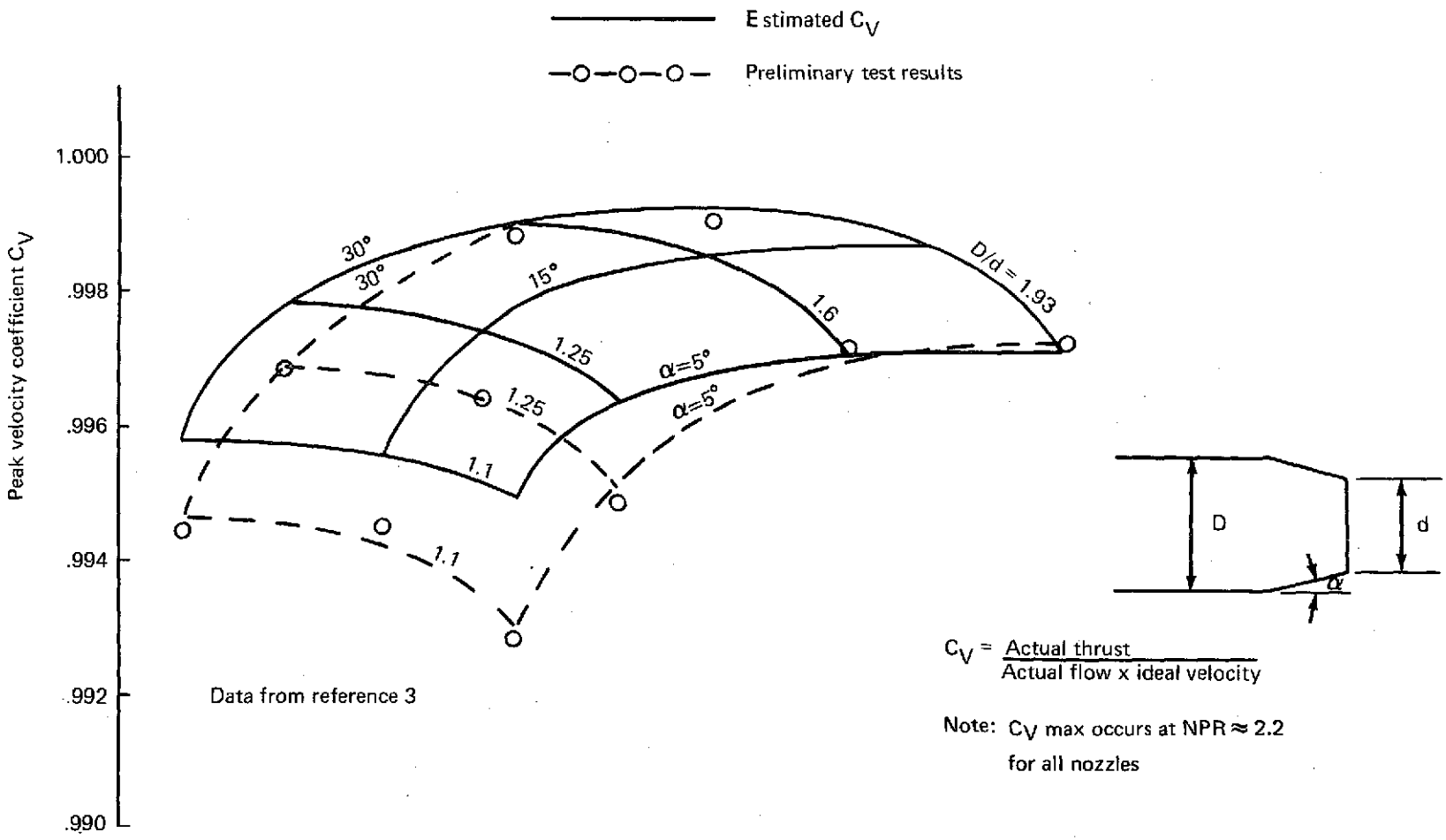

FIGURE 39.—EFFECT OF CONICAL NOZZLE ONE-HALF ANGLE AND DIAMETER RATIO ON PEAK VELOCITY COEFFICIENT

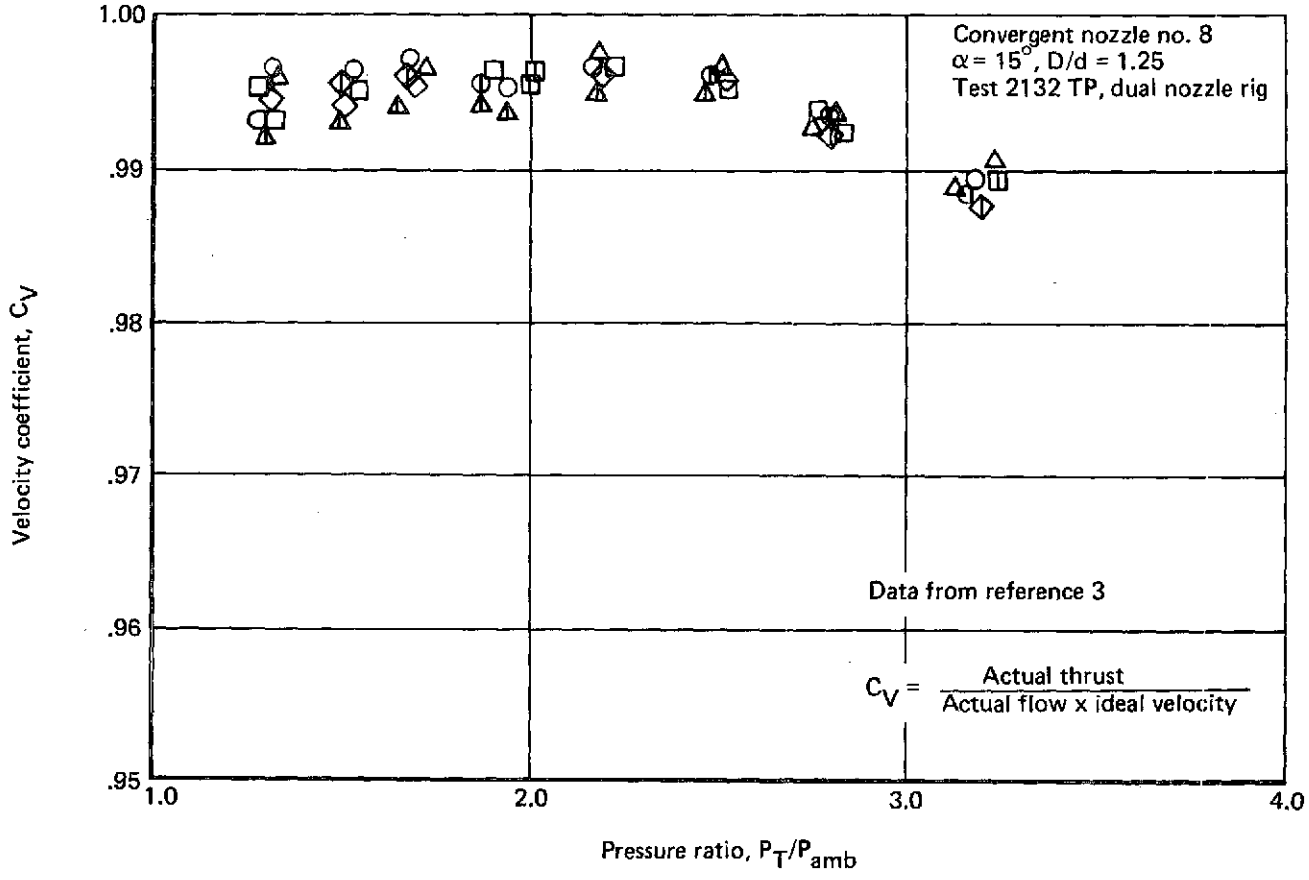

FIGURE 40.—EFFECT OF NOZZLE PRESSURE RATIO ON VELOCITY COEFFICIENT

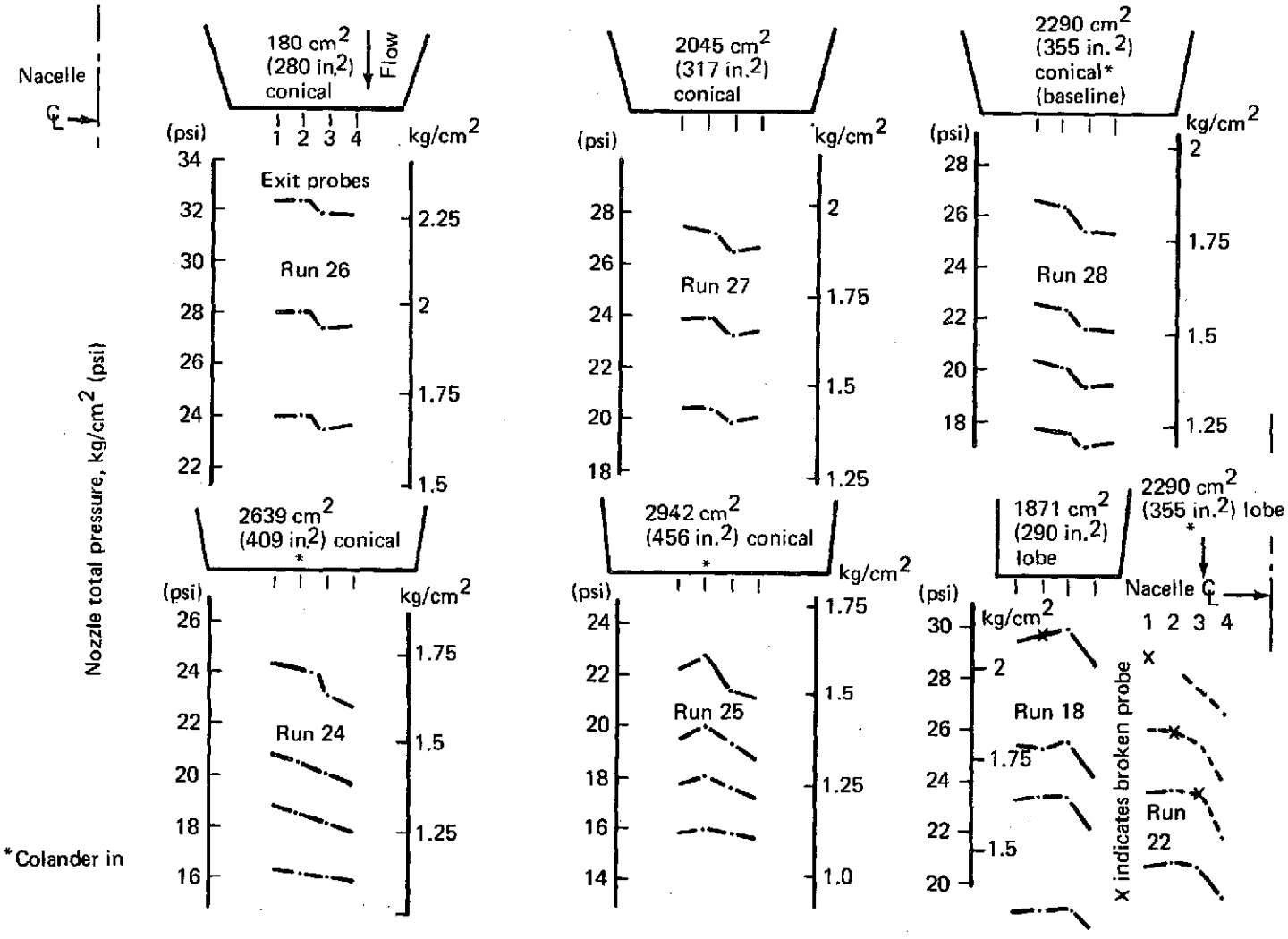

FIGURE 41.—NOZZLE EXIT TOTAL PRESSURE DATA

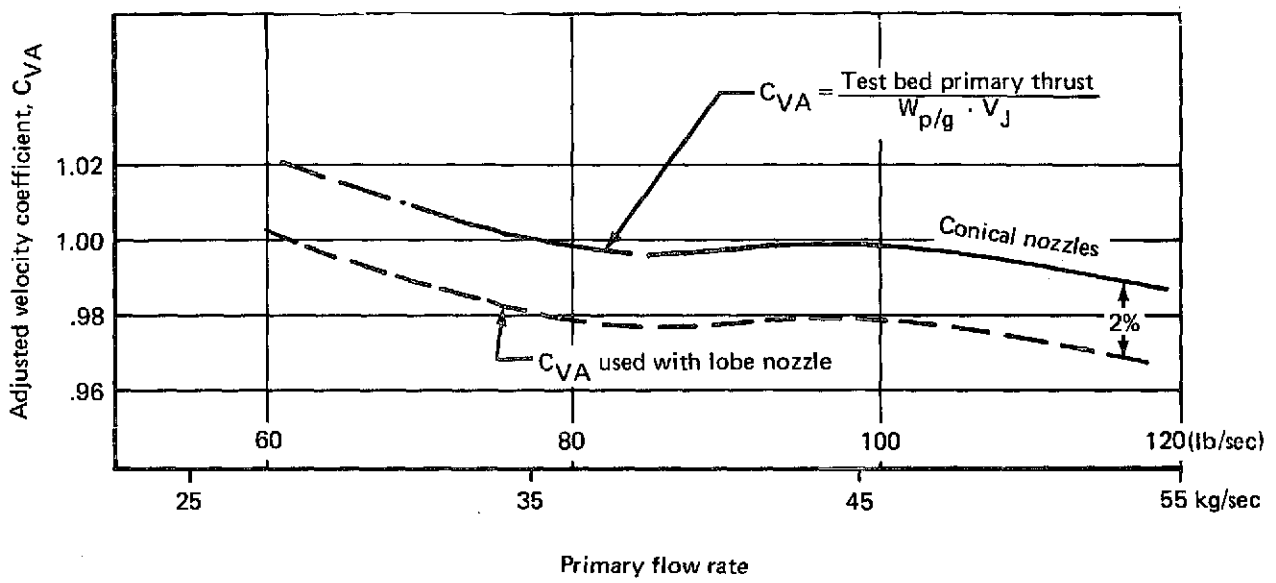

FIGURE 42.–NOZZLE VELOCITY COEFFICIENT (ADJUSTED) AS FUNCTION OF PRIMARY FLOW RATE

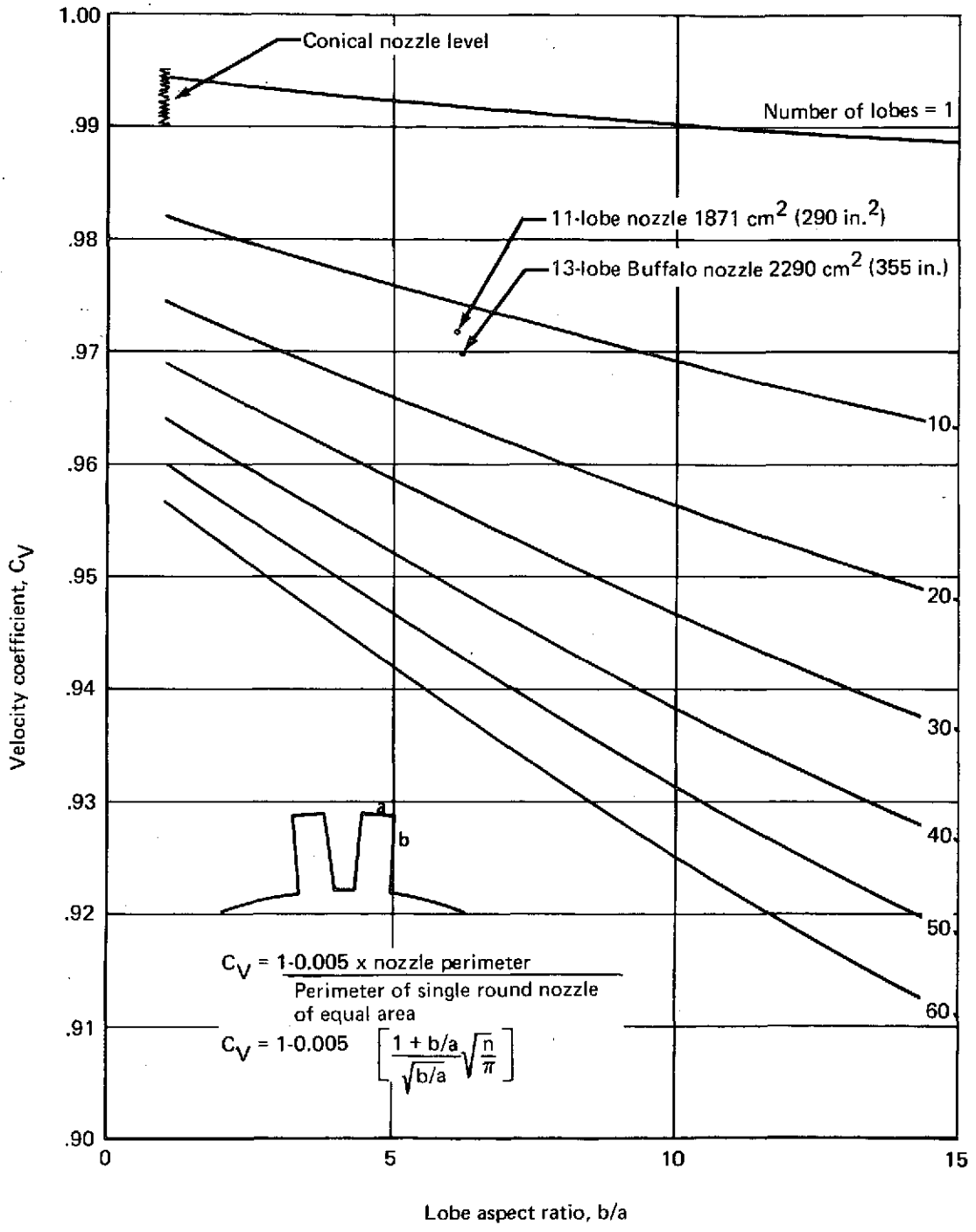

FIGURE 43.–ESTIMATED VELOCITY COEFFICIENTS FOR LOBE TYPE SUPPRESSOR NOZZLES

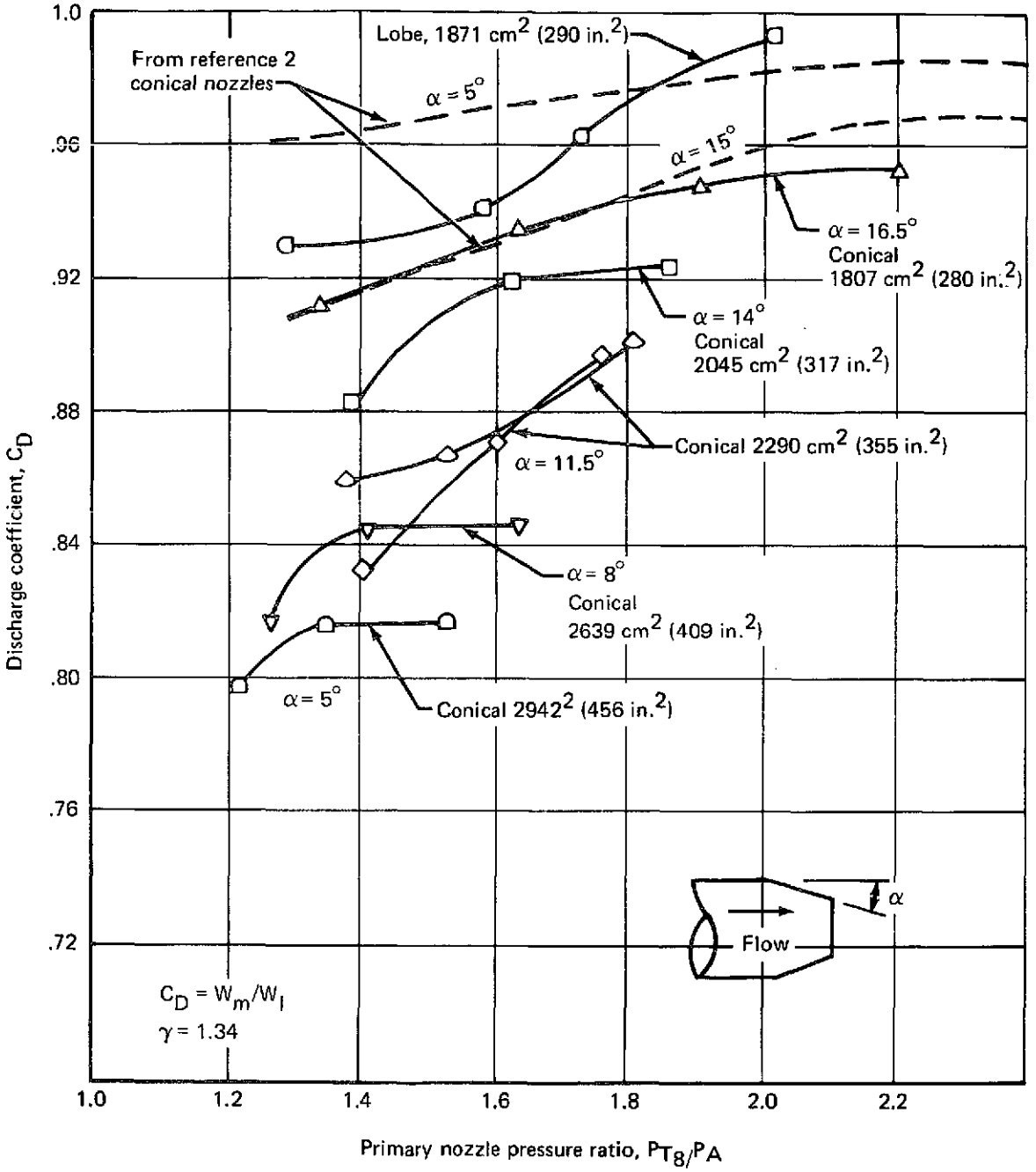

FIGURE 44.–NOZZLE OR SYSTEM DISCHARGE COEFFICIENTS

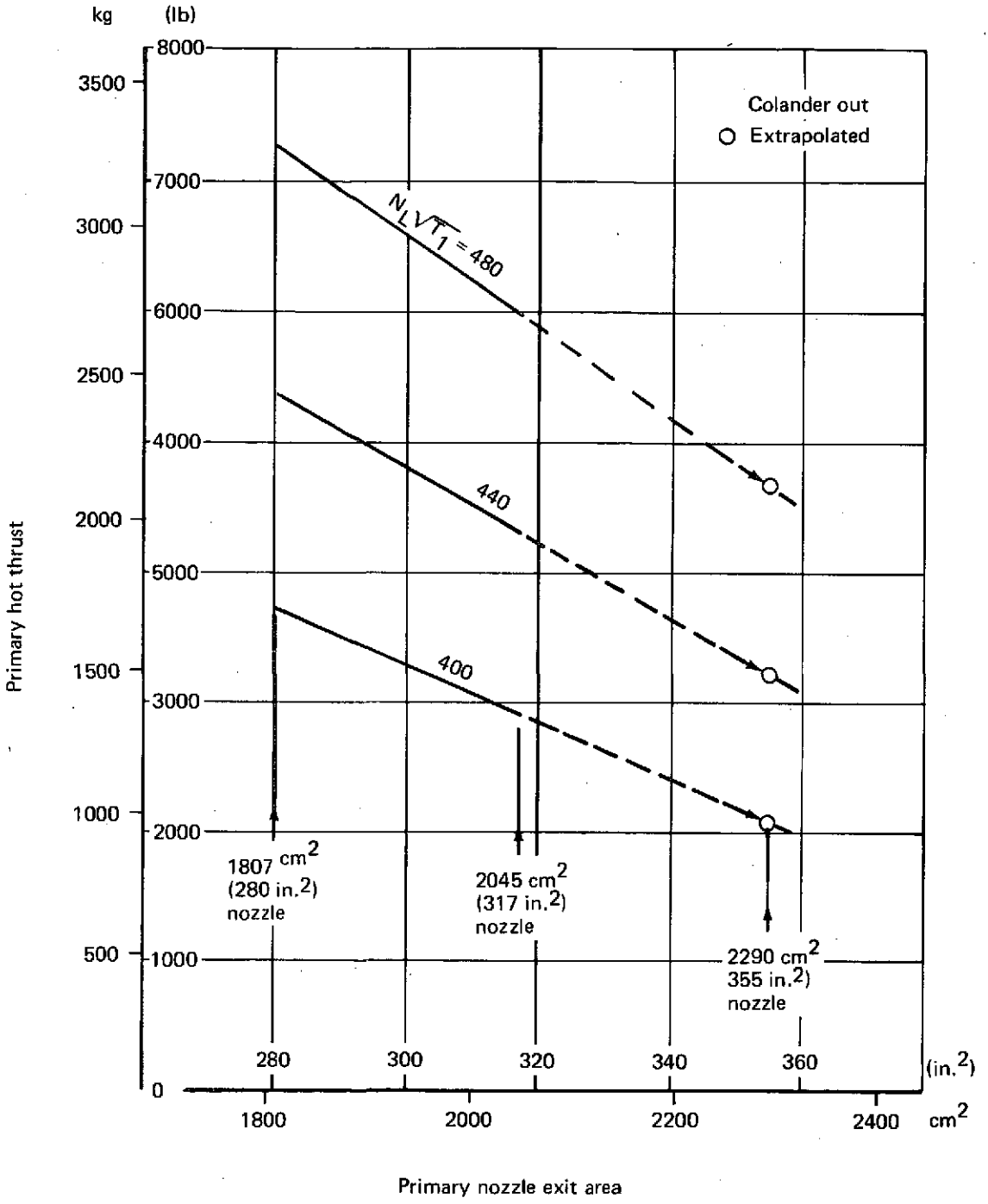

FIGURE 45.—CONICAL NOZZLE HOT THRUST DETERMINATION BY LINEAR EXTRAPOLATION

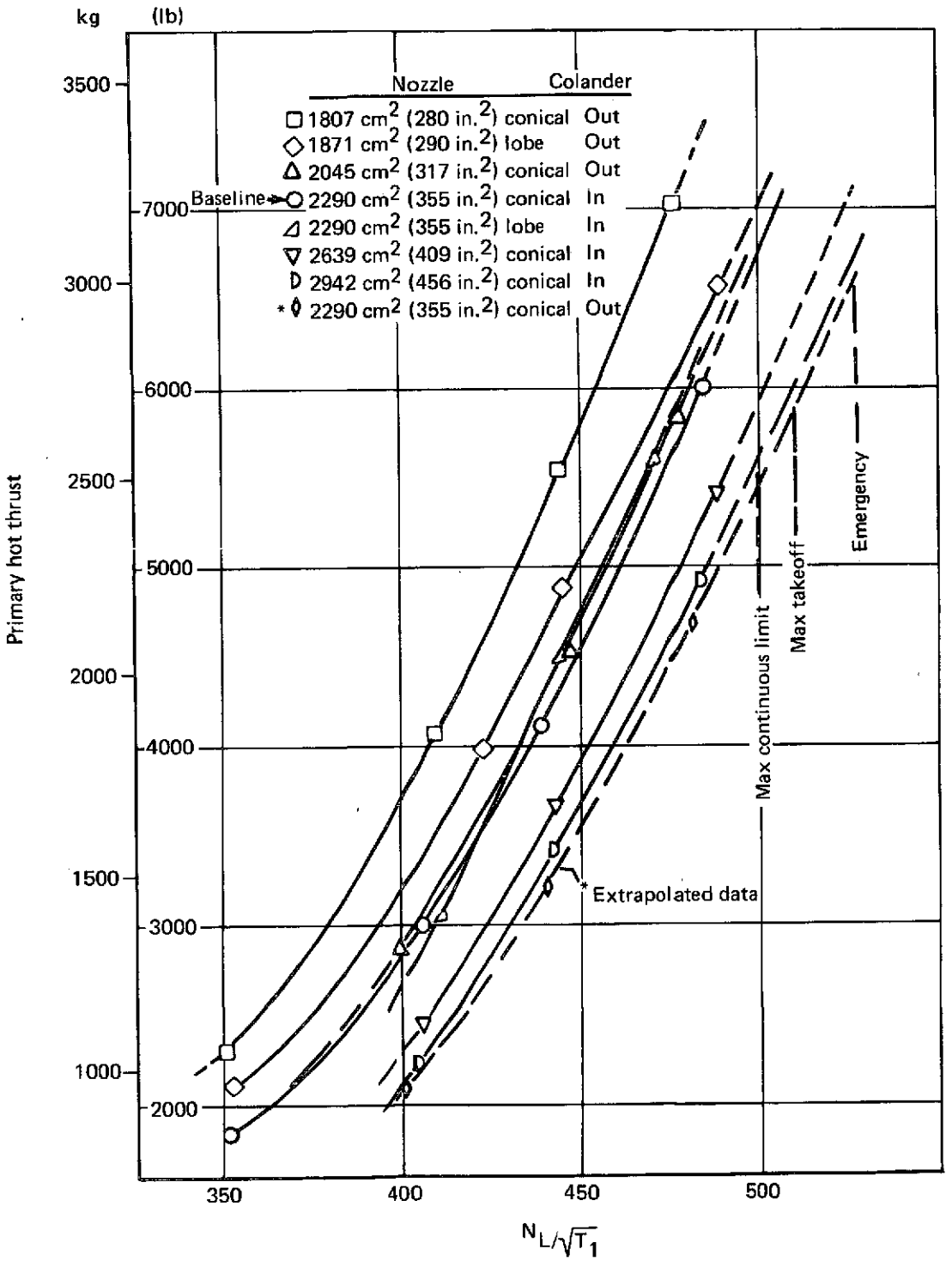

FIGURE 46.–COMPUTED PRIMARY THRUST

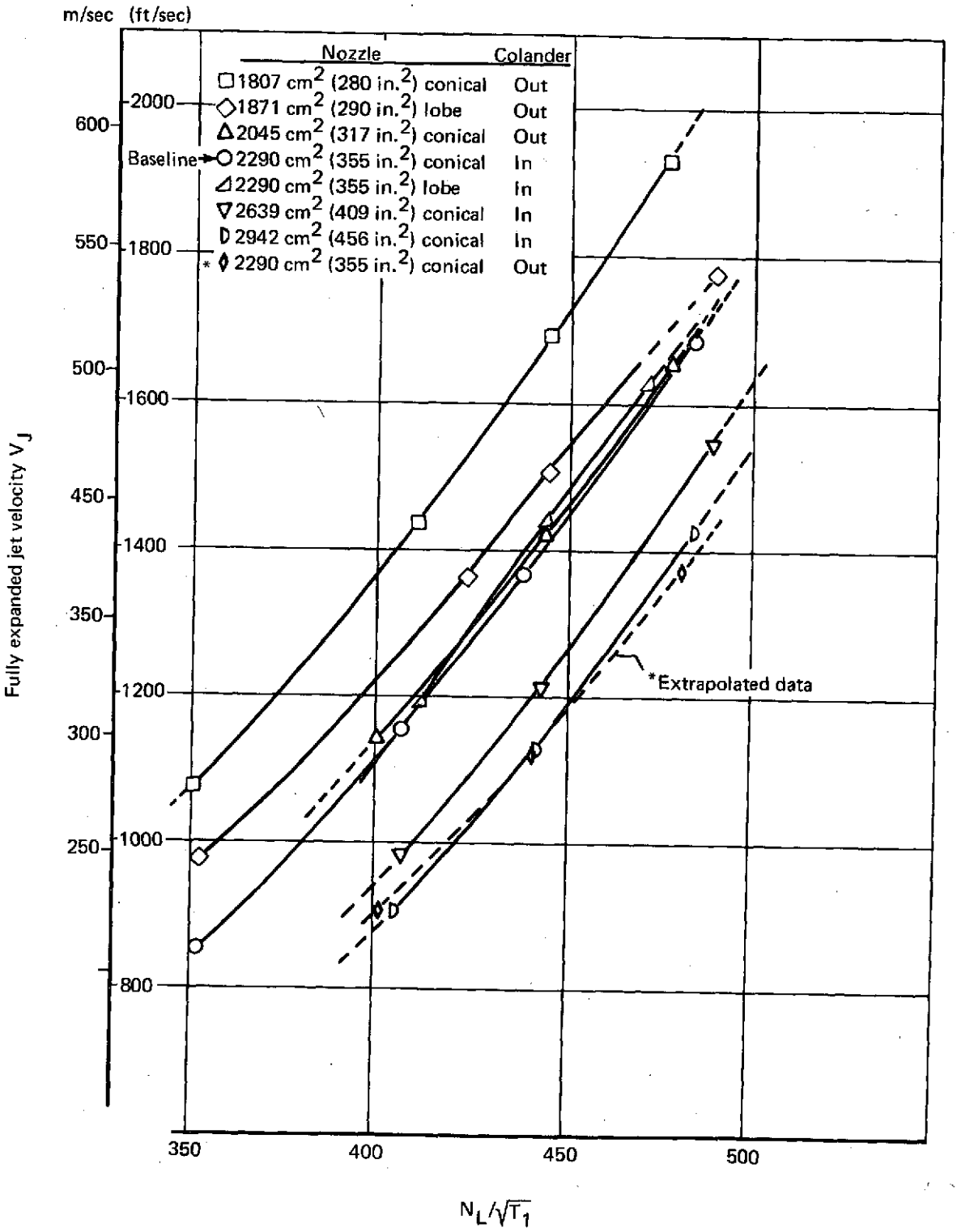

FIGURE 47.—FULLY EXPANDED JET VELOCITY VERSUS $N_L/\sqrt{T_1}$

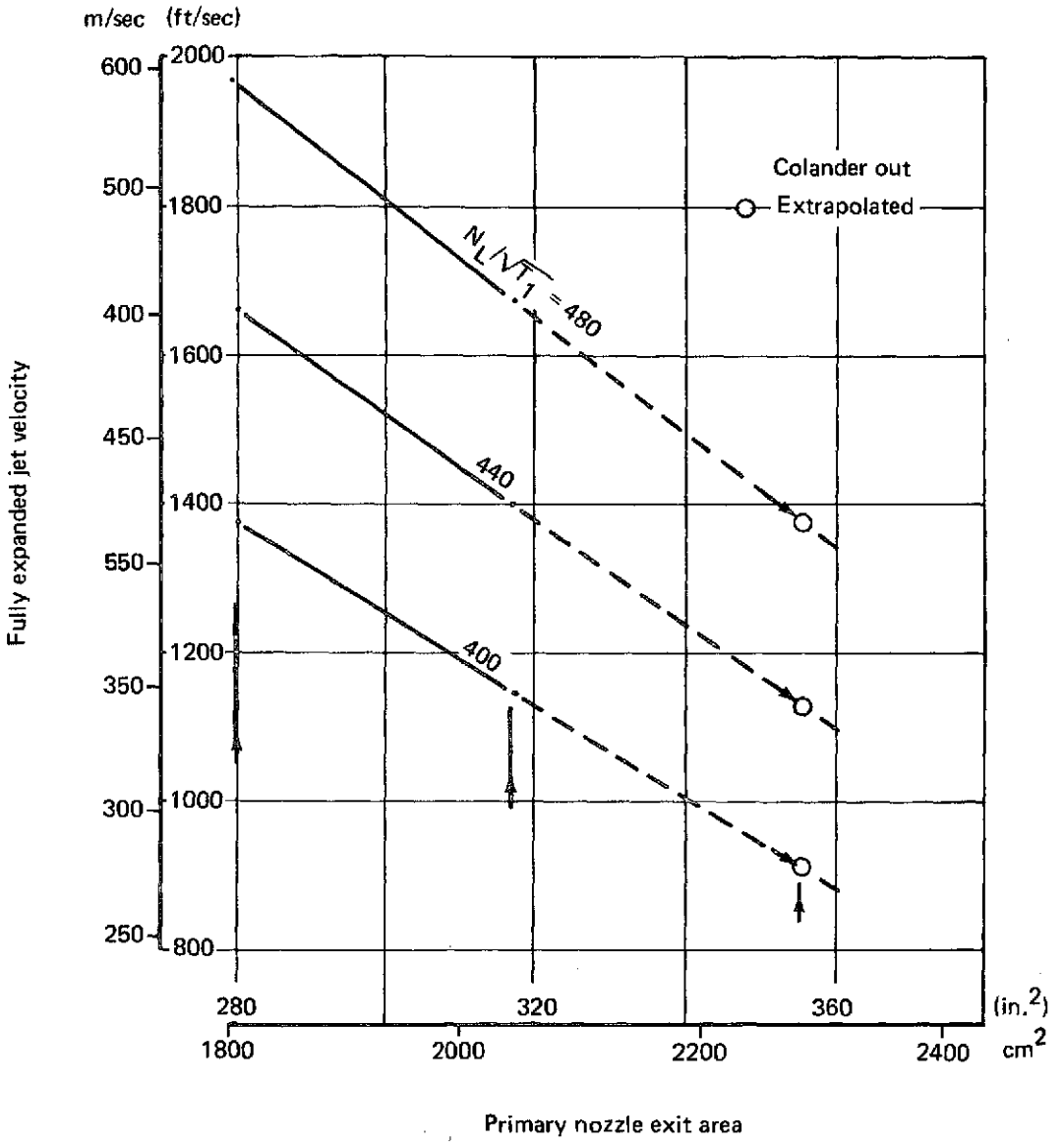

FIGURE 48.–CONICAL NOZZLE JET VELOCITY DETERMINATION BY LINEAR EXTRAPOLATION

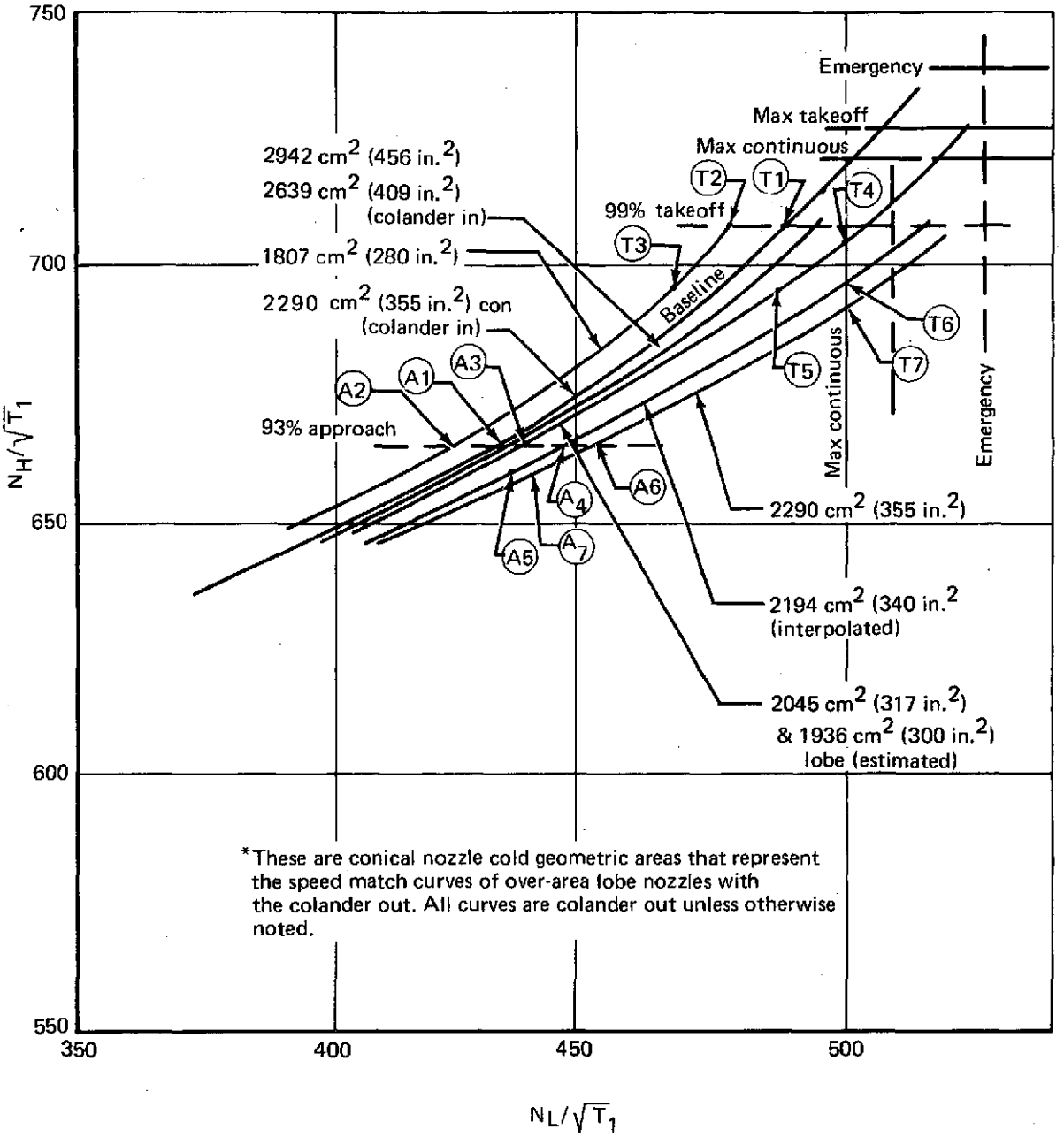

FIGURE 49.—ENGINE SPEED MATCH CHARACTERISTICS

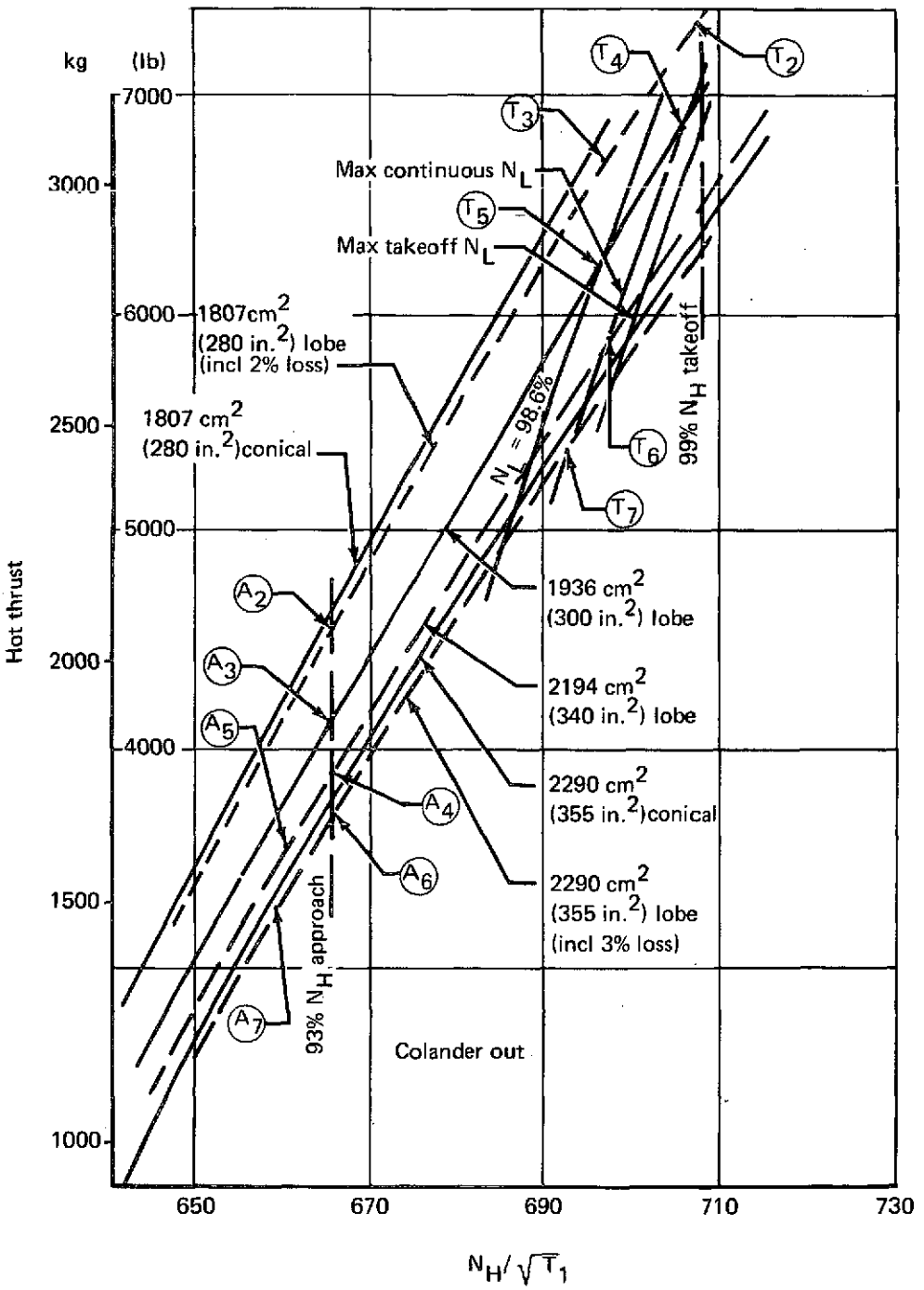

FIGURE 50.–COMPUTED HOT THRUST VALUES

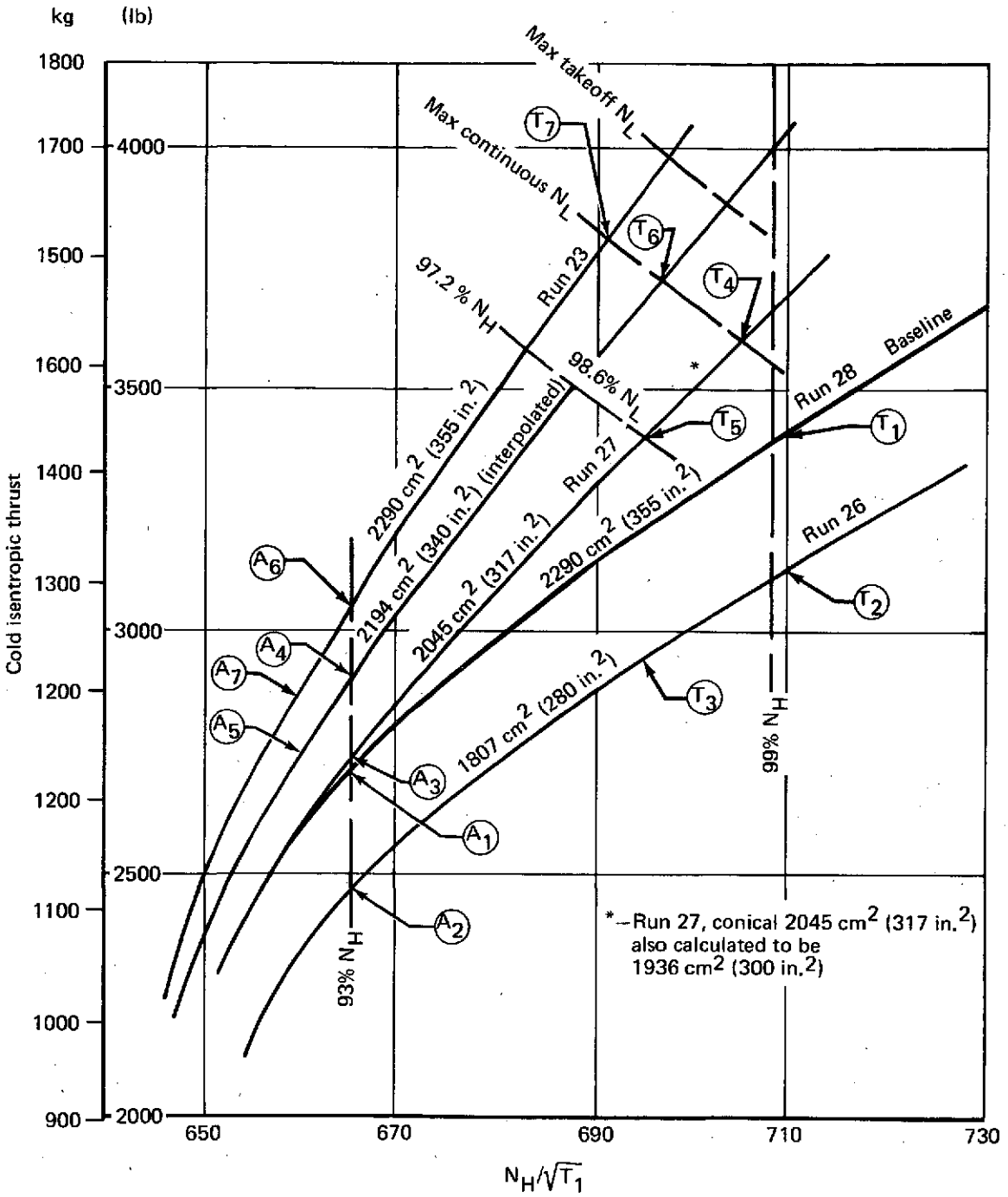

FIGURE 51.—COMPUTED COLD THRUST VALVES

C-12